The Islamic University–Gaza
Research and Postgraduate Affairs
Faculty of Science
Master of Physics

الجامعـــــــة الإســـلاميـة – غـزة
شئون البحث العلمي والدراسات العليا
كليـــة العلوم
ماجستير الفيزياء

Theoretical Analysis of Metamaterial – Multilayer Waveguide Structures for Solar Cells

التحليل النظري لبنية مرشد موجي متعدد الطبقات يحتوي على مواد يسارية للخلايا الشمسية

Samer J. Abu Lebda

Supervised by

Prof. Dr. Mohammed M. Shabat

Professor of Theoretical Physices and Applied Mathematices

A thesis submitted in partial fulfillment of the requirements for the degree of Master of Pyhsices

November/2016

إقـــــرار

أنا الموقع أدناه مقدم الرسالة التي تحمل العنوان:

Theoretical Analysis of Metamaterial – Multilayer Waveguide Structures for Solar Cells

التحليل النظري لبنية مرشد موجي متعدد الطبقات يحتوي على مواد يسارية للخلايا الشمسية

أقر بأن ما اشتملت عليه هذه الرسالة إنما هو نتاج جهدي الخاص، باستثناء ما تمت الإشارة إليه حيثما ورد، وأن هذه الرسالة ككل أو أي جزء منها لم يقدم من قبل الاخرين لنيل درجة أو لقب علمي أو بحثي لدى أي مؤسسة تعليمية أو بحثية أخرى.

Declaration

I understand the nature of plagiarism, and I am aware of the University's policy on this.

The work provided in this thesis, unless otherwise referenced, is the researcher's own work, and has not been submitted by others elsewhere for any other degree or qualification.

Student's name:	سامر جبر أبو لبدة	اسم الطالب:
Signature:		التوقيع:
Date:	2016/12/28	التاريخ:

بسم الله الرحمن الرحيم

الجامعة الإسلامية غزة
The Islamic University of Gaza

مكتب نائب الرئيس للبحث العلمي والدراسات العليا هاتف داخلي: 1150

الرقم: ج س غ/35/ Ref:

التاريخ: 2016/12/28 Date:

نتيجة الحكم على أطروحة ماجستير

بناءً على موافقة شئون البحث العلمي والدراسات العليا بالجامعة الإسلامية بغزة على تشكيل لجنة الحكم على أطروحة الباحث/ **سامر جبر السيد ابو لبده** لنيل درجة الماجستير في **كلية العلوم** قسم **الفيزياء** وموضوعها:

التحليل النظري لبنية مرشد موجي متعدد الطبقات يحتوي على مواد يسارية للخلايا الشمسية

Theoretical Analysis of Metamaterial – Multilayer Waveguide Structures for Solar Cells

وبعد المناقشة العلنية التي تمت اليوم الأربعاء 29 ربيع أول 1438هـ، الموافق 2016/12/28م الساعة الثانية عشرة ظهراً في قاعة مؤتمرات مبنى القدس، اجتمعت لجنة الحكم على الأطروحة والمكونة من:

أ.د. محمد موسى شبات	مشرفاً و رئيساً	.....
د. معين فتحي عبيد	مناقشاً داخلياً	.....
د. زياد إسماعيل السحار	مناقشاً خارجياً	.....

وبعد المداولة أوصت اللجنة بمنح الباحث درجة الماجستير في **كلية العلوم**/ قسم **الفيزياء**.

واللجنة إذ تمنحه هذه الدرجة فإنها توصيه بتقوى الله ولزوم طاعته وأن يسخر علمه في خدمة دينه ووطنه.

والله ولي التوفيق،،،

نائب الرئيس لشئون البحث العلمي والدراسات العليا

أ.د. عبدالرؤوف علي المناعمة

+97082644400 +97082644800 public@iugaza.edu.ps www.iugaza.edu.ps iugaza iugaza mediaiug iugaza
P.O Box 108, Rimal,Gaza,Palestine ص.ب 108 الرمال . غزة . فلسطين

Abstract

Solar cells are photoelectric devices convert sun light to electric power through semiconductors. The main problem of solar cells is the limit of the transmission and absorption of the sun light which causes the low efficiency. When used as Anti-Reflection Coatings (ARCs), Metamaterials under certain conditions could be a useful choice to increase the transmision and the absorption of the incident radiation.

The main purpose of this study is to suggest a new waveguide structure containing a metamaterial ARC capable of reducing the reflection and enhancing both the transmission and the absorption of the sun light incident on the solar cell in order to increase its efficiency. The proposed structure of the ARC consists of 4-layers (air, metamaterial, silicon nitride (SiN_x) and Gallium Arsenide (GaAs) as a substrate). Analytical and mathematical methods such as the boundary conditions, transfer matrix and Fresnel's equations are used to calculate the reflection, transmission and absorption and determined the optimal values of the parameters for each layer as the electric permittivity (ε), magnetic permeability (μ) and thickness, in addition to the angle of incidence. A computer software (Maple 13) is used to analyse and carry out the results.

The study shows that the maximum transmittance and absorbance are achieved under certain conditions when the Gallium Arsenide (GaAs) solar cells are covered by the proposed ARCs.

الملخص

الخلايا الشمسية هي أجهزة كهروضوئية تحول أشعة الشمس الى كهرباء باستخدام أشباه الموصلات. المشكلة الرئيسية في الخلايا الشمسية هي محدودية نفاذ وامتصاص أشعة الشمس والذي يتسبب في خفض كفاءة تلك الخلايا الشمسية. وعندما تستخدم المواد الاصطناعية (اليسارية) المسماة (Metamaterials) تحت ظروف معينة كطبقة ضمن الغطاء المضاد للانعكاس (Anti-Reflection Coating) فإنها تشكل خياراً جيداً لزيادة النفاذية والامتصاص للأشعة الساقطة على الخلية الضوئية.

ويهدف هذا البحث بشكل رئيس إلى اقتراح نموذج مرشد موجي جديد من الخلايا الشمسية يحتوي غطاؤه على مواد اصطناعية (يسارية) (Metamaterials) قادرة على تقليل الانعكاس وتحسين كل من النفاذية والامتصاص لأشعة الشمس الساقطة على الخلايا الشمسية الأمر الذي يزيد من كفاءتها. البنية المقترحة من الغطاء المضاد للانعاكاس (ARC) يتكون من أربع طبقات (هواء و مادة اصطناعية (Metamaterial) و نيتريد السيلكون (SiN_x) بالإضافة إلى أرسينيد الجاليوم (GaAs) كطبقة تحتية). وقد تم هنا استخدام الطرق النظرية والرياضية كالشروط الحدية (boundary conditions) و مصفوفة التحويل (Transfer Matrix) بالإضافة لمعادلات فرينيل (Fresnel's equations) من أجل حساب قيم الانعكاس والنفاذية بالإضافة للامتصاص وتحديد القيم المثلى لمعاملات كل طبقة كالسماحية الكهربائية (ε) والنفاذية المغناطيسية (μ) والسمك ويضاف إلى ذلك زاوية السقوط. استخدم برنامج محوسب (Maple 13) من أجل إجراء الحسابات ورسم الأشكال البيانية.

ولقد خلصت الدراسة إلى أن النفاذية والامتصاص يصلان إلى قيمة عظمى تحت ظروف معينة عندما يتم استخدام ذلك الغطاء العاكس المقترح في الخلايا الشمسية المصنوعة من أرسينيد الجاليوم (GaAs).

Dedication

To the fountain of patience, support and love

father and mother

To my wife

To my beloved son, Adam

To my brothers, sisters and family

To my homeland Palestine.

I dedicate this work

Samer J. Abu Lebda

Acknowledgment

Gratitude to Allah who guided me to complete this work and helped me throughout the path of knowledge.

I'd like to express my profound gratitude to my supervisor Prof. Dr. Mohammed M. Shabat, for his useful comments, remarks and guidance throughout this work.

I'd like also to thank Dr. Mazen M. Alabadla for his cooperation and comments in several aspects throughout this work.

My appreciation goes also to the members of Physics Department in the Islamic University of Gaza for their willingness to help whenever I asked.

Finally, I'm very grateful to all my friends and relatives, especially my parents and wife for their patience, support and encouragement.

Table of Contents

List of Figures

List of Abbreviations

ARC	Anti-Reflection Coating
FDTD	Finite Difference Time Domain
GaAs	Gallium Arsenide
LHM	Left Handed Material
PV	Photovoltaic
RHM	Right Handed Material
SiN_x	Silicon Nitride
TCL	Transparent Conductive Layer
TE	Transfer Electric Field
TM	Transfer Magnetic Field

Preface

Since the last few decades, solar energy has been taking a large space of researches due to its advantages with respect to the none-renewable energy. One of the most important ways to generate electricity from the solar energy is the use of solar cells, which runs under photovoltaic effect and gives an electric current (Zeman, 2003; Nelson, 2003; Crabtree and Lewis, 2007). All research activities are looking to increase its efficiency with several ways such as using texturing surface, nanostructure and Anti-Reflection Coatings (ARCs) (Yu and Chen, 2008; Al-Turk, 2011; Hashmi and Rafique, 2013; El-Amassi, El-Khozondar, and Shabat, 2015).

ARCs consist of different numbers of layers and several types of materials. One of the most important materials that are used as a medium of light trapping is metamaterial, which is characterized by unusual properties arising from the electric permittivity (ε), magnetic permeability (μ) and refractive index all being simultaneously negative (Markoš and Soukoulis, 2008; Smith and Kroll, 2000).

The proposed structure of the ARC consists of 4-layers. The first layer is air, the second is a metamaterial layer, the third is silicon nitride (SiN_x) and the last layer is Gallium Arsenide (GaAs) as a substrate. Transfer matrix method is used to analyze the optical properties of the ARC as transmission, absorption and reflection. With the aid of Maple 13 program, suitable cods have been developed to solve and plot the behavior of transmission, reflection and absorption with several variables.

This work consists of five chapters. In chapter one, the solar cells and metamaterials will be introduced. Chapter two is devoted to theoretical basis of the work, where the transfer matrix approach, Fresnel equations and boundary conditions in both TE and TM cases are being applied. The third chapter deals with the numerical results, charts and discussions of reflection and transmission for the proposed ARC in TE and TM cases and their average as well. The fourth chapter discusses the absorption for the same ARC structures dealt with in chapter 3 after changing places of the second and the third layers. Finally, conclusion remarks are included in chapter five.

Chapter 1

Introduction

Chapter 1

Introduction

1.1 Solar Energy

A long time ago, solar energy attracted the world's interest because of its various advantages such as renewability, environmental friendship and being alternative to oil and fossil fuels, where the demand is growing for them, as shown in Figure (1.1)

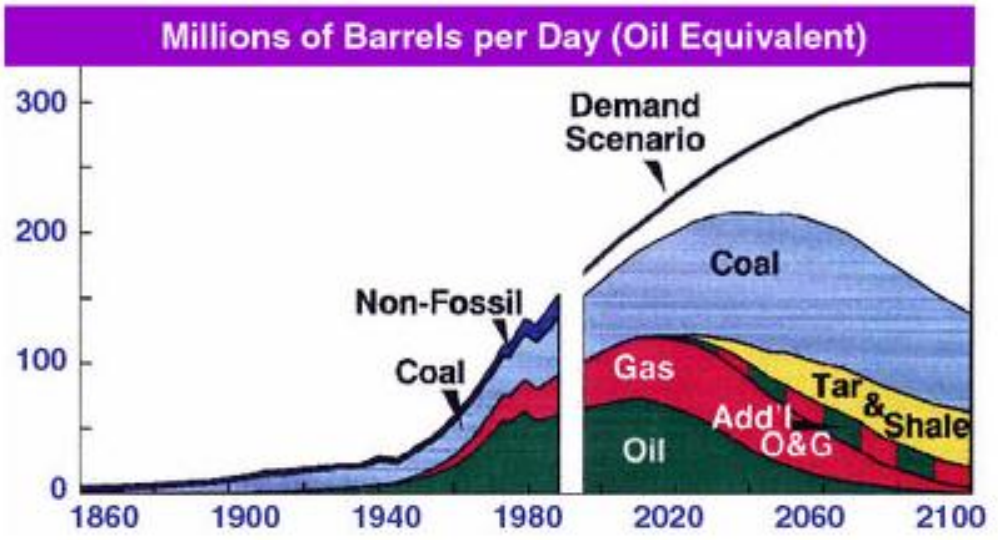

Figure (1.1): Historical and projected view of supply and demand of energy (Al-Turk, 2011).

The sun provides us with about 1.2×10^5 TW per hour continuously while the world consumes about 13 TW. This means the sun delivers about 10000 times more than the present energy consumption. The energy delivered to Earth from the sun in just one hour is equal to the total energy consumed in one year (Zeman, 2003; Crabtree and Lewis, 2007; Al-Turk, 2011). However, there are difficulties facing good exploitation of that power such as its dispersion, the large plate areas to absorb radiation and the cost of the necessary equipment to deal with it.

Solar energy is the radiant light and heat from the sun which man has always been trying to control by using a range of ever evolving technologies such as solar heating, solar cells and solar thermal electricity.

Solar cells are p-n junction devices which convert photon energy into electrical power by using photovoltaic effect (Zeman, 2003; Al-Turk, 2011).

The basic parts of a solar cell are semiconductor layers since the solar cells depend on the absorption of sun photons and supply them to charge carriers within the semiconductor materials. Silicon is a perfect example of semiconductor where it is using to build typical solar cells. Figure (1.2) represents the structure of a solar cell. The p-n junction consists of an absorber material moderately doped p-type wafer, the top layer is doped to be n^+-type and in bottom p^+-type. The n^+-type layer is often a shiny reflective material in order to send photons bouncing away before they enter the p^+-type layer.

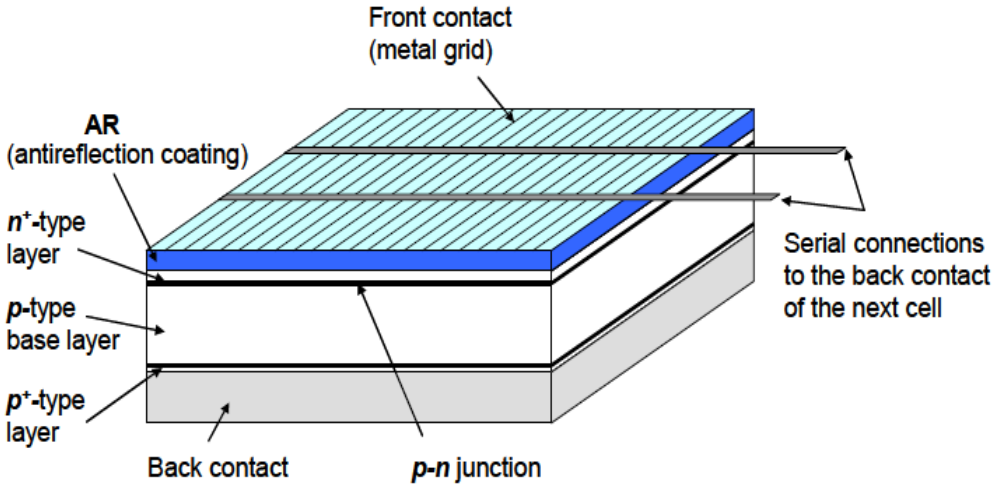

Figure (1.2): Basic structure of a solar cell (Zeman, 2003).

Solar cells also consist of metallic grid which is put on a top and bottom to collect the charge carriers and represent the part that connect with load (Zeman, 2003; Hashmi and Rafique, 2013). As a way to trapping light, Anti-Reflection Coating (ARC) covers the cell which decreases the reflection of light. There are some other techniques of light trapping such as (Al-Turk, 2011):

1- Surface texturing of silicon.

2- Using structural components on the nano scale where called (Nanostructures).

3- Transparent conductive layers (TCL).

The structure of solar cells in the end is covered by glass or other transparent materials to protect the cell from the environmental effects.

Photovoltaic effect is the generation of potential difference at the p-n junction of two material by visible or any electromagnetic waves (Zeman, 2003). If the incident photon on the cell hold energy greater than the band gab "the difference potential between the conducting band and valance band in the semiconductor" the electron is excited to higher energy states and moved to conduction band and leave hole behind it in the valance band, these electrons from the n^+-type layer and holes from p^+-type layer diffuse across the junction through the depletion region and that's gives electrical current (Nelson, 2003; Al-Turk, 2011).

1.2 Metamaterials

The types of materials can be characterize by permittivity (ε) and permeability (μ) as the following (Ubeid, Shabat, and Sid-Ahmed, 2013, a):

1- Materials with $\varepsilon > 0$ and $\mu > 0$, gives regular materials called RHMs due to satisfying the right hand rule to determine the directions for the electric field (E), the magnetic field (H) and the wave propagation (k). These materials allow forward propagation with positive refractive index like dielectrics.

2- Materials with $\varepsilon < 0$ and $\mu > 0$, like metals.

3- Materials with $\varepsilon > 0$ and $\mu < 0$, like ferrites.

For both the second and the third materials, evanescent waves appear when electromagnetic waves propagate inside them.

4- Materials with $\varepsilon < 0$ and $\mu < 0$ which are called Metamaterial or left handed materials (LHMs) because of using the left hand rule to determine the directions for the electric field (E), the magnetic field (H) and the wave propagation (k). LHMs also have negative refractive index with backward propagation so that these materials are sometimes referred to as negative index materials, they are also called metamaterials due to the unusual properties.

Figure (1.3) explains the four types of materials, based on the electric permittivity (ε) and magnetic permeability (μ).

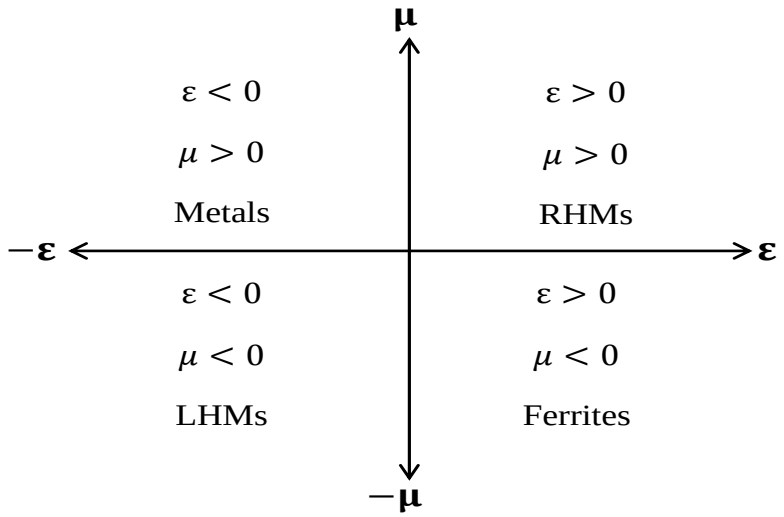

Figure (1.3): Types of materials which depending on the sign of electric permittivity (ε) and magnetic permeability (μ), after (Ubeid et al., 2013, a).

1.2.1 Definition of Metamaterials

Metamaterials or Left-Handed Materials (LHMs) are artificial effectively homogeneous electromagnetic structures, where its electromagnetic properties differ qualitatively from the conventional materials, dielectric or metal and not readily available in nature.

Metamaterials became well-known because of the negativity of both permittivity (ε) and permeability (μ) that gives antiparallel orientation of the wave vector ($\vec{k}$) and the Poynting vector ($\vec{S}$).

1.2.2 History of Metamaterials

In the last few years, Metamaterials had been considered in the scientific community due to the unusual properties. LHMs historically introduced theoretically by Veselago (Veselago, 1968), when he analyzed the propagation of plane waves in a materials having negative permittivity and permeability. Pendry et al. (Pendry, Holden, Stewart, and Youngs, 1996) suggested the artificial periodic wire, where the negative permittivity appears, then the split-rings model was presented, where the negative permeability appears (Pendry, Holden, Robbins, and Stewart, 1998).

In 2000, smith et al. (Smith and Kroll, 2000; Smith, Padilla, Vier, Nemat-Nasser, and Schultz, 2000) constructed the LHM using the combination of split-rings and periodic wires. They prepared several microwave experiments to find the properties of this material. After one year, Shelby et al. (Shelby, Smith, and Schultz, 2001) attained the first experimental investigation of negative index of refraction on the LHMs at microwave frequencies.

Kong (Kong, 2002) studied the electromagnetic waves interaction with stratified LHMs isotropic media. He studded the transmission and reflection waves, field solution of guided waves and linear dipole antennas in stratified structure of LHMs.

Engheta (Engheta, 2003) discussed some of electromagnetic properties of LHM, physics remark and the probably future applications.

Chew (Chew, 2005) had investigated the reflection on the LHM and the LHM energy conservation property.

Sabah et al. (Sabah, Ogucu, and Uckun, 2006; Sabah and Uckun, 2007) used transfer matrix method to determine the reflection and transmission powers due to the interaction of electromagnetic waves with a double slab of metamaterials.

Cory and Zach (Cory and Zach, 2004) carried out the analysis of the reflection and transmission in multilayer structures containing Metamaterials and dielectric slaps.

Several researches were done by Ubeid and Shabat and others to determine the propagation through Metamaterials, reflection and transmission through it and other properties (Oraizi and Abdolali, 2009; Ubeid, Shabat, and Sid-Ahmed, 2011; Ubeid, Shabat, and Sid-Ahmed, 2012, a; Ubeid, Shabat, and Sid-Ahmed, 2012, b; Ubeid et al., 2013, a; Ubeid, Shabat, and Sid-Ahmed, 2013, b; Shabat and Ubeid, 2014).

1.2.3 Properties of Metamaterials

1.2.3.1 Maxwell's Equations and Left Handed Rule

Wave propagation through any media based on the Maxwell's equations are given as:

$$\vec{\nabla} \times \vec{E} = -\frac{\partial \vec{B}}{\partial t} \quad (1.1)$$

$$\vec{\nabla} \times \vec{H} = \frac{\partial \vec{D}}{\partial t} + \vec{j} \quad (1.2)$$

$$\vec{\nabla} . \vec{D} = \rho \quad (1.3)$$

$$\vec{\nabla} . \vec{B} = 0 \quad (1.4)$$

Where $\vec{E}$ and $\vec{H}$ are the electric field (V/m) and magnetic field (A/m), respectively. The quantities $\vec{D}$ and $\vec{B}$ are electric flux density (C/m^2) and magnetic flux density (T), respectively. The quantities ρ and $\vec{j}$ are electric charge density (C/m^3) and current density (A/m^2); respectively (Jackson, 1999).

The material response to external electric and magnetic fields characterized by electric permittivity ε and the magnetic permeability μ, where:

$$\vec{D} = \varepsilon \vec{E} \quad (1.5)$$

$$\vec{B} = \mu \vec{H} \quad (1.6)$$

For a plane wave, the electric and magnetic fields can be expressed as:

$$\vec{E}(r, t) = \vec{E}_0 e^{i(\vec{k}.\vec{r} - \omega t)} \quad (1.7)$$

$$\vec{H}(r, t) = \vec{H}_0 e^{i(\vec{k}.\vec{r} - \omega t)} \quad (1.8)$$

Where ω is the frequency of the field, $\vec{k}$ is the wave vector, $\vec{E}_0$ and $\vec{H}_0$ are amplitude and the direction of the vector $\vec{E}$ and $\vec{H}$; respectively (Markoš and Soukoulis, 2008). For dielectric materials without free charges and no currents, $\rho = 0$ and $\vec{j} = 0$ (Jackson, 1999).

Based on of the above definitions Maxwell's equations can be written as (Kong, 2002):

$$\vec{k} \times \vec{E} = \omega \mu \vec{H} \quad (1.9)$$

$$\vec{k} \times \vec{H} = -\omega \varepsilon \vec{E} \quad (1.10)$$

$$\vec{k} . \vec{E} = 0 \quad (1.11)$$

$$\vec{k} . \vec{H} = 0 \quad (1.12)$$

In RHMs the vectors $\vec{E}, \vec{H}$ and $\vec{k}$ follow the right handed rule of vector and the Poyniting vector $\vec{S} /\!/ \vec{k}$. Due to $\varepsilon, \mu < 0$ for LHMs Maxwell's equations became:

$$\vec{k} \times \vec{E} = -\omega|\mu|\vec{H} \tag{1.13}$$

$$\vec{k} \times \vec{H} = \omega|\varepsilon|\vec{E} \tag{1.14}$$

This gives left-handed rule of vectors $\vec{E}$, $\vec{H}$ and $\vec{k}$; hence the name LHM. Also vectors $\vec{k}$ and $\vec{S}$ have opposite orientations (Al-Turk, 2011), as shown in Figure (1.4).

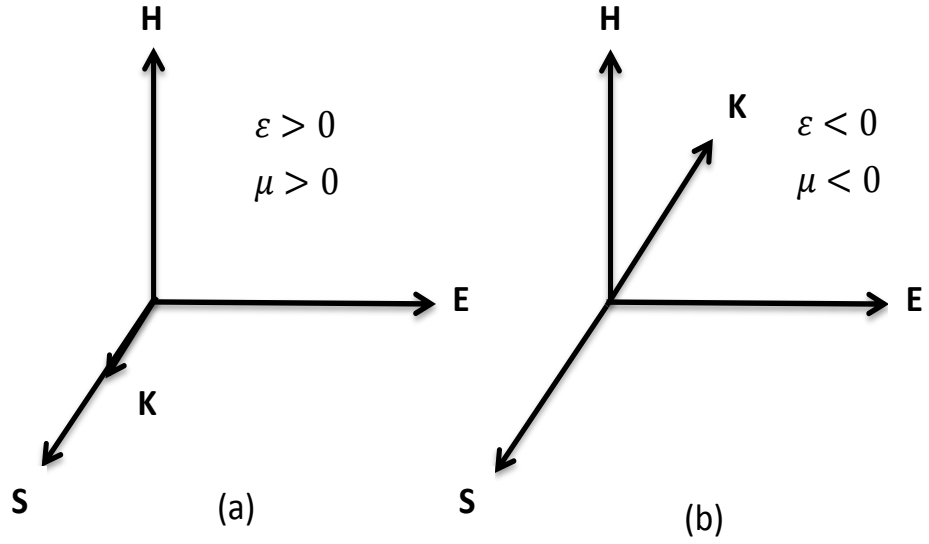

Figure (1.4): Orientation of the electric field ($\vec{E}$), magnetic field ($\vec{H}$), wave vector ($\vec{k}$) and Poynting vector ($\vec{S}$), (a) RHM and (b) LHM, after (Markoš and Soukoulis, 2008).

Note that, for LHMs the direction of the propagation of the electromagnetic waves is determined by the orientation of the Poynting vector $\vec{S}$. The opposite sign of $\vec{k}$ only means that the phase velocity of the wave inside the medium is negative (Markoš and Soukoulis, 2008; Reza, 2008).

1.2.3.2 Poynting Vector

Poynting vector is the cross product of the electric and magnetic fields, and represents the time rate of flow of the electromagnetic energy per unit area, it also gives the direction of energy propagation. The Poynting vector is still following the right hand rule for all materials including LHMs in the direction of energy

propagation from the relation (Markoš and Soukoulis, 2008; Ubeid et al., 2013, a; Xiong and Sha, 2013):

$$\vec{S} = \vec{E} \times \vec{H} \tag{1.15}$$

Where $\vec{S}$ is the Poynting vector (W/m^2).

Poynting vector takes a real value due to the physical meaning of energy so it can be written as:

$$\vec{S} = \mathrm{Re}\{\vec{E} \times \vec{H}^*\} \tag{1.16}$$

For plane waves given in equations (1.7) and (1.8) and by using Maxwell's equations (1.13) and (1.14) through (1.6) we can obtain:

$$S = \frac{1}{2\mu_0\omega}\mathrm{Re}\left\{\frac{k}{\mu}\right\}|E|^2 = \frac{1}{2\varepsilon_0\omega}\mathrm{Re}\left\{\frac{k}{\varepsilon}\right\}|H|^2 \tag{1.17}$$

Where ε_0 and μ_0 are the electric permittivity and the magnetic permeability in the air.

1.2.3.3 Refractive Index and Snell's Law

One of the unusual properties of LHMs is the negative-index of refraction, there are several experimental and theoretical studies to prove that e.g. (Smith and Kroll, 2000; Shelby, Smith and Schultz, 2001).

In a simple proof for this, we start with wave number k in the case of an isotropic substance which is given by:

$$k = n\omega/c \tag{1.18}$$

where n is refractive index of the substance that is given by:

$$n = c/v = \pm\sqrt{\varepsilon\mu} \tag{1.19}$$

where c: speed of light in vacuum, v: speed of light in medium.

Since k has negative sign for LHMs, from (1.18) we can obtain that refractive index must be negative also. So we have now $k < 0$, $\varepsilon < 0$, $\mu < 0$ and $n < 0$ for LHMs.

For Snell's law which appears when the light transmit through the interface between two different media and takes the form:

$$n_1 \sin\theta_1 = n_2 \sin\theta_2 \qquad (1.\ 20)$$

If the refraction occurs at the interface between two media one of them LHM, Snell's law does not change, but we will get negative refractive angle (i.e. $\theta_2 < 0$) due to the negative refractive index of the LHM (Al-Turk, 2011), as in Figure (1.5).

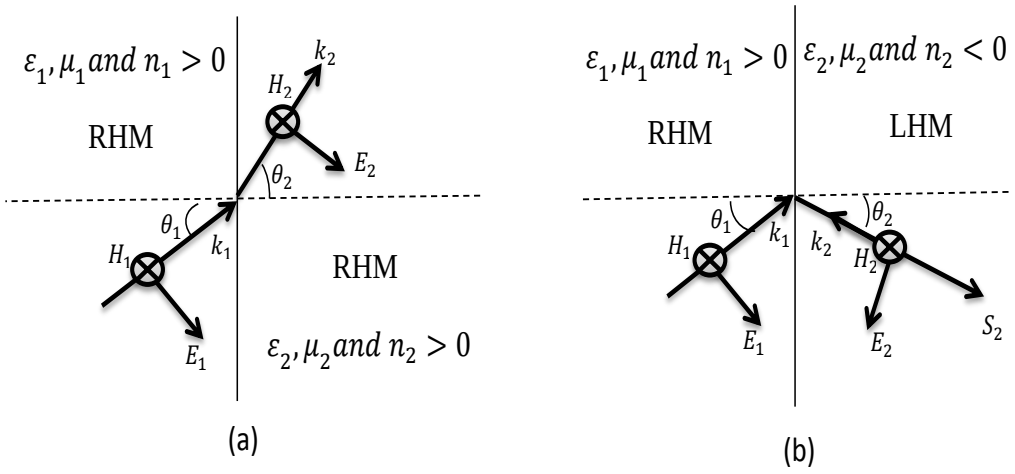

Figure (1.5): Refraction of electromagnetic plane wave on the interface between: (a) two RHM materials with positive refraction, (b) two materials one of them LHM with negative refraction (the wave propagates in the direction of negative angle).

There are another properties of Metamaterials such as reversal of Doppler effect and focusing see (Veselago, 1968; Smith et al., 2000; Markoš and Soukoulis, 2008; Reza, 2008).

Chapter 2

Theory

Chapter 2

Theory

2.1 Introduction

When a beam of light falls on a transparent material, it will be divided into three parts: one part reflects back, another transmits into the material and the third is absorbed by the material. Accordingly; the reflectance (R), transmittance (T) and absorbance (A) are determined. There are several ways to determine these quantities such as the Round Method (Heavens, 1991), Finite Difference Time Domain (FDTD) (Xiong and Sha, 2013) and Transfer Matrix Method (Heavens, 1991; Pedrotti F. L. and Pedrotti L. S., 1993; Macleod, 2001; Markoš and Soukoulis, 2008). In this chapter, we adopt the Transfer Matrix Method and its application in Transfer Magnetic Field (TM) and Transfer Electric Field (TE) polarizations to discuss the theoretical analysis of light through material and determine R,T and A.

2.2 Matrix Method

The analysis of the wave propagation of light through multilayer films requires mathematical approach. In this thesis, the matrix treatment commonly known as Transfer Matrix Method is used to study the proposed structures.

Figure (2.1) shows the scattering of incident waves on one dimensional sample. Scattering means that the wave is either reflecting back or transmitting through the sample. The transmission (T) and reflection (R) can be determined through the Transfer Matrix (Heavens, 1991; Pedrotti F. L. and Pedrotti L. S., 1993; Macleod, 2001; Goodman, 2005; Markoš and Soukoulis, 2008; Al-Turk, 2011).

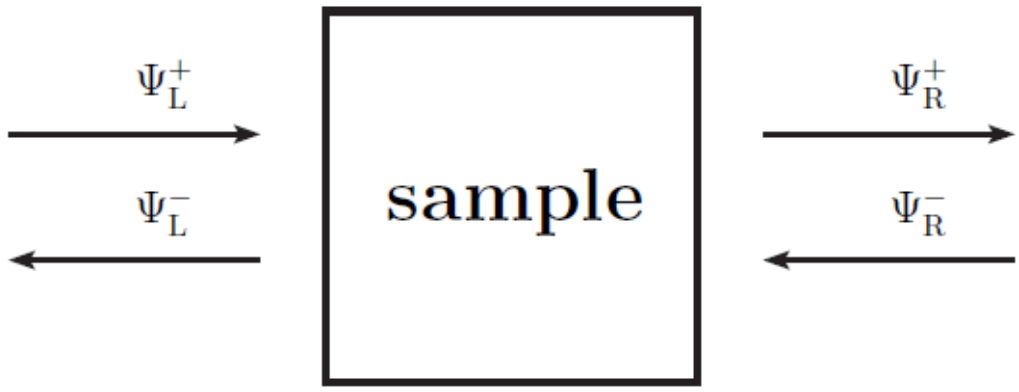

Figure (2.1): A scattering experiment for a wave through a sample. Ψ_L^+ and Ψ_R^- are incoming waves, Ψ_L^- and Ψ_R^+ are outgoing waves (Markoš and Soukoulis, 2008).

Equation (2.1) relates the waves amplitude of the right side of the sample in terms of the waves on the left side as:

$$\begin{bmatrix} \Psi_R^+ \\ \Psi_R^- \end{bmatrix} = M \begin{bmatrix} \Psi_L^+ \\ \Psi_L^- \end{bmatrix} \tag{2.1}$$

where M is the transfer matrix.

Transfer Matrix (M) is a matrix that solves the wave function on the right hand side of the sample (the layer) in terms of the wave function on the left hand side and takes the formula (Markoš and Soukoulis, 2008):

$$M = \begin{bmatrix} m_{11} & m_{12} \\ m_{21} & m_{22} \end{bmatrix} \tag{2.2}$$

2.3 Properties of Transfer Matrix

The transfer matrix has some properties as multiplication of transfer matrix, bound states, propagation states and others. In this section we present multiplication of transfer matrix that we will need it (Pedrotti F. L. and Pedrotti L. S., 1993; Macleod, 2001; Markoš and Soukoulis, 2008).

Consider a wave scattered by two samples as shown in Figure (2.2). The study of transmission and reflection can be taken by two steps:

a- Using the transfer matrices M_1 and M_2, which determine the scattering properties of each sample alone.

b- Using the transfer matrix M_{12}.

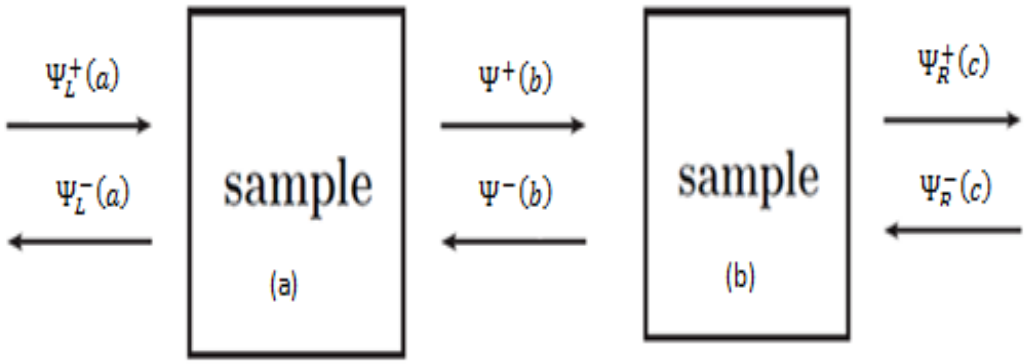

Figure (2.2): A scattering experiment on two sample (a) and (b).

Through the definition of transfer matrix M given by equation (2.1), we get:

$$\begin{bmatrix}\Psi_L^+(a)\\ \Psi_L^-(a)\end{bmatrix} = M_1 \begin{bmatrix}\Psi^+(b)\\ \Psi^-(b)\end{bmatrix} \tag{2.3}$$

And

$$\begin{bmatrix}\Psi^+(b)\\ \Psi^-(b)\end{bmatrix} = M_2 \begin{bmatrix}\Psi_R^+(c)\\ \Psi_R^-(c)\end{bmatrix} \tag{2.4}$$

Substituting equation (2.4) into equation (2.3), we get:

$$\begin{bmatrix}\Psi_L^+(a)\\ \Psi_L^-(a)\end{bmatrix} = M_1 M_2 \begin{bmatrix}\Psi_R^+(c)\\ \Psi_R^-(c)\end{bmatrix} \tag{2.5}$$

Which can be written as:

$$\begin{bmatrix}\Psi_L^+(a)\\ \Psi_L^-(a)\end{bmatrix} = M_{12} \begin{bmatrix}\Psi_R^+(c)\\ \Psi_R^-(c)\end{bmatrix} \tag{2.6}$$

where

$$M_{12} = M_1 M_2 \tag{2.7}$$

In general, for multilayers of N layer (sample) each layer is associated with its own transfer matrix that's give:

$$\begin{bmatrix}\Psi_L^+\\ \Psi_L^-\end{bmatrix} = M_1 M_2 \dots M_{N-1} M_N \begin{bmatrix}\Psi_R^+\\ \Psi_R^-\end{bmatrix} \tag{2.8}$$

2.4 Reflection

When a beam of light is incident on the boundary between two materials, a part of its energy is reflected back into the first medium and the rest is transmitted into the second. The reflected and transmitted quantities depend on (Al-Turk, 2011):

1- The polarization of the incident light;

2- The thickness of each layer of coating;

3- Differences in the refractive index of the media;

4- The angle of incidence upon the boundary.

The polarization of the oblique incidence of light can take two forms, the first is p-polarization (TM) and the second is s-polarization (TE). In this section, we introduce both polarizations separately to determine the transmission and the reflection amplitudes for the two polarizations through Fresnel equation and boundary condition for wave at interface as the derivation in (Pedrotti F. L. and Pedrotti L. S., 1993; Smith and Kroll, 2000; Macleod, 2001; Yeh and Shimabukuro, 2008; Al-Turk, 2011).

2.4.1 Fresnel Equation and Boundary Condition for TE Polarization

TE polarization (s-polarization) means that the electric field $\vec{E}$ is parallel to the interface and the magnetic field $\vec{H}$ lies in the plane of incidence, i.e.: $\vec{E} = (0, E_y, 0)$has one component and $\vec{H} = (H_x, 0, H_z)$ has two components, as shown in Figure (2.3).

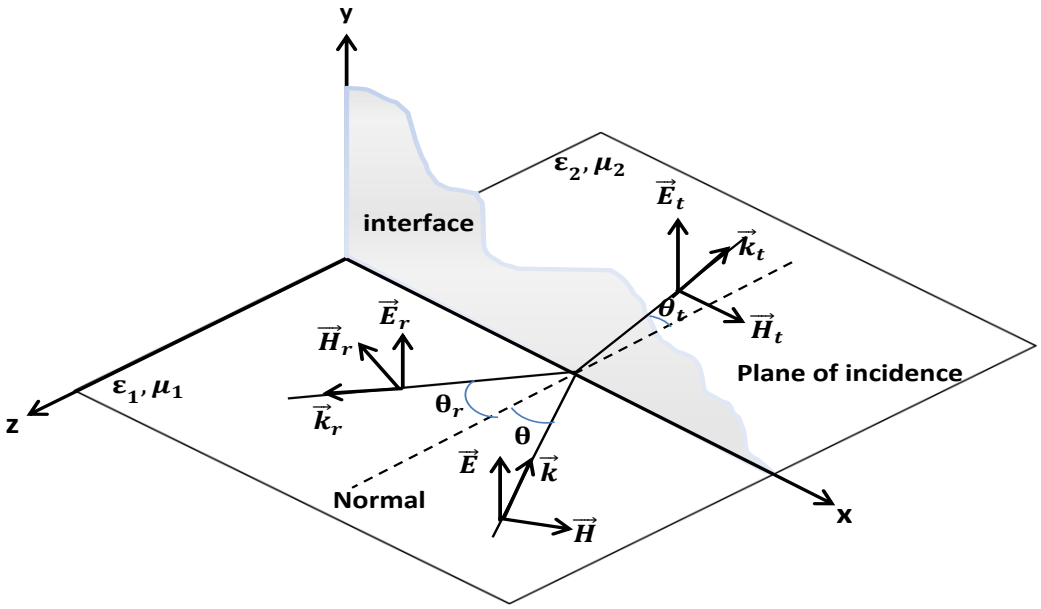

Figure (2.3): Light incident on the interface between two media for TE polarization.

Figure (2.3) shows an incident, reflected and transmitted waves on the interface between two media, where the waves satisfy the definition of the TE polarization. The x-y plane is called boundary interface and the x-z plane is called the plane of incidence. Applying boundary conditions at the interface for parallel electric field and the parallel components of magnetic field which must be continuous at both sides of the interface (Pedrotti F. L. and Pedrotti L. S., 1993; Al-Turk, 2011) we get:

$$E + E_r = E_t \tag{2.9}$$

where $E, E_r \; and \; E_t$ are the amplitudes of incident, reflected and transmitted electric fields; respectively.

$$H_x - H_{rx} = H_{tx} \tag{2.10}$$

Using Maxwell's equation, given by equation (1.9)

$$\vec{k} \times \vec{E} = \mu\omega\vec{H}$$

to express the magnetic field $\vec{H}$ in eq. (2.10) in terms of $\vec{E}$:

$$k_{1z}\mathrm{E} = \mu_1\omega H_x \,, \quad k_{1z}\mathrm{E}_r = \mu_1\omega H_{rx} \,, \quad k_{2z}\mathrm{E}_t = \mu_2\omega H_{tx} \tag{2.11}$$

where $\mathrm{k_{1z}} = \mathrm{k_1}\cos\theta$ and $\mathrm{k_{2z}} = \mathrm{k_2}\cos\theta_\mathrm{t}$ and they represent the normal components of the wave vectors.

Inserting equation (2.11) in the equation of the boundary condition (2.10), we obtain:

$$\frac{k_{1z}}{\mu_1\omega}E - \frac{k_{1z}}{\mu_1\omega}E_r = \frac{k_{2z}}{\mu_2\omega}E_t \tag{2.12}$$

Substitution for E_t from equation (2.9) in equation (2.12):

$$\frac{k_{1z}}{\mu_1}E - \frac{k_{1z}}{\mu_1}E_r = \frac{k_{2z}}{\mu_2}(E + E_r) \tag{2.13}$$

Upon rearranging the above equation, we get:

$$E(\frac{k_{1z}}{\mu_1} - \frac{k_{2z}}{\mu_2}) = E_r(\frac{k_{1z}}{\mu_1} + \frac{k_{2z}}{\mu_2}) \tag{2.14}$$

The reflection amplitude for the electric field can be written as:

$$r_s = \frac{E_r}{E} = \frac{\frac{k_{1z}}{\mu_1} - \frac{k_{2z}}{\mu_2}}{\frac{k_{1z}}{\mu_1} + \frac{k_{2z}}{\mu_2}} \tag{2.15}$$

$$r_s = \frac{\mu_2 k_{1z} - \mu_1 k_{2z}}{\mu_2 k_{1z} + \mu_1 k_{2z}} \tag{2.16}$$

Similarly, we can obtain the transmission amplitude from the relation:

$$t_s = \frac{E_t}{E} = \frac{2\mu_2 k_{1z}}{\mu_2 k_{1z} + \mu_1 k_{2z}} \tag{2.17}$$

Equations (2.15) and (2.17) are called Fresnel equations.

Fresnel equations are equations that determine the reflection and transmission amplitudes by taking the ratio of both reflected and transmitted E-field amplitudes to incident E-field amplitude and it can be determined by taking H-field amplitude instead of E-field amplitude (Pedrotti F. L. and Pedrotti L. S., 1993; Markoš and Soukoulis, 2008; Yeh and Shimabukuro, 2008).

2.4.2 Fresnel Equation and Boundary Condition for TM Polarization

TM polarization (p-polarization) means that the magnetic field $\vec{H}$ is parallel to the interface and the electric field lies in the plane of incidence, i.e.: $\vec{H} = (0, H_y, 0)$ has one component and $\vec{E} = (E_x, 0, E_z)$ has two components, as shown in Figure (2.4).

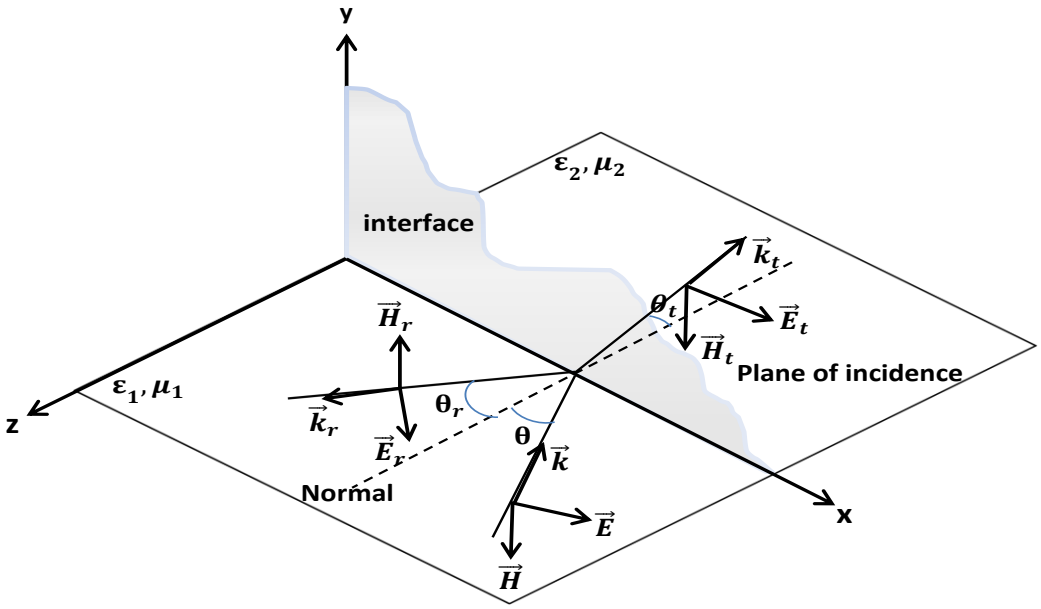

Figure (2.4): Light incident on the interface between two media for TM polarization.

Figure (2.4) demonstrates an incident, reflected and transmitted waves on the interface between two media, where the waves satisfy the definition of the TM polarization. Applying the boundary conditions at the interface for parallel magnetic field and the parallel components of electric field which must be continuous at both sides of the interface (Pedrotti F. L. and Pedrotti L. S., 1993; Al-Turk, 2011) we get:

$$-H + H_r = -H_t \tag{2.18}$$

where $H, H_r \; and \; H_t$ are the amplitudes of incident, reflected and transmitted magnetic field; respectively.

$$E_x + E_{rx} = E_{tx} \tag{2.19}$$

Using the Maxwell's equation, given by equation (1.10)

$$\vec{k} \times \vec{H} = -\varepsilon\omega\vec{E}$$

to express the electric field $\vec{E}$ in eq. (2.19) in terms of $\vec{H}$:

$$k_{1z}\mathrm{H} = \varepsilon_1\omega E_x, \quad k_{1z}\mathrm{H}_r = \varepsilon_1\omega E_{rx}\,, \quad k_{2z}\mathrm{H}_t = \varepsilon_2\omega E_{tx} \tag{2.20}$$

Inserting (2.10) in the equation of boundary condition (2.19), we obtain:

$$\frac{k_{1z}}{\varepsilon_1\omega}\mathrm{H} + \frac{k_{1z}}{\varepsilon_1\omega}H_r = \frac{k_{2z}}{\varepsilon_2\omega}H_t \tag{2.21}$$

If one substitutes for H_t from equation (2.18) in equation (2.21) then:

$$\frac{k_{1z}}{\varepsilon_1}\mathrm{H} + \frac{k_{1z}}{\varepsilon_1}H_r = \frac{k_{2z}}{\varepsilon_2}(H - H_r) \tag{2.22}$$

Rearranging the last equation gives:

$$H\left(\frac{k_{2z}}{\varepsilon_2} - \frac{k_{1z}}{\varepsilon_1}\right) = H_r\left(\frac{k_{1z}}{\varepsilon_1} + \frac{k_{2z}}{\varepsilon_2}\right) \tag{2.23}$$

Applying Fresnel equations to determine reflection amplitude for the magnetic field as:

$$r_p = \frac{H_r}{H} = \frac{\frac{k_{2z}}{\varepsilon_2} - \frac{k_{1z}}{\varepsilon_1}}{\frac{k_{1z}}{\varepsilon_1} + \frac{k_{2z}}{\varepsilon_2}} \tag{2.24}$$

$$r_p = \frac{\epsilon_1 k_{2z} - \epsilon_2 k_{1z}}{\epsilon_2 k_{1z} + \epsilon_1 k_{2z}} \tag{2.25}$$

Using the same way, the transmission amplitude can be calculated from the relation:

$$t_p = \frac{H_t}{H} = \frac{2\epsilon_2 k_{1z}}{\epsilon_2 k_{1z} + \epsilon_1 k_{2z}} \tag{2.26}$$

2.5 Reflection and Transmission in TE Polarization Using the Transfer Matrix Method

To calculate reflection and transmission coefficients in more than one layer we have a long mathematical way to do that. Using the transfer matrix method, this manipulation is highly abbreviated. This section explains the calculation of both reflection and transmission coefficients in TE polarization ($R_s \; and \; T_s$) through transfer matrix method.

If we have a homogenous thin film with thickness L on a substrate as shown in Figure 2.6, where a beam of light is scattering at the film, there are two reflections that happen, the first on the interface (1) between the air and the film and the second on the interface (2) between the film and the substrate.

The variables in Figure (2.5) represent the following: E_0 and E_{r1} are the collection of the incoming and the reflecting beams; respectively on the interface (1) from the left in the air. E_{t1} and E_{i1} are the collections of the transmitting and incident beams; respectively on the interface (1) from the right in the film. E_{i2} and E_{r2} are the collections of the incident and the reflecting beams; respectively on the interface (2)

from the left in the film. E_t is the collection of the transmitting (outgoing) beams on the interface (2) from the right in the substrate.

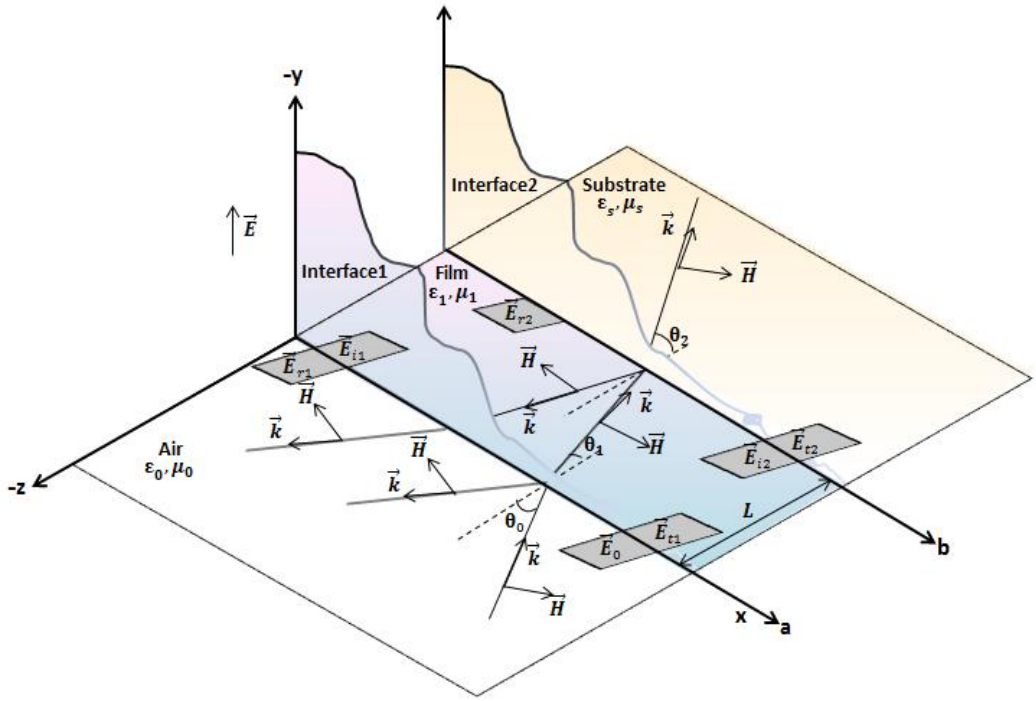

Figure (2.5): Light incident on a thin film on a substrate, for TE polarization.

Applying the boundary conditions for the parallel electric field and the parallel components of magnetic field, which must be continuous at each boundary, we get:

$$E_a = E_0 + E_{r1} = E_{t1} + E_{i1} \tag{2.27}$$

$$E_b = E_{i2} + E_{r2} = E_{t2} \tag{2.28}$$

$$H_a = H_{0x} - H_{rx1} = H_{tx1} - H_{ix1} \tag{2.29}$$

$$H_b = H_{ix2} - H_{rx2} = H_{tx2} \tag{2.30}$$

Using Maxwell's equation, given by equation (1.9):

$$\vec{k} \times \vec{E} = \mu\omega\vec{H}$$

which give: $H_{0x} = \frac{k_{0z}}{\omega\mu_0} E_0$, $H_{rx1} = \frac{k_{0z}}{\omega\mu_0} E_{r1}$, $H_{tx1} = \frac{k_{1z}}{\omega\mu_1} E_{t1}$, $H_{ix1} = \frac{k_{1z}}{\omega\mu_1} E_{i1}$,

$H_{ix2} = \frac{k_{1z}}{\omega\mu_1} E_{i2}$, $H_{rx2} = \frac{k_{1z}}{\omega\mu_1} E_{r2}$ and $H_{tx2} = \frac{k_{sz}}{\omega\mu_s} E_{t2}$

then substitution for the magnetic field $\vec{H}$ in equations (2.29) and (2.30) in terms of $\vec{E}$, we obtain:

$$H_a^* = \frac{k_{0z}}{\mu_0}(E_0 - E_{r1}) = \frac{k_{1z}}{\mu_1}(E_{t1} - E_{i1}) \tag{2.31}$$

$$H_b^* = \frac{k_{1z}}{\mu_1}(E_{i2} - E_{r2}) = \frac{k_{sz}}{\mu_s}E_{t2} \tag{2.32}$$

where $H_b^* = \omega H_b$, $H_a^* = \omega H_a$.

We can write the electric field as:

$$E_{i2} = E_{t1}e^{-i\delta} \text{ and } E_{i1} = E_{r2}e^{-i\delta} \Rightarrow E_{r2} = E_{i1}e^{i\delta} \tag{2.33}$$

Where δ is the phase difference is given by (Pedrotti F. L. and Pedrotti L. S., 1993):

$$\delta = k_0\Delta_1 = \left(\frac{2\pi}{\lambda_0}\right)\sqrt{\mu_1\varepsilon_1}L\cos\theta_1 \tag{2.34}$$

Where $\Delta_1 = \sqrt{\mu_1\varepsilon_1}L\cos\theta_1$ is called the optical path difference.

Using equation (2.33) in equations (2.28) and (2.32) instead of E_{i2} and E_{r2} we get:

$$E_b = E_{t1}e^{-i\delta} + E_{i1}e^{i\delta} = E_{t2} \tag{2.35}$$

$$H_b^* = \frac{k_{1z}}{\mu_1}(E_{t1}e^{-i\delta} - E_{i1}e^{i\delta}) = \frac{k_{sz}}{\mu_s}E_{t2} \tag{2.36}$$

Solving E_{t1} and E_{i1} in terms of E_b and H_b^* we fined:

$$E_{t1} = \left(\frac{k_{1z}E_b + \mu_1 H_b^*}{2k_{1z}}\right)\mathrm{e}^{\mathrm{i}\delta} \tag{2.37}$$

$$E_{i1} = \left(\frac{k_{1z}E_b - \mu_1 H_b^*}{2k_{1z}}\right)\mathrm{e}^{-\mathrm{i}\delta} \tag{2.38}$$

Applying Euler formula $e^{\pm i\delta} = \cos\delta \pm i\sin\delta$ in equations (2.37) and (2.38) then substituting in equations (2.27) and (2.31) we get:

$$E_a = E_b \cos\delta + H_b^* \left(\frac{i\mu_1 \sin\delta}{k_{1z}} \right) \tag{2.39}$$

$$H_a^* = E_b (i \frac{k_{1z}}{\mu_1} \sin\delta) + H_b^* \cos\delta \tag{2.40}$$

The above equations can be written in the matrix form as:

$$\begin{bmatrix} E_a \\ H_a^* \end{bmatrix} = \begin{bmatrix} \cos\delta & \frac{\mathrm{i}\mu_1 \sin\delta}{k_{1z}} \\ i \frac{k_{1z}}{\mu_1} \sin\delta & \cos\delta \end{bmatrix} \begin{bmatrix} E_b \\ H_b^* \end{bmatrix} \tag{2.41}$$

where $$\begin{bmatrix} \cos\delta & \frac{\mathrm{i}\mu_1 \sin\delta}{k_{1z}} \\ i \frac{k_{1z}}{\mu_1} \sin\delta & \cos\delta \end{bmatrix} = \begin{bmatrix} \mathrm{m}_{11} & \mathrm{m}_{12} \\ \mathrm{m}_{21} & m_{22} \end{bmatrix}$$

is the transfer matrix in TE polarization for three layers (air, film and substrate), which represents the incoming wave in term of the outgoing wave.

To derive the reflection and transmission amplitudes, one takes the remaining parts in equations (2.27), (2.28), (2.31) and (2.32), we have:

$$E_a = E_0 + E_{r1} \tag{2.42}$$

$$E_b = E_{t2} \tag{2.43}$$

$$H_a^* = \frac{k_{0z}}{\mu_0} (E_0 - E_{r1}) \tag{2.44}$$

$$H_b^* = \frac{k_{sz}}{\mu_s} E_{t2} \tag{2.45}$$

Equations (2.42) to (2.45) can be substituted in equation (2.41) to give:

$$\begin{bmatrix} E_0 + E_{r1} \\ \frac{k_{0z}}{\mu_0} (E_0 - E_{r1}) \end{bmatrix} = \begin{bmatrix} m_{11} & m_{12} \\ m_{21} & m_{22} \end{bmatrix} \begin{bmatrix} E_{t2} \\ \frac{k_{sz}}{\mu_s} E_{t2} \end{bmatrix} \tag{2.46}$$

The equivalent equations to the matrix system (2.46) are:

$$E_0 + E_{r1} = m_{11}E_{t2} + m_{12}\frac{k_{sz}}{\mu_s}E_{t2} \tag{2.47}$$

$$\frac{k_{0z}}{\mu_0}(E_0 + E_{r1}) = m_{21}E_{t2} + m_{22}\frac{k_{sz}}{\mu_s}E_{t2} \tag{2.48}$$

Dividing equations (2.47) and (2.48) by E_0 and using the definition of Fresnel equations where reflection and transmission amplitudes can be calculated from the relations $r = E_{r1}/E_0$ and $t = E_{t2}/E_0$ respectively, we obtain:

$$1 + r = m_{11}t + m_{12}\frac{k_{sz}}{\mu_s}t \tag{2.49}$$

$$\frac{k_{0z}}{\mu_0}(1 - r) = m_{21}t + m_{22}\frac{k_{sz}}{\mu_s}t \tag{2.50}$$

The solution of equations (2.49) and (2.50) give the reflection and transmission amplitudes in TE polarization (r_s and t_s):

$$r_s = \frac{\frac{k_{0z}}{\mu_0}m_{11} + \frac{k_{0z}}{\mu_0}\frac{k_{sz}}{\mu_s}m_{12} - m_{21} - \frac{k_{sz}}{\mu_s}m_{22}}{\frac{k_{0z}}{\mu_0}m_{11} + \frac{k_{0z}}{\mu_0}\frac{k_{sz}}{\mu_s}m_{12} + m_{21} + \frac{k_{sz}}{\mu_s}m_{22}} \tag{2.51}$$

$$\mathrm{t_s} = \frac{2}{m_{11} + \frac{k_{sz}}{\mu_s}m_{12} + \frac{\mu_0}{k_{0z}}m_{21} + \frac{\mu_0}{k_{0z}}\frac{k_{sz}}{\mu_s}m_{22}} \tag{2.52}$$

The last two equations are used to determine the reflectance from the relation:

$$R_s = |r_s|^2 \tag{2.53}$$

And the transmittance from the relation:

$$T_s = \frac{S_t}{\mathrm{S_0}} \tag{2.54}$$

where the Poynting vectors S and S_t from equation (1.17) can be written as:

$$\mathrm{S_0} = \frac{1}{2\mu_0\omega}\mathrm{Re}\left\{\frac{\mathrm{k_{oz}}}{\mu_0}\right\}|E_0|^2 \tag{2.55}$$

$$S_t = \frac{1}{2\mu_0\omega}\mathrm{Re}\{\frac{k_{sz}}{\mu_s}\}|E_t|^2 \tag{2.56}$$

Inserting equations (2.55) and (2.56) into equation (2.54) we can obtain:

$$T_s = \mathrm{Re}\{\frac{k_{sz}\mu_0}{k_{oz}\mu_s}\}|t_s|^2 \tag{2.57}$$

Note that: the addition of equations (2.53) and (2.57) must equal 1 in the case with zero absorption, that means:

$$T_s + R_s = 1 \tag{2.58}$$

2.6 Reflection and Transmission in TM Polarization Using the Transfer Matrix Method

To complete the study of the reflection and transmission in more than one layer, we view in this section the transfer matrix in the TM polarization, and then we use it to determine the reflection and transmission coefficients in TM polarization (R_p and T_p) through Fresnel equations.

Figure (2.6) shows a homogeneous thin film with thickness *L* on a substrate and a beam of light in TM polarization incident on it.

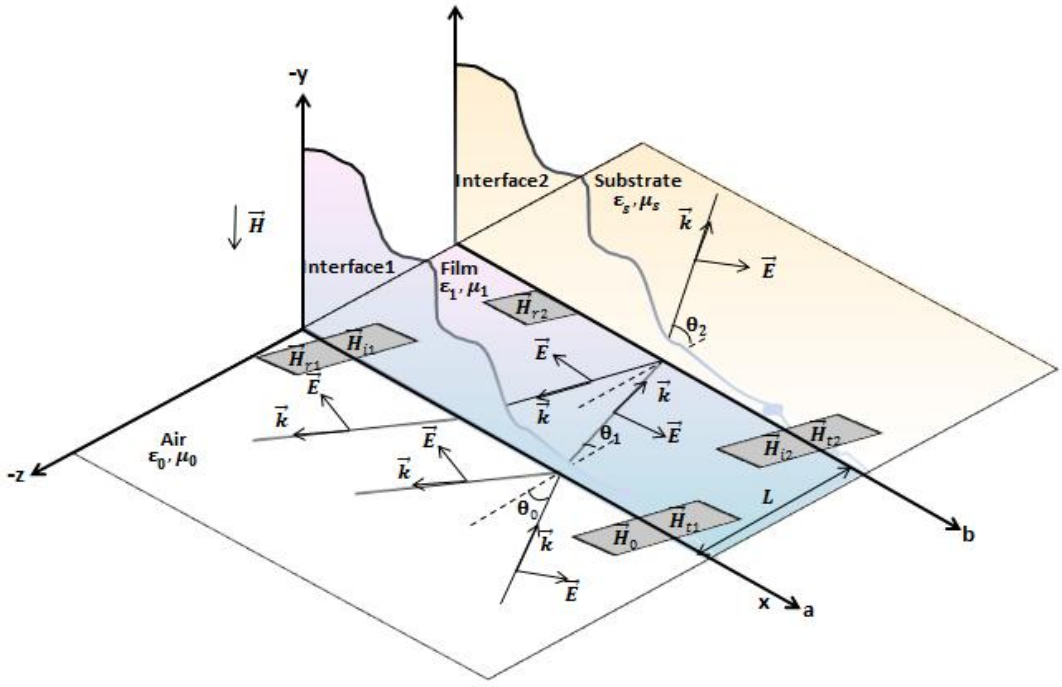

Figure (2.6): Light incident on a thin film on a substrate, for TM polarization.

Applying the boundary conditions for the parallel magnetic field and the parallel components of electric field, which must be continuous at each boundary as:

$$H_a = H_0 + H_{r1} = H_{t1} + H_{i1} \tag{2.59}$$

$$H_b = H_{i2} + H_{r2} = H_{t2} \tag{2.60}$$

$$E_a = E_{0x} - E_{rx1} = E_{tx1} - E_{ix1} \tag{2.61}$$

$$E_b = E_{ix2} - E_{rx2} = E_{tx2} \tag{2.62}$$

Using Maxwell's equation, given by equation (1.10):

$$\vec{k} \times \vec{H} = -\varepsilon\omega\vec{E}$$

which give: $E_{0x} = \frac{k_{0z}}{\omega\varepsilon_0} H_0$, $E_{rx1} = \frac{k_{0z}}{\omega\varepsilon_0} H_{r1}$, $E_{tx1} = \frac{k_{1z}}{\omega\varepsilon_1} H_{t1}$, $E_{ix1} = \frac{k_{1z}}{\omega\varepsilon_1} H_{i1}$,

$E_{ix2} = \frac{k_{1z}}{\omega\varepsilon_1} H_{i2}$, $E_{rx2} = \frac{k_{1z}}{\omega\varepsilon_1} H_{r2}$ and $E_{tx2} = \frac{k_{sz}}{\omega\varepsilon_s} H_{t2}$

then express the electric field $\vec{E}$ in equations (2.61) and (2.62) in terms of $\vec{H}$, we obtain:

$$E_a^* = \frac{k_{0z}}{\varepsilon_0}(H_0 - H_{r1}) = \frac{k_{1z}}{\varepsilon_1}(H_{t1} - H_{i1}) \tag{2.63}$$

$$E_b^* = \frac{k_{1z}}{\varepsilon_1}(H_{i2} - H_{r2}) = \frac{k_{sz}}{\varepsilon_s} H_{t2} \tag{2.64}$$

where $E_b^* = \omega E_b$, $E_a^* = \omega E_a$.

The magnetic field can be written as:

$$H_{i2} = H_{t1} e^{-i\delta} \text{ and } H_{i1} = H_{r2} e^{-i\delta} \Rightarrow H_{r2} = H_{i1} e^{i\delta} \tag{2.65}$$

Where δ is the phase difference is given by equation (2.34).

Using equation (2.65) in equations (2.59) and (2.64) we get:

$$H_b = H_{t1} e^{-i\delta} + H_{i1} e^{i\delta} \tag{2.66}$$

$$E_b^* = \frac{k_{1z}}{\varepsilon_1}(H_{t1}e^{-i\delta} - H_{i1}e^{i\delta}) \tag{2.67}$$

Solving H_{t1} & H_{i1} in terms of E_b^* & H_b, we find:

$$H_{t1} = \left(H_b + \frac{\varepsilon_1 E_b^*}{k_{1z}}\right)\frac{\mathrm{e}^{\mathrm{i}\delta}}{2} \tag{2.68}$$

$$H_{i1} = \left(H_b - \frac{\varepsilon_1 E_b^*}{k_{1z}}\right)\frac{\mathrm{e}^{-\mathrm{i}\delta}}{2} \tag{2.69}$$

Applying Euler formula $e^{\pm i\delta} = \cos\delta \pm i\sin\delta$ in equations (2.68) and (2.69) and substituting in equations (2.59) and (2.63) we obtain:

$$H_a = H_b\cos\delta + E_b^*\left(\frac{i\varepsilon_1\sin\delta}{k_{1z}}\right) \tag{2.70}$$

$$E_a^* = H_b(i\frac{k_{1z}}{\varepsilon_1}\sin\delta) + E_b^*\cos\delta \tag{2.71}$$

The last two equations can be written in the matrix form as:

$$\begin{bmatrix} H_a \\ E_a^* \end{bmatrix} = \begin{bmatrix} \cos\delta & \mathrm{i}\frac{\varepsilon_1}{k_{1z}}\sin\delta \\ \mathrm{i}\frac{k_{1z}}{\varepsilon_1}\sin\delta & \cos\delta \end{bmatrix}\begin{bmatrix} H_b \\ E_b^* \end{bmatrix} \tag{2.72}$$

where $\begin{bmatrix} \cos\delta & \mathrm{i}\frac{\varepsilon_1}{k_{1z}}\sin\delta \\ \mathrm{i}\frac{k_{1z}}{\varepsilon_1}\sin\delta & \cos\delta \end{bmatrix} = \begin{bmatrix} \mathrm{m}_{11} & \mathrm{m}_{12} \\ \mathrm{m}_{21} & m_{22} \end{bmatrix}$

is the transfer matrix in TM polarization for three layers.

Taking the remaining parts in equations (2.59), (2.60), (2.63) and (2.64) and insert them in the matrix equation (2.72), we get:

$$\begin{bmatrix} H_0 + H_{r1} \\ \frac{k_{0z}}{\varepsilon_0}(H_0 - H_{r1}) \end{bmatrix} = \begin{bmatrix} m_{11} & m_{12} \\ m_{21} & m_{22} \end{bmatrix}\begin{bmatrix} H_{t2} \\ \frac{k_{sz}}{\varepsilon_s}H_{t2} \end{bmatrix} \tag{2.73}$$

The matrix system in the last equation can be written as two equations:

$$H_0 + H_{r1} = m_{11} H_{t2} + m_{12} \frac{k_{sz}}{\varepsilon_s} H_{t2} \tag{2.74}$$

$$\frac{k_{0z}}{\varepsilon_0}(H_0 - H_{r1}) = m_{21} H_{t2} + m_{22} \frac{k_{sz}}{\varepsilon_s} H_{t2} \tag{2.75}$$

To reach the definition of Fresnel equations, equations (2.74) and (2.75) are divided by H_0 and the relations $r = H_{r1} / H_0$ and $t = H_{t2} / H_0$ are used to represent the reflection and transmission amplitudes:

$$1 + r = (m_{11} + m_{12} \frac{k_{sz}}{\varepsilon_s}) t \tag{2.76}$$

$$1 - r = (m_{21} \frac{k_{sz}}{\varepsilon_s} + m_{22}) \frac{\varepsilon_0}{k_{0z}} t \tag{2.77}$$

Solving equations (2.75) and (2.76), we obtain:

$$r_p = \frac{\frac{k_{0z}}{\varepsilon_0} m_{11} + \frac{k_{0z}}{\varepsilon_0}\frac{k_{sz}}{\varepsilon_s} m_{12} - m_{21} - \frac{k_{sz}}{\varepsilon_s} m_{22}}{\frac{k_{0z}}{\varepsilon_0} m_{11} + \frac{k_{0z}}{\varepsilon_0}\frac{k_{sz}}{\varepsilon_s} m_{12} + m_{21} + \frac{k_{sz}}{\varepsilon_s} m_{22}} \tag{2.78}$$

$$\mathrm{t_p} = \frac{2}{m_{11} + \frac{k_{sz}}{\varepsilon_s} m_{12} + \frac{\varepsilon_0}{k_{0z}} m_{21} + \frac{\varepsilon_0}{k_{0z}}\frac{k_{sz}}{\varepsilon_s} m_{22}} \tag{2.79}$$

Similarly, in TE polarization the reflection and transmission amplitudes are used to determine the reflectance and transmittance.

The reflectance in TM polarization is given by:

$$R_p = |r_p|^2 \tag{2.80}$$

and the transmittance can be written as:

$$T_p = \frac{S_t}{S_0} \tag{2.81}$$

As above mentioned, the Poynting's vectors S and S_t from equation (1.17) can be written as:

$$S_0 = \frac{1}{2\varepsilon_0\omega}\,\mathrm{Re}\left\{\frac{k_{oz}}{\varepsilon_0}\right\}|H_0|^2 \tag{2.82}$$

$$S_t = \frac{1}{2\varepsilon_0\omega}\,\mathrm{Re}\left\{\frac{k_{sz}}{\varepsilon_s}\right\}|H_t|^2 \tag{2.83}$$

Substituting for the Poynting's vectors S and S_t from equations (2.82) and (2.83) into equation (2.81) we obtain:

$$T_p = \mathrm{Re}\{\frac{k_{sz}\varepsilon_0}{k_{oz}\varepsilon_s}\}\left|t_p\right|^2 \tag{2.84}$$

Chapter 3

Four Layers Anti-Reflection Coating

Chapter 3

Four Layers Anti-Reflection Coating

3.1 Introduction

Since the solar cells technology is considered as one of the most important ways to generate the electric power, there are several investigations were implemented to enhance its efficiency. One of most common ways is using ARCs as a method of light trapping. The ARCs is a structure that minimizes the reflection from solar cells surfaces and is put on the front surfaces of the photovoltaic cells. In 1817 Fraunhofer fabricated the first of the ARCs (Macleod, 2001). To achieve a high efficiency of the solar cell, there are several variables must be considered, such as the material in the structure, the number of layers, the thickness of each layer, the angle of incidence and the range of wavelengths incident on the ARCs.

In this study, we investigate the multilayers ARC structure containing left handed materials (LHM) used to enhance the efficiency of the solar cells, for examples see (Chen et al., 2010; Dena et al., 2015; Hamouche and Shabat, 2016). We also present an analytical analysis to study the reflection and transmission of this structure in both TE and TM polarizations of light.

3.2 The Model Structure

To design a structure of the ARC with minimum reflection, we assume a structure that consists of 4-layers (air, LHM, dielectric and substrate) as illustrated in Figure (3.1). We study the Gallium Arsenide solar cells in which the GaAs layer (electric permittivity $\varepsilon_s = 12.7$) is considered as a substrate (Chen et al., 2010). The band gap of GaAs equals 1.424ev that makes it one of the optimal materials to improve solar cells efficiency (Zdanowicz, Rodziewicz, and Zabkowska-Waclawek, 2005).

Air, dielectric and substrate are all nonmagnetic materials with magnetic permeability equals 1. The electric permittivity for air also equals 1. The LHM has both negative electric permittivity (ε_1) and magnetic permeability (μ_1). In numerical simulation, $\varepsilon_1\mu_1$ is taken to be 4 so that the refractive index equals -2 from the relation $n_1 = -\sqrt{\varepsilon_1\mu_1} = -2$ (Kim, Cho, Tae and Lee, 2006). The dielectric is chosen

to be Silicon Nitride (SiN_x) which is characterized by its high value of refractive index. Upon varying the deposition parameter, the refractive index of SiN_x takes on values ranging from 1.8 to 2.3 (Lee et al., 2012).

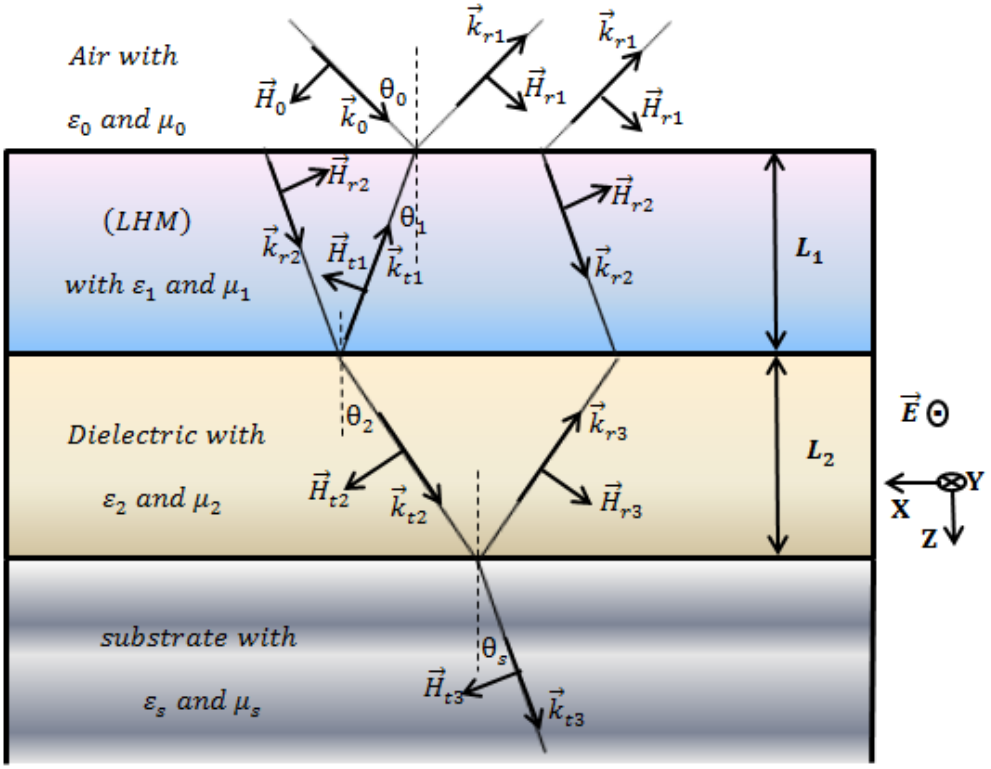

Figure (3.1): The propagation of light in four layers ARC in TE mode.

In Figure (3.1) we assume the beams of light in TE polarization incident with angles θ_0 on a four-layers structure. In the first interface between air and LHM some of beams are reflected back and some transmit to the LHM with a refraction angle θ_1. It is worth mentioning that we have a negative refraction and negative direction of the wave vector in the LHM layers that appears in Figure (3.1) as we mentioned in chapter 1. Again, some of the beams incident on the second interface between the LHM and dielectric layers will reflect back and some will transmit to the dielectric layer with refraction angle θ_2. Finally, some of the beams reflect on the third interface between the dielectric and the semiconductor GaAs substrate while the others transmit with a refraction angle θ_s. We can determine the reflection angles θ_1, θ_2 *and* θ_s from Snell's law given in equation (1.20). L_1 *and* L_2 represent the thickness of LHM and dielectric; respectively.

3.3 TE Polarization in Four Layers ARC

For the polarization of the incident light, only the two types of polarization (TE and TM) are considered. In the first of the analysis of the reflectance and transmittance to our ARC structure, we start with the TE polarization through its definition in chapter 2 as in Figure (3.1). In this section, the reflectance and transmittance for four layers are calculated through transfer matrix method and apply them in our structure to verify its optical properties by using the Maple 13 software program.

3.3.1 Transfer Matrix for Four Layers in TE Case

The transfer matrix for n layers depends on the number of layers (n) as shown in equation (2.8). In chapter 2, the transfer matrix for TE polarization for three layers was viewed in equation (2.41) in the form:

$$M_s = \begin{bmatrix} \cos\delta & \frac{i\mu_1}{k_{1z}}\sin\delta \\ i\frac{k_{1z}}{\mu_1}\sin\delta & \cos\delta \end{bmatrix}$$

Using the Multiplication property of the transfer matrix that given in equation (2.7) and (2.8), the transfer matrix can be given by:

$$\mathrm{M_{12}} = \mathrm{M_1 M_2}$$

Where $\mathrm{M_1}$ the transfer matrix through the LHM layer and $\mathrm{M_2}$ is the transfer matrix through the dielectric layer, by inserting equation (2.41) into the above we get:

$$M_s = \begin{bmatrix} \cos(\delta_1) & \frac{i\mu_1}{k_{1z}}\sin(\delta_1) \\ i\frac{k_{1z}}{\mu_1}\sin(\delta_1) & \cos(\delta_1) \end{bmatrix} \begin{bmatrix} \cos(\delta_2) & \frac{i\mu_2}{k_{2z}}\sin(\delta_2) \\ i\frac{k_{2z}}{\mu_2}\sin(\delta_2) & \cos(\delta_2) \end{bmatrix} \quad (3.1)$$

Where δ_1 and δ_2 are the phase differences in the LHM and dielectric; respectively. They are given as:

$$\delta_1 = \mathrm{k_0}\sqrt{\varepsilon_1\mu_1}\,\mathrm{L_1}\cos\theta_1 \text{ and } \delta_2 = \mathrm{k_0}\sqrt{\varepsilon_2\mu_2}\mathrm{L_2}\cos\theta_2$$

The components of the wave vector normal to the interface can be written as:

$$k_{1z} = k_1 \cos\theta_1,\ k_{2z} = k_2 \cos\theta$$

Applying the matrix product in equation (3.1), we get:

$$M_s = \begin{bmatrix} \cos(\delta_1)\cos(\delta_2) - \frac{\mu_1 k_{2z}}{\mu_2 k_{1z}} \sin(\delta_1)\sin(\delta_2) & \frac{\mathrm{i}\mu_2}{k_{2z}} \cos(\delta_1)\sin(\delta_2) + \frac{\mathrm{i}\mu_1}{k_{1z}} \sin(\delta_1)\cos(\delta_2) \\ \mathrm{i}\frac{k_{1z}}{\mu_1} \sin(\delta_1)\cos(\delta_2) + i\frac{k_{2z}}{\mu_2} \cos(\delta_1)\sin(\delta_2) & \cos(\delta_1)\cos(\delta_2) - \frac{\mu_2 k_{1z}}{\mu_1 k_{2z}} \sin(\delta_1)\sin(\delta_2) \end{bmatrix} \quad (3.2)$$

This is the transfer matrix for four layers in TE mode.

3.3.2 Reflection and Transmission for Four Layers ARC in TE Case

The propagation and the study of the transmission and reflection of electromagnetic waves within a waveguide depend on several variables as the type of the polarization.

In this section, the reflection and transmission equations in TE polarization for proposed four layers structure model are determined.

Depending on Figure (3.1) and the transfer matrix in equation (3.2) to calculate the reflection in four layers for TE case, and by recalling equation (2.51) which takes the form:

$$r_s = \frac{\frac{k_{0z}}{\mu_0} m_{11} + \frac{k_{0z}}{\mu_0}\frac{k_{sz}}{\mu_s} m_{12} - m_{21} - \frac{k_{sz}}{\mu_s} m_{22}}{\frac{k_{0z}}{\mu_0} m_{11} + \frac{k_{0z}}{\mu_0}\frac{k_{sz}}{\mu_s} m_{12} + m_{21} + \frac{k_{sz}}{\mu_s} m_{22}}$$

Inserting the elements of transfer matrix in equation (3.2), where the elements can be written as:

$$m_{11} = \cos(\delta_1)\cos(\delta_2) - \frac{\mu_1 k_{2z}}{\mu_2 k_{1z}} \sin(\delta_1)\sin(\delta_2) \quad (3.3)$$

$$m_{12} = i\frac{\mu_2}{k_{2z}} \cos(\delta_1)\sin(\delta_2) + i\frac{\mu_1}{k_{1z}} \sin(\delta_1)\cos(\delta_2) \quad (3.4)$$

$$m_{21} = \mathrm{i}\frac{k_{1z}}{\mu_1} \sin(\delta_1)\cos(\delta_2) + i\frac{k_{2z}}{\mu_2} \cos(\delta_1)\sin(\delta_2) \quad (3.5)$$

$$m_{22} = \cos(\delta_1)\cos(\delta_2) - \frac{\mu_2 k_{1z}}{\mu_1 k_{2z}} \sin(\delta_1)\sin(\delta_2) \quad (3.6)$$

Then the reflection amplitude takes the form:

$$r_s = \frac{A + iB - iC - D}{A + iB + iC + D} \tag{3.7}$$

Where A, B, C and D are given by:

$$A = \frac{k_{0z}}{\mu_0}\left(\cos(\delta_1)\cos(\delta_2) - \frac{\mu_1 k_{2z}}{\mu_2 k_{1z}}\sin(\delta_1)\sin(\delta_2)\right) \tag{3.8}$$

$$B = \frac{k_{0z}}{\mu_0}\frac{k_{sz}}{\mu_s}\left(\frac{\mu_2}{k_{2z}}\cos(\delta_1)\sin(\delta_2) + \frac{\mu_1}{k_{1z}}\sin(\delta_1)\cos(\delta_2)\right) \tag{3.9}$$

$$C = \left(\frac{k_{1z}}{\mu_1}\sin(\delta_1)\cos(\delta_2) + \frac{k_{2z}}{\mu_2}\cos(\delta_1)\sin(\delta_2)\right) \tag{3.10}$$

$$D = \frac{k_{sz}}{\mu_s}\left(\cos(\delta_1)\cos(\delta_2) - \frac{\mu_2 k_{1z}}{\mu_1 k_{2z}}\sin(\delta_1)\sin(\delta_2)\right) \tag{3.11}$$

From equation (2.53), the reflectance is given by:

$$\mathrm{R_s} = |\mathrm{r_s}|^2 = \mathrm{r}.\mathrm{r}^*$$

Substituting equation (3.7) in the last equation (2.53), we get:

$$\mathrm{R_s} = |\mathrm{r_s}|^2 = \mathrm{r}.\mathrm{r}^* = \frac{A + iB - iC - D}{A + iB + iC + D}.\frac{A - iB + iC - D}{A - iB - iC + D} \tag{3.12}$$

Then the reflectance for four layers in TE polarization is given by:

$$\mathrm{R_s} = \frac{A^2 + B^2 + C^2 + D^2 - 2(AD + BC)}{A^2 + B^2 + C^2 + D^2 + 2(AD + BC)} \tag{3.13}$$

Now, recalling equation (2.52) to determine the transmission in four layers in TE case:

$$t_s = \frac{2}{m_{11} + \frac{k_{sz}}{\mu_s}m_{12} + \frac{\mu_0}{k_{0z}}m_{21} + \frac{\mu_0}{k_{0z}}\frac{k_{sz}}{\mu_s}m_{22}}$$

Substituting the elements of transfer matrix from equation (3.2) in the previous equation, the transmission amplitude can be written as:

$$t_s = \frac{2k_{0z}/\mu_0}{A + iB + iC + D} \tag{3.14}$$

To calculate the total transmission, equation (2.57) is used:

$$T_s = \mathrm{Re}\{\frac{k_{sz}\mu_0}{k_{oz}\mu_s}\}|t_s|^2$$

From equation (3.14) and equation (2.57), we get:

$$T_s = \frac{k_{sz}\mu_0}{k_{0z}\mu_s}\, t \cdot t^* = \frac{k_{sz}\mu_0}{k_{0z}\mu_s} \cdot \frac{2k_{0z}/\mu_0}{A + iB + iC + D} \cdot \frac{2k_{0z}/\mu_0}{A - iB - iC + D} \tag{3.15}$$

The total transmission in four layers for TE polarization takes the form:

$$T_s = \frac{k_{sz}k_{0z}}{\mu_0\mu_s} \cdot \frac{4}{A^2 + B^2 + C^2 + D^2 + 2(AD + BC)} \tag{3.16}$$

Using a computer software to solve and analyze the total reflectance and transmittance equations (3.13) and (3.16).

3.3.3 Results and Discussions in TE case

For the proposed structure, the relative electric permittivity of air is $\varepsilon_0 = 1$ and the relative magnetic permeability is also $\mu_0 = 1$. The electric permittivity and the magnetic permeability ε_1 and μ_1 for LHM are both negative and are chosen such that $\varepsilon_1\mu_1 = 4$ (Kim et al., 2006), i.e. the refractive index of the LHM is $n_1 = -2$. The chosen dielectric SiN_x has magnetic permeability $\mu_2 = 1$ with electric permittivity varying from 1.8^2 to 2.5^2 (Lee et al., 2012). For the GaAs substrate the electric permittivity is $\varepsilon_s = 12.7$ and its magnetic permeability is $\mu_s = 1$ (Chen et al., 2010). The thicknesses of both LHM and SiN_x are assumed to be $L_1 = 75\,nm$ and $L_2 = 83.33\,nm$; respectively. All calculations and diagrams in this section are carried out depending on equations (3.13) and (3.16) in addition to Snell's law to determine the angles of refraction.

In the beginning of the study of the suggested ARC, we start with the LHM parameters as its electric permittivity, magnetic permeability and the thickness of the LHM layer.

Figure (3.2) and (3.3) illustrate the variation in the reflection and transmission coefficients for the ARC when the ε_1 and μ_1 for LHM layer is changed, where they take on the values (-1,-4), (-2,-2), (-3,-4/3) and (-4,-1) for the pair (ε_1,μ_1); respectively and the SiN_x layer is assumed with $\varepsilon_2 = 1.8^2$ and $\mu_2 = 1$. The optimal value of ε_1 and μ_1 of the lowest value of reflectance and maximum transmittence are observed at $\varepsilon_1 = \mu_1 = -2$ when the reflection goes to be zero and the transmittence becomes very close to 1 approximately at 600 nm wavelength. The value $\varepsilon_1 = -4$ and $\mu_1 = -1$ for LHM also can give a minimum reflectance for another structure, see (Dena et al., 2015).

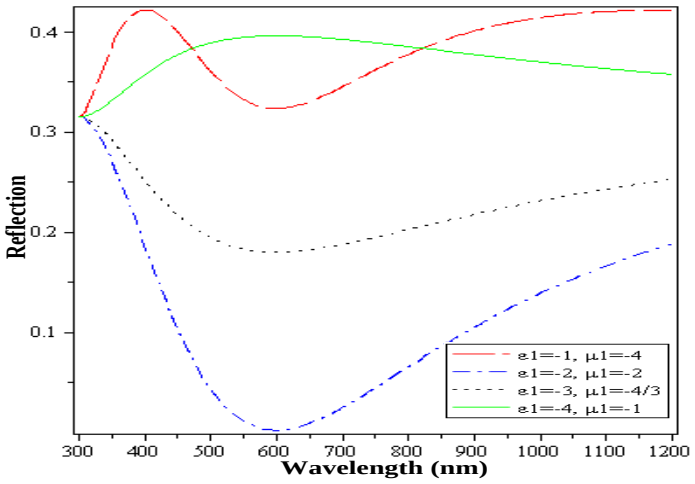

Figure (3.2): The reflectance versus the wavelength under normal incidence in TE case for different values of ε_1 and μ_1. Here, $L_1 = 75$ nm, $L_2 = 83.33\ nm$, $\varepsilon_2 = 1.8^2$ and $\mu_2 = 1$.

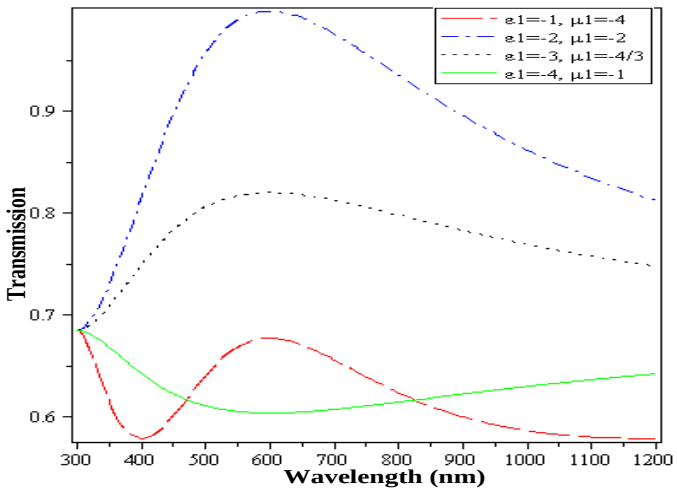

Figure (3.3): The transmittance versus the wavelength under normal incidence in TE case for different values of ε_1 and μ_1. Here, $L_1 = 75$ nm, $L_2 = 83.33\ nm$, $\varepsilon_2 = 1.8^2$ and $\mu_2 = 1$.

In other hand all values of ε_1 *and* μ_1 for the LHM in Figure (3.2) can give the same minimum reflection in different wavelengths, if we choose a thin film of the LHM in the range between 5 nm to 25 nm as have been shown in Figures (3.4) and (3.5), where the supposed thickness is 10 nm.

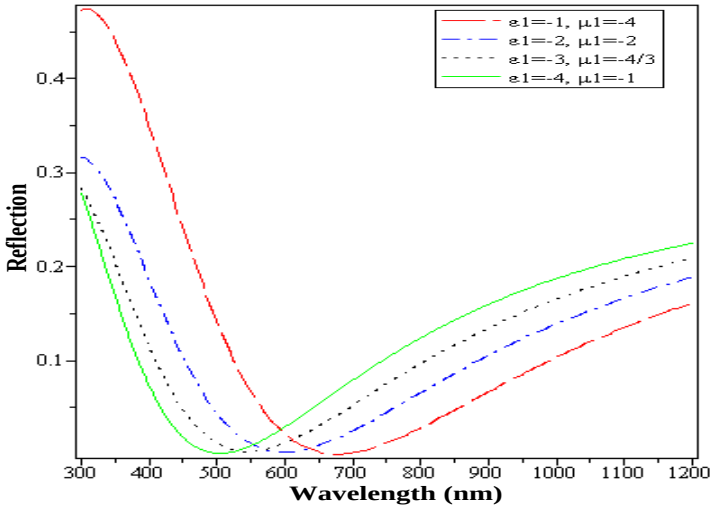

Figure (3.4): The reflectance versus the wavelength under normal incidence in TE case for different values of ε_1 and μ_1. Here, $L_1 = 10$ nm, $L_2 = 83.33\ nm$, $\varepsilon_2 = 1.8^2$ and $\mu_2 = 1$.

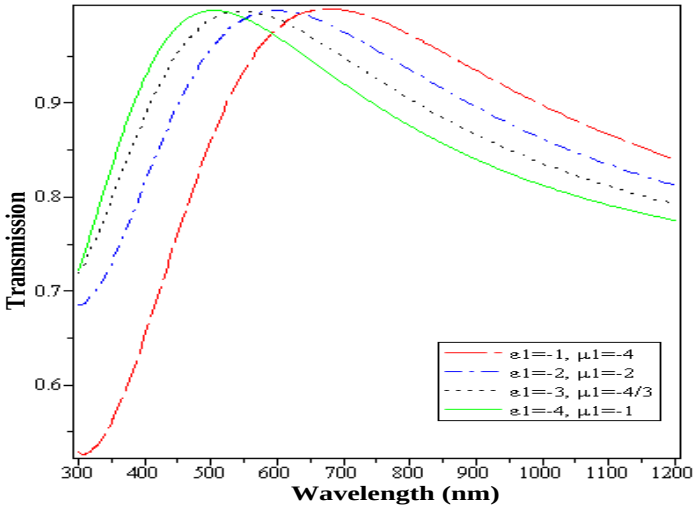

Figure (3.5): The transmittance versus the wavelength under normal incidence in TE case for different values of ε_1 and μ_1. Here, $L_1 = 10$ nm, $L_2 = 83.33\ nm$, $\varepsilon_2 = 1.8^2$ and $\mu_2 = 1$.

Although there are more than one minor value for reflection, we chose $\varepsilon_1 = -2$ and $\mu_1 = -2$ because it gives the maximum transmission at the middle of the desired photon flux (600 nm) as the previous figures show.

To study the effect of the LHM thickness, reflectance and transmittance are plotted against wavelength for different thicknesses as illustrated in Figures (3.6) and (3.7). The LHM thickness (L_1=10, 50, 75 and 100) nm are chosen with the same SiN_x layer of $\varepsilon_2 = 1.8^2$ and the angle of incidence is fixed to 30°.

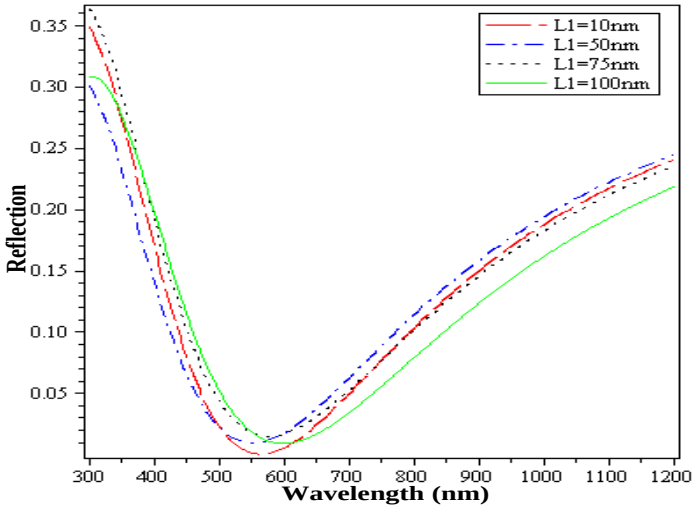

Figure (3.6): The reflectance versus the wavelength for different thicknesses of the LHM in TE case. Here, $\varepsilon_1 = \mu_1 = -2, L_2 = 83.33\ nm, \varepsilon_2 = 1.8^2$, $\mu_2 = 1$.and $\theta_0 = 30^\circ$.

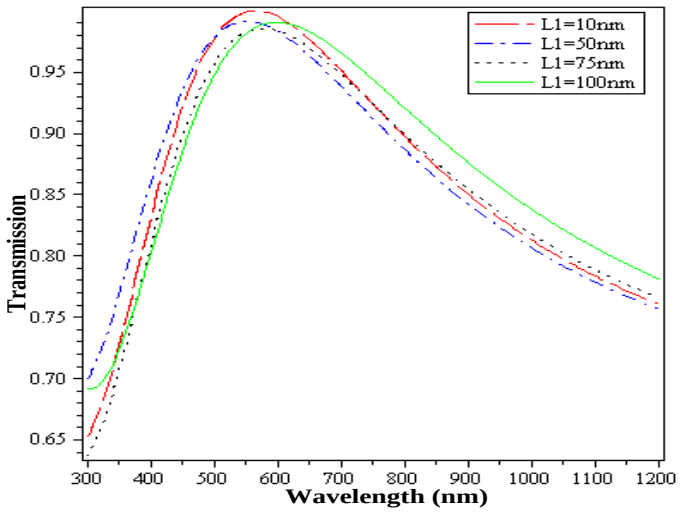

Figure (3.7): The transmittance versus the wavelength for different thicknesses of the LHM in TE case. Here, $\varepsilon_1 = \mu_1 = -2, L_2 = 83.33\ nm, \varepsilon_2 = 1.8^2, \mu_2 = 1$ and $\theta_0 = 30^\circ$.

As the last figures indicate, both reflection and transmission are slightly affected by changing the thickness of the LHM. The preferred thickness that gives a minimum reflection and maximum transmission is 10 nm at angle of incidence equal 30° which

gives the best results, but if we change the angle of incidence the thickness will change as in Figures (3.8) and (3.9).

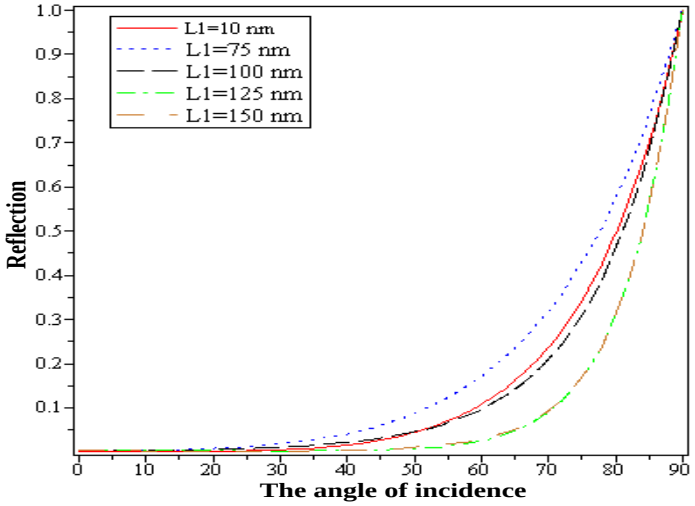

Figure (3.8): The reflectance versus the angle of incidence at 600 nm wavelength for different thicknesses of the LHM in TE case. Here, $\varepsilon_1 = \mu_1 = -2, L_2 = 83.33\, nm, \varepsilon_2 = 1.8^2\ and\ \mu_2 = 1$.

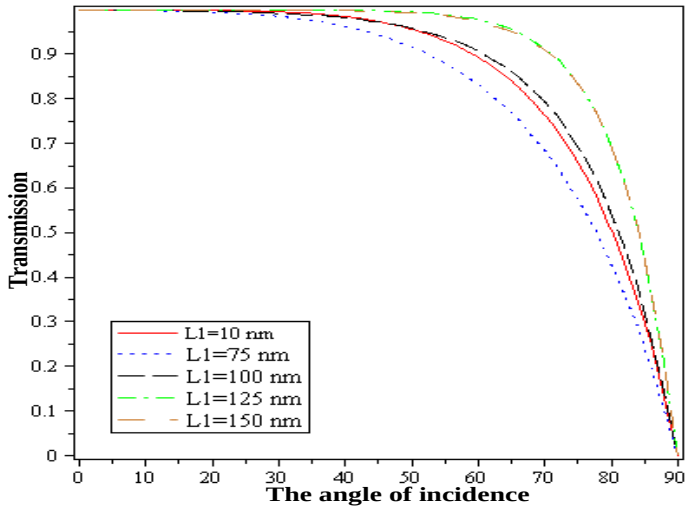

Figure (3.9): The transmittance versus the angle of incidence at 600 nm wavelength for different thicknesses of the LHM in TE case. Here, $\varepsilon_1 = \mu_1 = -2, L_2 = 83.33\, nm, \varepsilon_2 = 1.8^2, \mu_2 = 1$ and $\theta_0 = 30^{\circ}$.

The last two figures display the behavior of both the reflectance and transmittance at 600 nm against the angle of incidence when the thickness of the LHM layer (L_1) change. It is clear that the thicknesses (125 and 150) nm give results better than the

10 nm for the angles larger than 30°. In this work the angle of incidence is assumed to be 30°, so the chosen thickness for the LHM is L_1= 10 nm.

In the second step of verifying the properties of the structure of the ARC, we study the effective variables of the dielectric layer (SiN_x) as its electric permittivity and thickness.

The variation in the electric permittivity ε_2 for the SiN_x also changes the efficiency of the solar cells where the reflection of the ARC is changed. Figure (3.10) and (3.11) illustrate these changes by consider the value $\varepsilon_1 = -2$ and $\mu_1 = -2$ for the LHM layer with thickness $L_1 = 10$ nm and varying ε_2 for the SiN_x in the range from 1.8^2 to 2.4^2 under normal incidence.

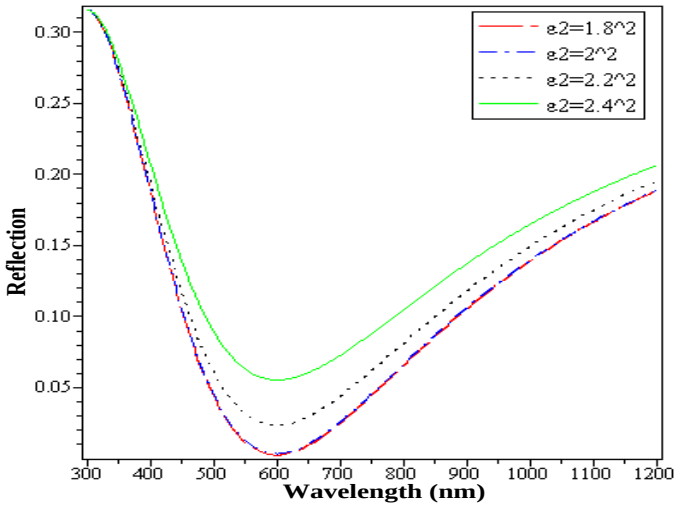

Figure (3.10): The reflectance versus the wavelength under normal incidence in TE case for different values of ε_2. Here, $\varepsilon_1 = \mu_1 = -2, L_1 = 10\ nm$ and $L_2 = 83.33\ nm$.

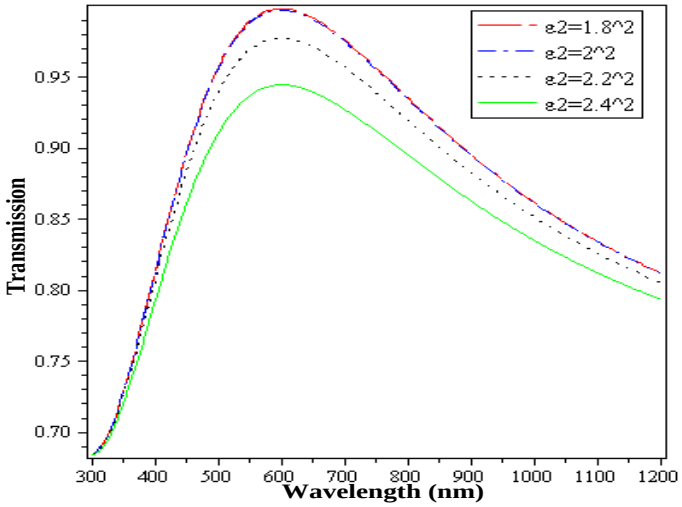

Figure (3.11): The transmittance versus the wavelength under normal incidence in TE case for different values of ε_2. Here, $\varepsilon_1 = \mu_1 = -2, L_1 = 10\ nm$ and $L_2 = 83.33\ nm$.

These two plots reveal that higher values of ε_2 for the SiN_x result in different behaviors of reflection and transmission whereas the lower values (here $\varepsilon_2 = 1.8^2$ and $\varepsilon_2 = 2^2$) tend to be the same and give optimal values at 600nm.

In order to study the effect of SiN_x layer thickness on both reflectance and transmittance, we plotted these two quantities against wavelength for different L_2 values as shown in Figures (3.12) and (3.13). Specifically; (L_2 =50, 75, 100 and 125 nm). The other parameters are: $\varepsilon_1 = -2$ and $\mu_1 = -2$ for the LHM layer with thickness $L_1 = 10\ nm$, $\varepsilon_2 = 1.8^2$ for the SiN_x layer at an angle of incidence of 30°.

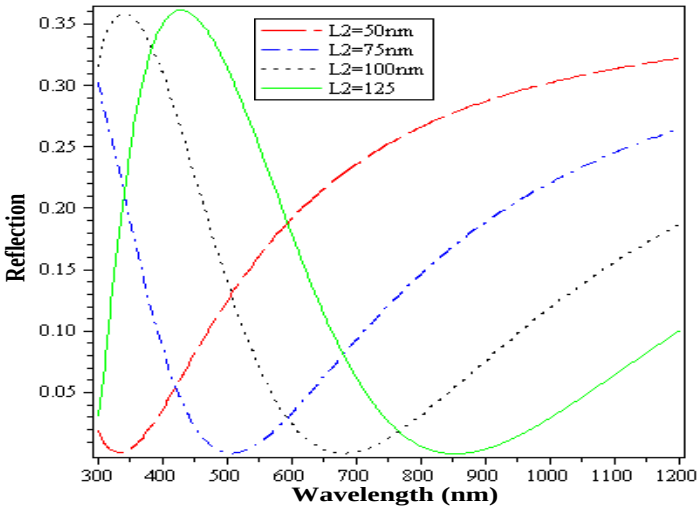

Figure (3.12): The reflectance versus the wavelength for different values of L_2 with $\varepsilon_2 = 1.8^2$, $\varepsilon_1 = \mu_1 = -2$, $L_1 = 10nm$ and $\theta_0 = 30^\circ$ in TE case.

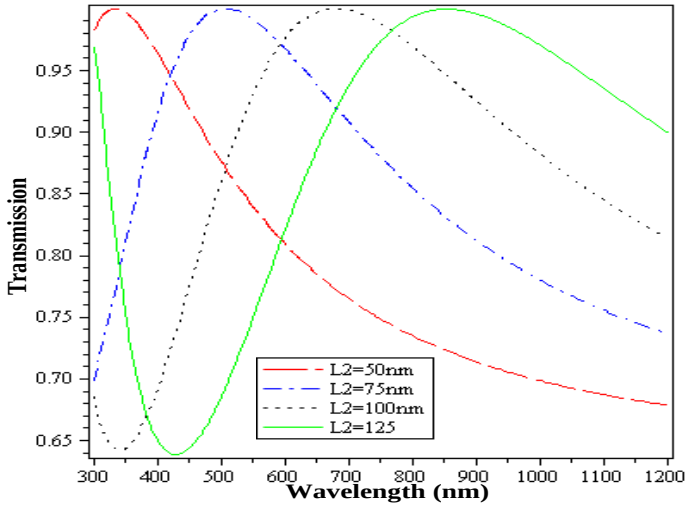

Figure (3.13): The transmittance versus the wavelength for different values of L_2 with $\varepsilon_2 = 1.8^2$, $\varepsilon_1 = \mu_1 = -2$, $L_1 = 10nm$ and $\theta_0 = 30^\circ$ in TE case.

Reflectance minima and transmittance maxima are all the same for various values of L_2 but they are shifted to the right with higher values. The best behavior is seen for the two middle values (75 nm and 100 nm) since they occur in the range between 500nm to 600nm in good agreement with the best value of L_2=83.33nm which is calculated from the relation: $L_x = \lambda/4|\sqrt{\varepsilon_x \mu_x}|$ at 600 nm wavelength.

In the following plots, we will check the effect of the angle of incidence on the reflectance and transmittance. These values of parameters are put into consideration: $\varepsilon_2 = 1.8^2$ is considered for the SiN_x layer and the LHM with $\varepsilon_1 = -2$, $\mu_1 = -2$ and $L_1 = 10$ nm. Minimum reflection and maximum transmission occurring about 600nm are attained at normal incidence as predicted from figures (3.14) and (3.15).

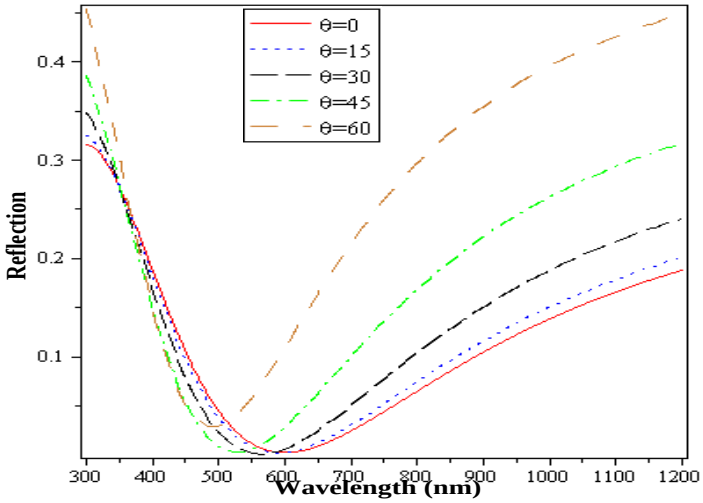

Figure (3.14): The reflectance versus the wavelength for different angles of incidence θ_0 in TE case. Here, $\varepsilon_1 = \mu_1 = -2$, $L_1 = 10$ nm, $\varepsilon_2 = 1.8^2$ and $L_2 = 83.33$ nm.

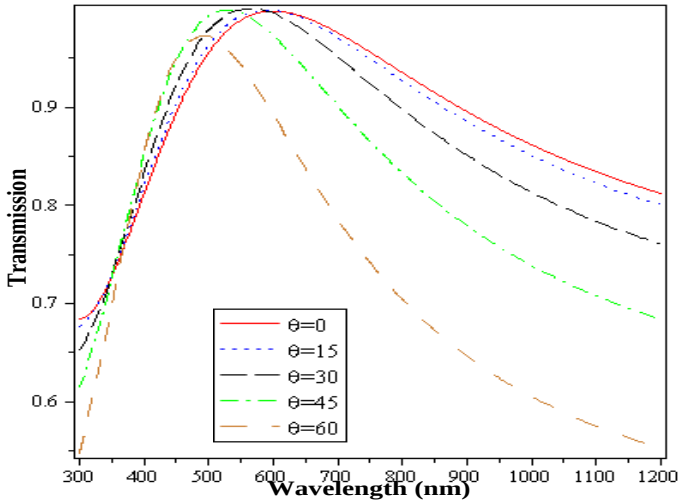

Figure (3.15): The transmittance versus the wavelength for different angles of incidence θ_0 in TE case. Here, $\varepsilon_1 = \mu_1 = -2$, $L_1 = 10$ nm, $\varepsilon_2 = 1.8^2$ and $L_2 = 83.33$ nm.

As the angle of incidence increases, the optimal values of reflectance and transmittance are shifted towards higher energy spectra but their extremes become no longer optimal.

For a deeper understanding, Figures (3.16) and (3.17) illustrate the change in the reflection and transmission with the angle of incidence in different wavelengths.

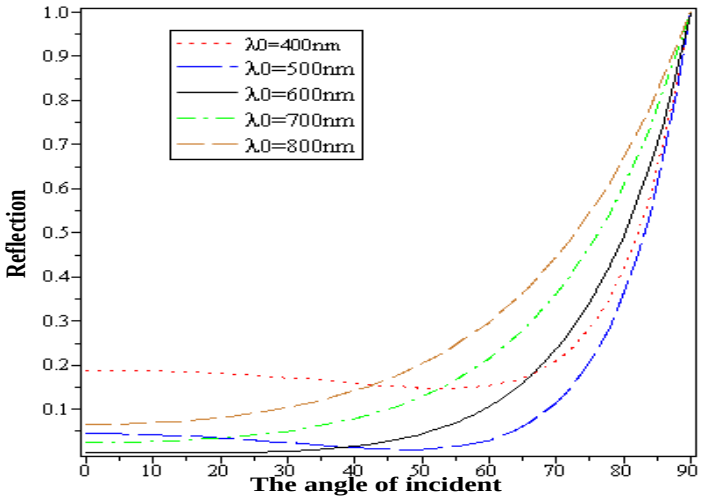

Figure (3.16): The reflectance versus the angles of incidence θ_0 for different wavelengths in TE case. Here, $\varepsilon_1 = \mu_1 = -2$, $L_1 = 10$ nm, $\varepsilon_2 = 1.8^2$ and $L_2 = 83.33$ nm.

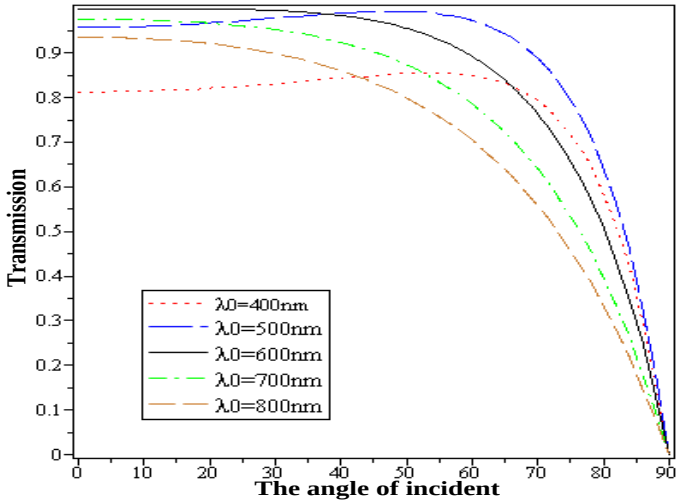

Figure (3.17): The transmittance versus the angles of incidence θ_0 for different wavelengths in TE case. Here, $\varepsilon_1 = \mu_1 = -2$, $L_1 = 10$ nm, $\varepsilon_2 = 1.8^2$ and $L_2 = 83.33$ nm.

It's clear from these two figures that the reflectance is very close to zero and the transmittance is nearly unity when the angle of incidence is less than 35° at 600nm. When the angle of incidence increases, the reflection increases but there is another wavelength giving a low reflection when the angle of incidence from 35° to 60° at 500nm. When the angle of incidence is greater than 60° the reflection increases significantly for all the range of the suitable wavelength for solar cells.

3.4 TM Polarization in Four Layers ARC

To study the properties of the proposed four layers ARC in TM mode, this section views the calculations and plottings for transmittance and reflectance by using transfer matrix method, Fresnel's equations, Snell's law and Mable 13 software program. Through the definition of the TM polarization in chapter 2, Figure (3.18) represents the ARC structure in TM polarization, where the variables in it and the negative refraction and direction of the wave vector in the LHM layers were explained in the previous section.

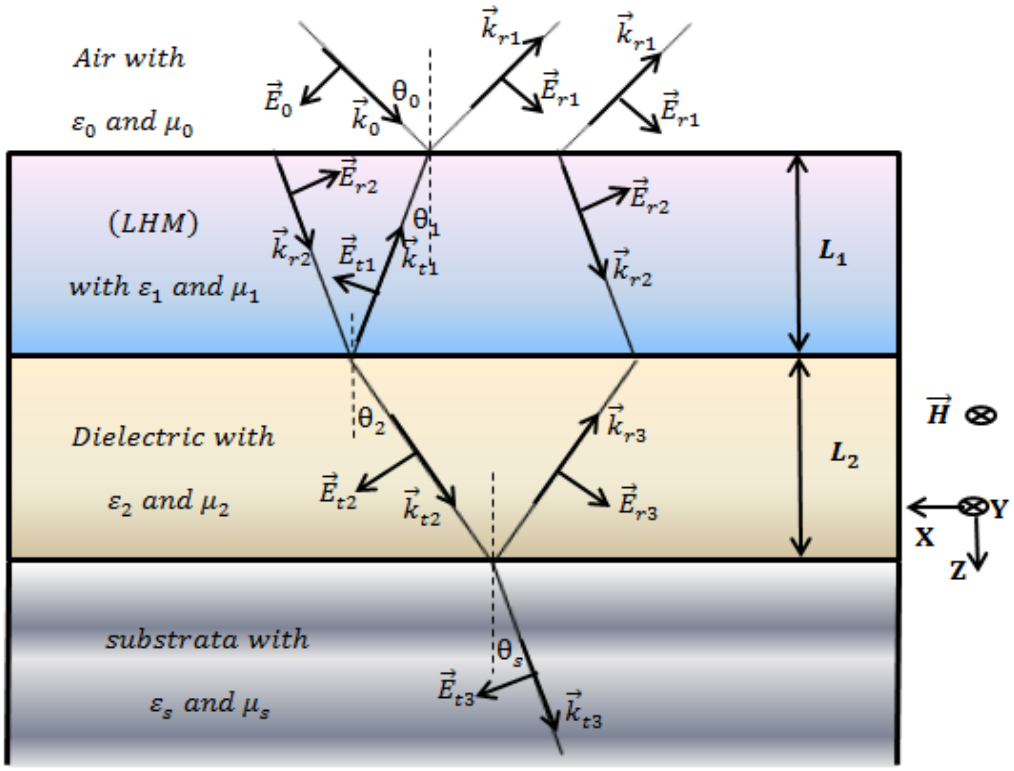

Figure (3.18): The propagation of light in four layers ARC in TM mode.

3.4.1 Transfer Matrix for Four Layers in TM Mode

To verify the transmittance and reflectance for four layers ARC, we introduce the transfer matrix for four layers in TM mode. Let us start from equation (2.72) which represents the transfer matrix for three layers in TM case:

$$M_p = \begin{bmatrix} \cos\delta & \frac{i\varepsilon_1}{k_{1z}}\sin\delta \\ i\frac{k_{1z}}{\varepsilon_1}\sin\delta & \cos\delta \end{bmatrix}$$

Using the Multiplication property for transfer matrix to multilayers coat that given by equations (2.7) and (2.8), which takes the form:

$$\mathrm{M}_{12} = \mathrm{M}_1\mathrm{M}_2$$

Where M_1 the transfer matrix through the LHM layer and M_2 is the transfer matrix through the dielectric layer, by inserting equation (2.72) in the above equation for the two transfer matrix we get:

$$M_p = \begin{bmatrix} \cos(\delta_1) & \mathrm{i}\frac{\varepsilon_1}{k_{1z}}\sin(\delta_1) \\ i\frac{k_{1z}}{\varepsilon_1}\sin(\delta_1) & \cos(\delta_1) \end{bmatrix} \begin{bmatrix} \cos(\delta_2) & \mathrm{i}\frac{\varepsilon_2}{k_{2z}}\sin(\delta_2) \\ i\frac{k_{2z}}{\varepsilon_2}\sin(\delta_2) & \cos(\delta_2) \end{bmatrix} \tag{3.17}$$

$$M_p = \begin{bmatrix} \cos(\delta_1)\cos(\delta_2) - \frac{\varepsilon_1 k_{2z}}{\varepsilon_2 k_{1z}}\sin(\delta_1)\sin(\delta_2) & \mathrm{i}\frac{\varepsilon_2}{k_{2z}}\cos(\delta_1)\sin(\delta_2) + \mathrm{i}\frac{\varepsilon_1}{k_{1z}}\sin(\delta_1)\cos(\delta_2) \\ \mathrm{i}\frac{k_{1z}}{\varepsilon_1}\sin(\delta_1)\cos(\delta_2) + i\frac{k_{2z}}{\varepsilon_2}\cos(\delta_1)\sin(\delta_2) & \cos(\delta_1)\cos(\delta_2) - \frac{\varepsilon_2 k_{1z}}{\varepsilon_1 k_{2z}}\sin(\delta_1)\sin(\delta_2) \end{bmatrix} \tag{3.18}$$

Where the elements of the transfer matrix can be written as:

$$m_{11} = \cos(\delta_1)\cos(\delta_2) - \frac{\varepsilon_1 k_{2z}}{\varepsilon_2 k_{1z}}\sin(\delta_1)\sin(\delta_2) \tag{3.19}$$

$$m_{12} = \mathrm{i}\frac{\varepsilon_2}{k_{2z}}\cos(\delta_1)\sin(\delta_2) + \mathrm{i}\frac{\varepsilon_1}{k_{1z}}\sin(\delta_1)\cos(\delta_2) \tag{3.20}$$

$$m_{21} = \mathrm{i}\frac{k_{1z}}{\varepsilon_1}\sin(\delta_1)\cos(\delta_2) + i\frac{k_{2z}}{\varepsilon_2}\cos(\delta_1)\sin(\delta_2) \tag{3.21}$$

$$m_{22} = \cos(\delta_1)\cos(\delta_2) - \frac{\varepsilon_2 k_{1z}}{\varepsilon_1 k_{2z}}\sin(\delta_1)\sin(\delta_2) \tag{3.22}$$

Equation (3.18) is called the transfer matrix for four layers in TM mode and is used to determine the optical properties of the coat of research as reflectance and transmittance in TM mode.

3.4.2 Reflection and Transmission for Four Layers in TM Case

In this section, the reflectance and transmittance equations for four layers in TM case are determined. From equation (2.78) which represents the reflection amplitude in three layers in TM case:

$$r = \frac{\frac{k_{0z}}{\varepsilon_0} m_{11} + \frac{k_{0z}}{\varepsilon_0}\frac{k_{sz}}{\varepsilon_s} m_{12} - m_{21} - \frac{k_{sz}}{\varepsilon_s} m_{22}}{\frac{k_{0z}}{\varepsilon_0} m_{11} + \frac{k_{0z}}{\varepsilon_0}\frac{k_{sz}}{\varepsilon_s} m_{12} + m_{21} + \frac{k_{sz}}{\varepsilon_s} m_{22}}$$

Substituting the elements of transfer matrix in equation (3.18) into the last equation (2.78), we get:

$$r_p = \frac{A' + iB' - iC' - D'}{A' + iB' - iC' - D'} \tag{3.23}$$

Where A', B', C' and D' are:

$$A' = \frac{k_{0z}}{\varepsilon_0}\left(\cos(\delta_1)\cos(\delta_2) - \frac{\varepsilon_1 k_{2z}}{\varepsilon_2 k_{1z}}\sin(\delta_1)\sin(\delta_2)\right) \tag{3.24}$$

$$B' = \frac{k_{0z}}{\varepsilon_0}\frac{k_{sz}}{\varepsilon_s}\left(\frac{\varepsilon_2}{k_{2z}}\cos(\delta_1)\sin(\delta_2) + \frac{\varepsilon_1}{k_{1z}}\sin(\delta_1)\cos(\delta_2)\right) \tag{3.25}$$

$$C' = \left(\frac{k_{1z}}{\varepsilon_1}\sin(\delta_1)\cos(\delta_2) + \frac{k_{2z}}{\varepsilon_2}\cos(\delta_1)\sin(\delta_2)\right) \tag{3.26}$$

$$D' = \frac{k_{sz}}{\varepsilon_s}\left(\cos(\delta_1)\cos(\delta_2) - \frac{\varepsilon_2 k_{1z}}{\varepsilon_1 k_{2z}}\sin(\delta_1)\sin(\delta_2)\right) \tag{3.27}$$

But the reflectance takes the form from equation (2.80):

$$\mathrm{R_p} = \left|\mathrm{r_p}\right|^2$$

Substituting equation (3.23) in the above equation, then the reflectance for four layers in TM case can written as:

$$\mathrm{R_p} = \frac{A'^2 + B'^2 + C'^2 + D'^2 - 2(A'D' + B'C')}{A'^2 + B'^2 + C'^2 + D'^2 + 2(A'D' + B'C')} \tag{3.28}$$

To compute the total transmittance by using equation (2.84):

$$\mathrm{T_p} = \mathrm{Re}\{\frac{\mathrm{k_{sz}}\varepsilon_0}{\mathrm{k_{oz}}\varepsilon_s}\}\left|\mathrm{t_p}\right|^2$$

Where the transmission amplitude from equation (2.79) equals:

$$t_p = \frac{2}{m_{11} + \frac{k_{sz}}{\varepsilon_s} m_{12} + \frac{\varepsilon_0}{k_{0z}} m_{21} + \frac{\varepsilon_0}{k_{0z}} \frac{k_{sz}}{\varepsilon_s} m_{22}}$$

After inserting the elements of transfer matrix from equation (3.18) it takes the form:

$$t_p = \frac{2 k_{0z}/\varepsilon_0}{A' + iB' + iC' + D'} \tag{3.29}$$

Substituting equation (3.29) into equation (2.84) and solving it, we can find the transmittance for four layers in TM case is given by the relation:

$$T_p = \frac{k_{sz} k_{0z}}{\varepsilon_0 \varepsilon_s} \cdot \frac{4}{A'^2 + B'^2 + C'^2 + D'^2 + 2(A'D' + B'C')} \tag{3.30}$$

3.4.3 Results and Discussions in TM case

Depending on the value of the all variables that given for each layer of the ARC in the sub section 3.3.3, where we need them in equations (3.28) and (3.30) to verify the reflectance and transmittance of the ARC in TM polarization. In this section, the optimum values of the parameters for the supposed structure in TM polarization are investigated.

In the study of the LHM parameters as the effective electric permittivity and magnetic permeability (ε_1, μ_1) in the supposed ARC in TM polarization, Figures (3.19) and (3.20) illustrate the changing in reflection and transmission due to the changing in ε_1 and μ_1, where we chose their products give 4 and assume the SiN_x layer with $\varepsilon_2 = 1.8^2$ and $\mu_2 = 1$.

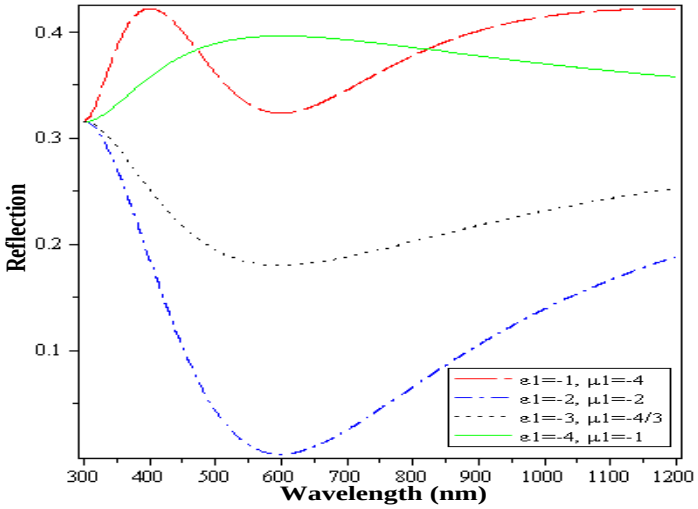

Figure (3.19): The reflectance versus the wavelength under normal incidence in TM case for different values of ε_1 and μ_1. Here, $L_1 = 75$ nm, $L_2 = 83.33\ nm$, $\varepsilon_2 = 1.8^2$ and $\mu_2 = 1$.

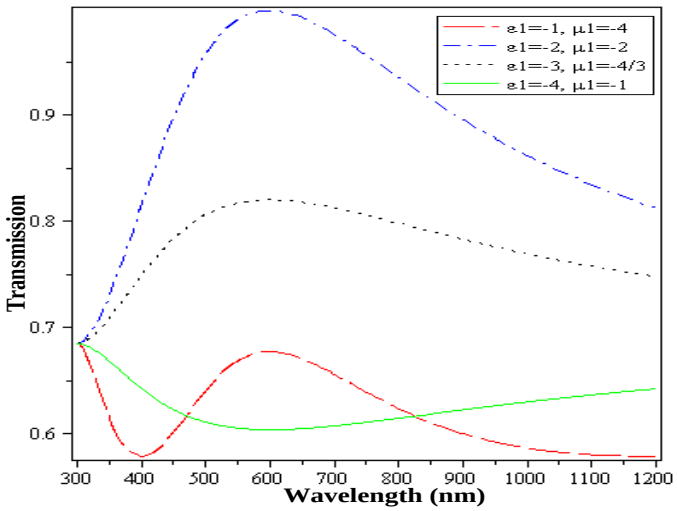

Figure (3.20): The transmittance the wavelength under normal incidence in TM case for different values of ε_1 and μ_1. Here, $L_1 = 75$ nm, $L_2 = 83.33\ nm$, $\varepsilon_2 = 1.8^2$ and $\mu_2 = 1$.

The previous Figures are matching with Figures (3.2) and (3.3), where they give the same results in the both polarization. The effective value of ε_1 and μ_1 of the LHM are ε_1=μ_1=-2, where the reflectance becomes very close to zero and the incidence light are transmitting through the ARC at 600nm. By changing the thickness of the LHM from $L_1 = 75$ nm to $L_1 = 10$ nm, all the values of ε_1 and μ_1 in the last Figures give the same transmission and reflection approximately in different wavelengths as Figures (3.21) and (3.22) show, but we still using -2 and -2 as values to ε_1 and μ_1, where they give the minimum reflection at the center of the required wavelength.

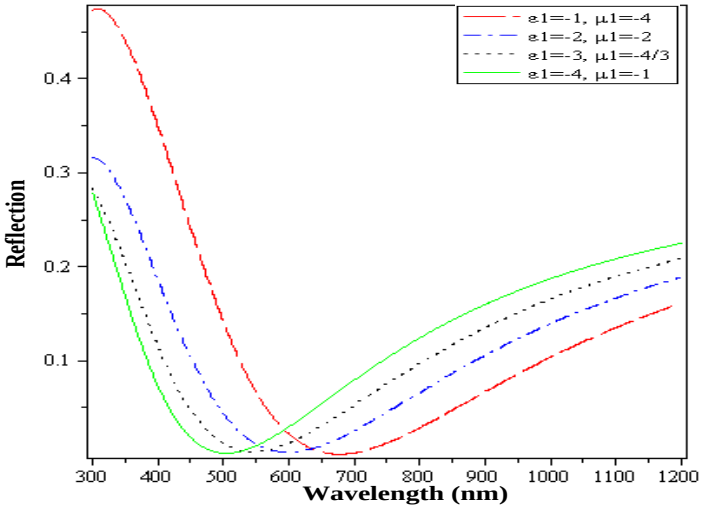

Figure (3.21): The reflectance versus the wavelength under normal incidence in TM case for different values of ε_1 and μ_1. Here, $L_1 = 10$ nm, $L_2 = 83.33\ nm$, $\varepsilon_2 = 1.8^2$ and $\mu_2 = 1$.

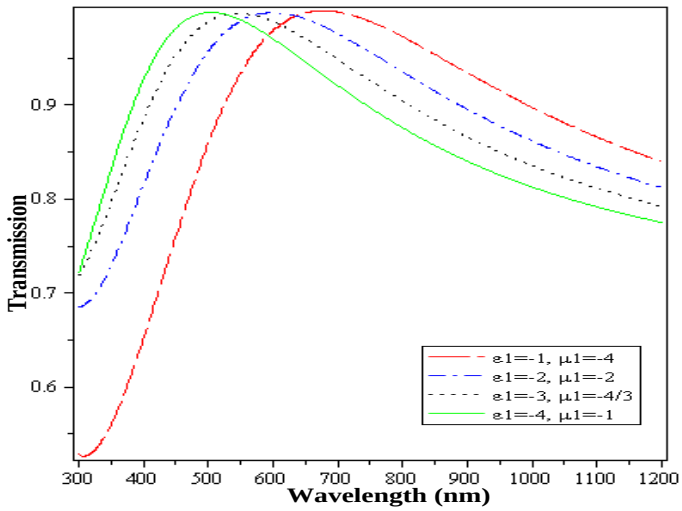

Figure (3.22): The transmittance versus the wavelength under normal incidence in TM case for different values of ε_1 and μ_1. Here, $L_1 = 10$ nm, $L_2 = 83.33\ nm$, $\varepsilon_2 = 1.8^2$ and $\mu_2 = 1$.

To check the effect of the LHM thickness (L_1), the reflectance and transmittance are plotted against wavelength for different thicknesses as illustrated in Figures (3.23) and (3.24). The LHM thickness (L_1=10, 50, 75 and 100) nm are chosen with the same SiN_x layer of $\varepsilon_2 = 1.8^2$ and the angle of incidence is fixed to 30°.

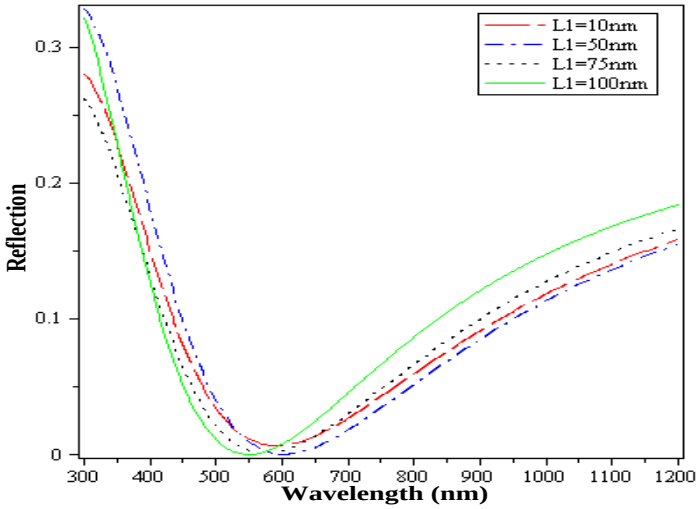

Figure (3.23): The reflectance versus the wavelength for different thicknesses of the LHM in TM case. Here, $\varepsilon_1 = \mu_1 = -2, L_2 = 83.33\ nm, \varepsilon_2 = 1.8^2$, $\mu_2 = 1$.and $\theta_0 = 30^\circ$.

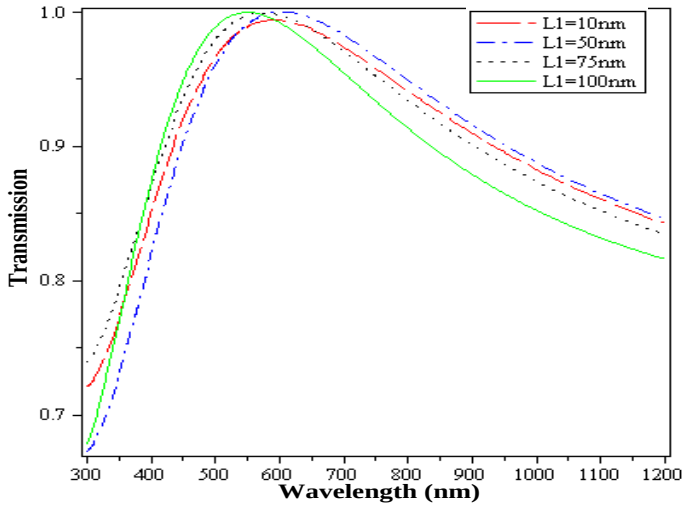

Figure (3.24): The transmittance versus the wavelength for different thicknesses of the LHM in TM case. Here, $\varepsilon_1 = \mu_1 = -2, L_2 = 83.33\ nm, \varepsilon_2 = 1.8^2$, $\mu_2 = 1$.and $\theta_0 = 30^\circ$.

The last two figures show that two thickness of the LHM layer give a minimum reflectance and maximum transmittance when $\theta_0 = 30^\circ$, where the thicknesses $L_1 = (50\ and\ 100)$ give a minimum reflection at (600 and 550) nm wavelength respectively. The angle of incidence has a greatly effect on the chosen thickness and the reflection as in Figures (3.25) and (3.26), and both reflection and transmission are slightly affected by changing the thickness of the LHM.

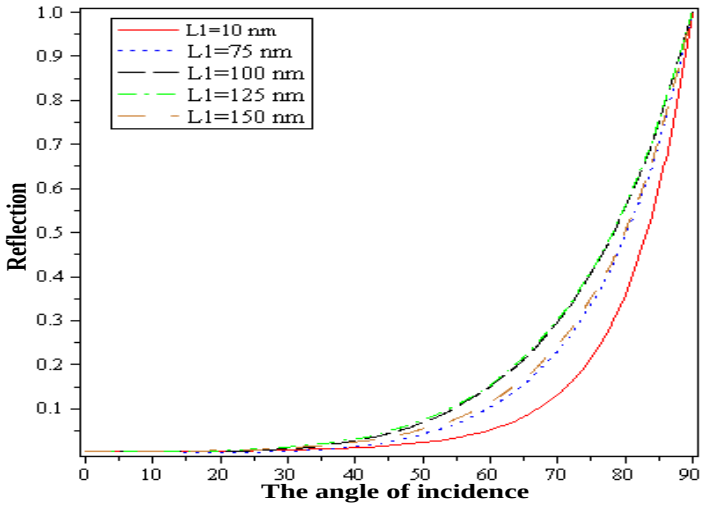

Figure (3.25): The reflectance versus the angle of incidence at 600 nm wavelength for different thicknesses of the LHM in TM case. Here, $\varepsilon_1 = \mu_1 = -2, L_2 = 83.33\, nm, \varepsilon_2 = 1.8^2$ *and* $\mu_2 = 1$.

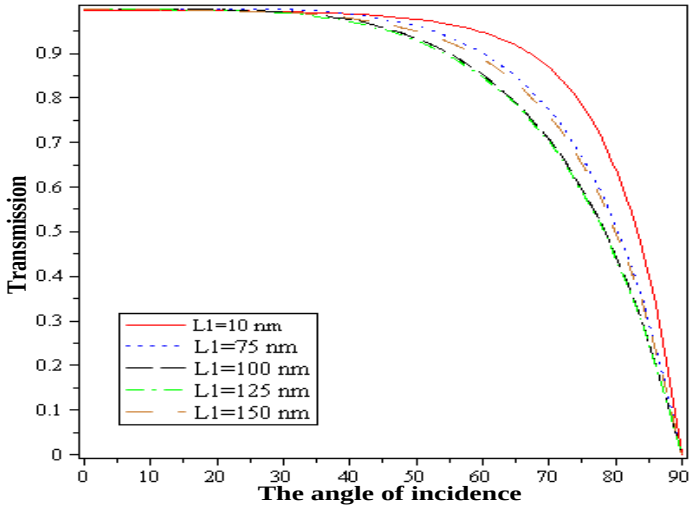

Figure (3.26): The transmittance versus the angle of incidence at 600 nm wavelength for different thicknesses of the LHM in TM case. Here, $\varepsilon_1 = \mu_1 = -2, L_2 = 83.33\, nm, \varepsilon_2 = 1.8^2$ *and* $\mu_2 = 1$.

There are a matching approximately in results between the thicknesses (75 and 150) nm where the both give the same interference. When the angle of incidence is greater than 30°, the perfect results at 600 nm wavelength is given by the thickness $L_1 = 10$ nm, but we chose the thickness of the LHM $L_1 = 50$ nm, where its minimum reflection is given at 600 nm when the angle of incidence equal 30°.

To search on the optimum values of the SiN_x variables, we start with the checking of the electric permittivity ε_2 for it. Assuming $\varepsilon_1 = -2$ and $\mu_1 = -2$ for the LHM layer with thicknesses $L_1 = 50\ nm$, Figures (3.27) and (3.28) indicate the changing in the reflectance and transmittance when ε_2 varying between (1.8^2 to 2.4^2) in the case of the normal incidence.

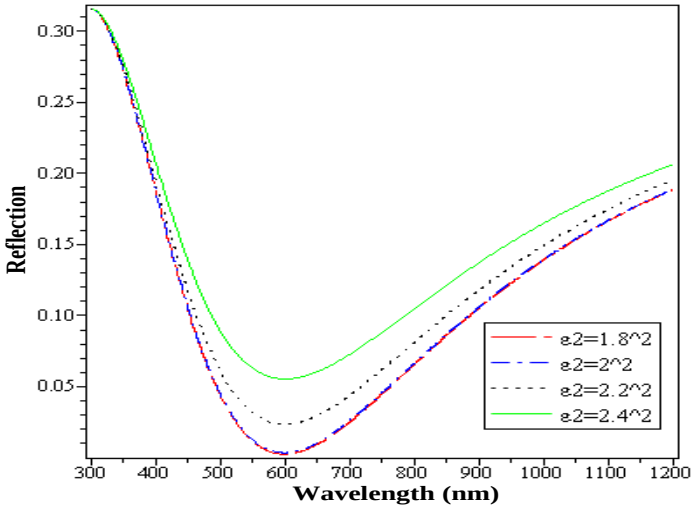

Figure (3.27): The reflectance versus the wavelength under normal incidence in TM case for different values of ε_2. Here, $\varepsilon_1 = \mu_1 = -2, L_1 = 50\ nm$ and $L_2 = 83.33\ nm$.

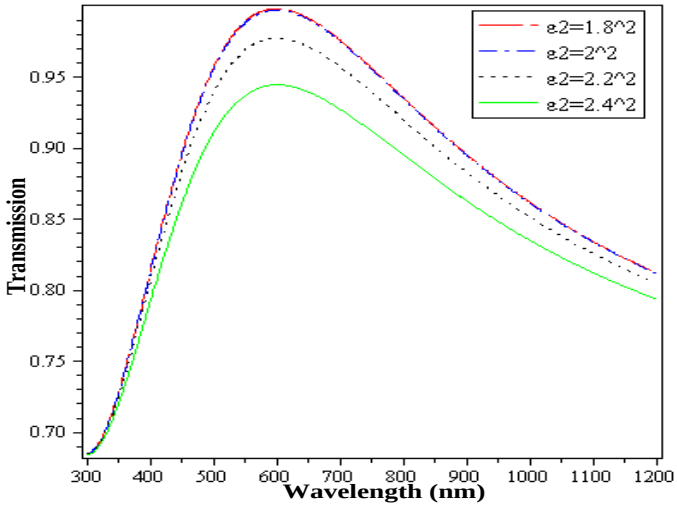

Figure (3.28): The transmittance versus the wavelength under normal incidence in TM case for different values of ε_2. Here, $\varepsilon_1 = \mu_1 = -2, L_1 = 50\ nm$ and $L_2 = 83.33\ nm$.

In the two cases of polarization, the structure of the ARC gives the same results of reflection and transmission under normal incidence when ε_2 change, where the

effective ε_2 for SiN_x layer can take two values (1.8^2 and 2^2) under normal incidence as Figures (3.10), (3.11), (3.27) and (3.28) illustrate.

Figures (3.29) and (3.30) illustrate a plotting of reflectance and transmission versus the wavelength. Reflectance minima and transmittance maxima are all the same for various values of L_2 but they are shifted to the right with higher values; but the values $L_2 = (50\ and\ 125\ )nm$ are ignored because there minimum reflection occur in the outside of the range (400-800) nm wavelengths. The optimal L_2that chosen in the structure is between (75-100) nm, where the thickness is determined at 600 nm wavelength from the relation ($L_x = \lambda/4|\sqrt{\varepsilon_x \mu_x}|$) that give $L_2 = 83.33$ nm and this results agree with TE results as Figures (3.12) and (3.13) show.

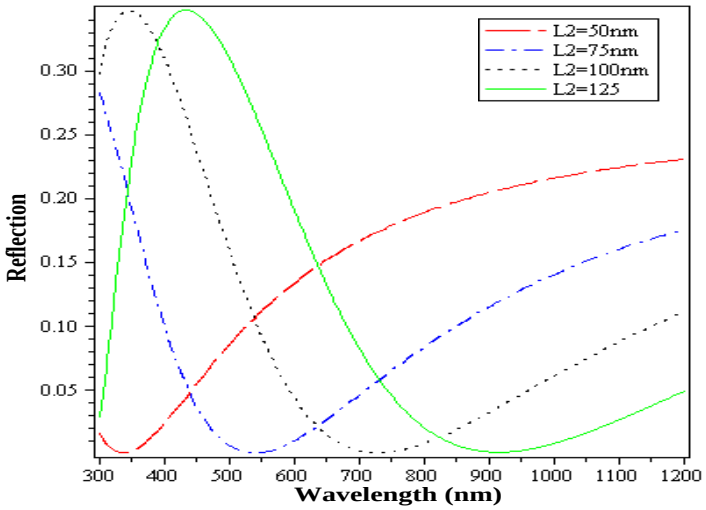

Figure (3.29): The reflectance versus the wavelength for different L_2 in TM case. Here, $\varepsilon_1 = \mu_1 = -2, \varepsilon_2 = 1.8^2$, $L_1 = 50nm$ and $\theta_0 = 30^\circ$.

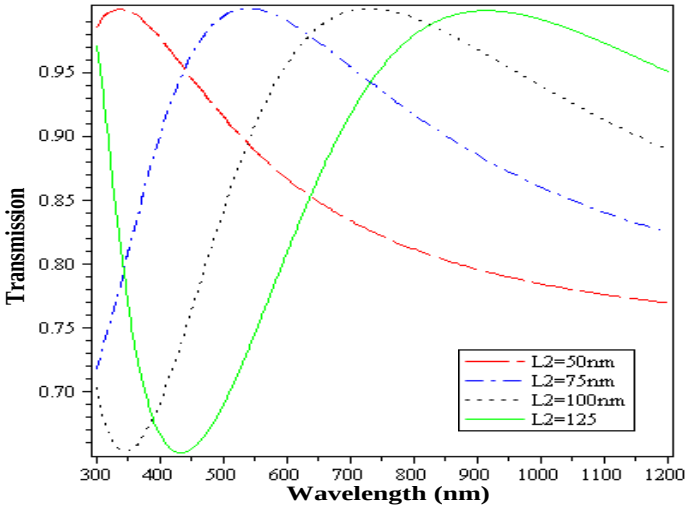

Figure (3.30): The transmittance versus the wavelength for different L_2 in TM case. Here, $\varepsilon_1 = \mu_1 = -2, \varepsilon_2 = 1.8^2$, $L_1 = 50nm$ and $\theta_0 = 30^\circ$.

The angle of incidence makes a large effect on the reflection and transmission through any sample. Figures (3.31) and (3.32) display the changing in reflection and transmission due to the variation in the angle of incidence against the wavelength for the light that incident in TM polarization.

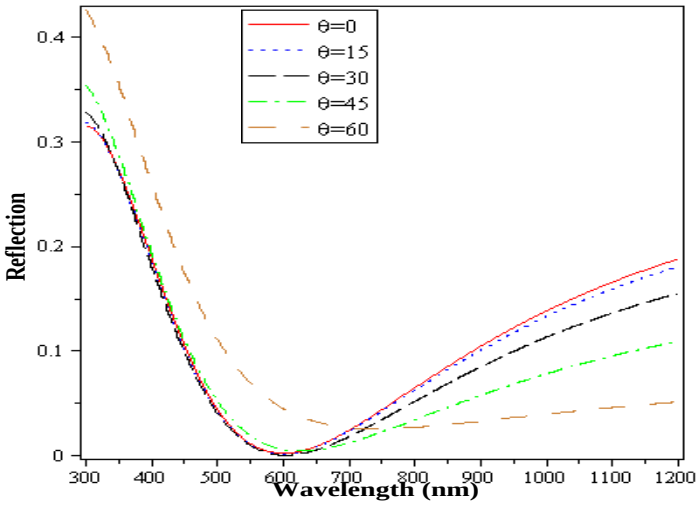

Figure (3.31): The reflectance versus the wavelength for different angles of incidence θ_0 in TM case. Here, $\varepsilon_1 = \mu_1 = -2$, $L_1 = 50nm, L_2 = 83.33\ nm$ and $\varepsilon_2 = 1.8^2$.

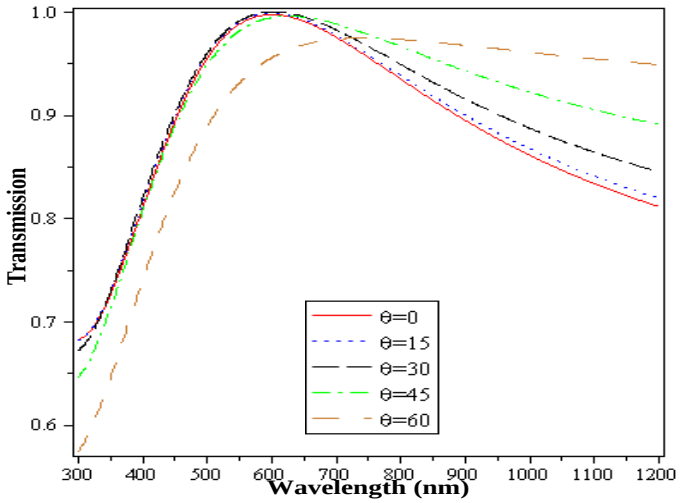

Figure (3.32): The transmittance versus the wavelength for different angles of incidence θ_0 in TM case. Here, $\varepsilon_1 = \mu_1 = -2$, $L_1 = 50nm$, $L_2 = 83.33\ nm$ and $\varepsilon_2 = 1.8^2$.

As the TE polarization, the minimum reflectance and maximum transmittance around 600 nm wavelength when the angle of incidence approaching to the normal incidence between $(0^\circ - 45^\circ)$, and as the angle of incidence increases, the optimal values of reflectance and transmittance are shifted towards smaller energy spectra but their extremes become no longer optimal.

Figures (3.33) and (3.34) indicate the reliance of the reflection and transmission on the angle of incidence for different wavelengths in the range of the desired photon flux , where the best angles of incidence that give a good ARC at 600 nm are between $(0^\circ - 45^\circ)$ in TM polarization.

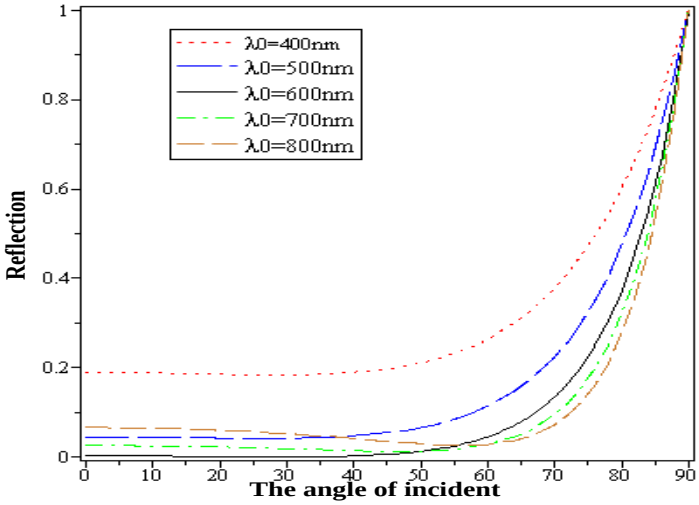

Figure (3.33): The reflectance versus the angles of incidence θ_0 with different wavelengths in TM case. Here, $\varepsilon_1 = \mu_1 = -2$, $L_1 = 50\ nm$, $L_2 = 83.33\ nm$ and $\varepsilon_2 = 1.8^2$.

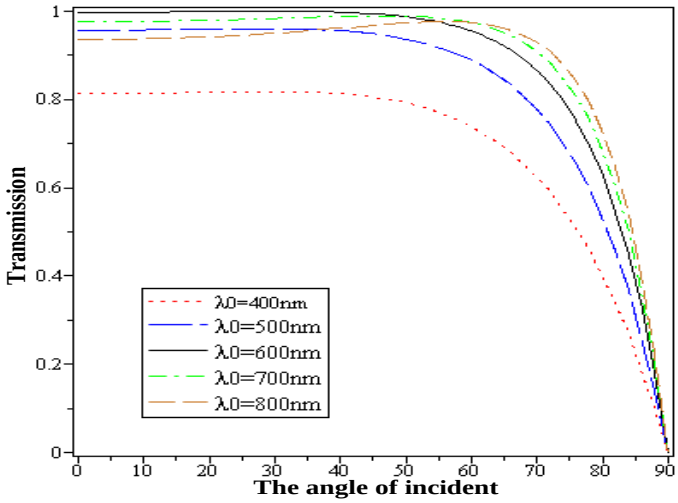

Figure (3.34): The transmittance versus the angles of incidence θ_0 with different wavelengths in TM case. Here, $\varepsilon_1 = \mu_1 = -2$, $L_1 = 50\ nm$, $L_2 = 83.33\ nm$ and $\varepsilon_2 = 1.8^2$.

3.5 The Average Results for TE and TM Polarizations

In this section we search on the optimal values for the proposed structure variables in the average of the two polarizations (TE and TM cases) to get a minimum reflectance and maximum transmittance. To compute the average of the reflectance and transmittance, we need the information in sections 3.2, 3.3 and 3.4 for the values of the structure variables and the results, by inserting them in the average equations of reflectance and transmittance, which can be given by:

$$R_{ave} = \frac{R_s + R_p}{2} \tag{3.31}$$

$$T_{ave} = \frac{T_s + T_p}{2} \tag{3.32}$$

where R_s, T_s, R_p and T_p are given by equations (3.13), (3.16), (3.28) and (3.30); respectively.

Let us start from the LHM layer where its thickness $L_1 = 75\,nm$ and the dielectric SiN_x with $\varepsilon_2 = 1.8^2$, $\mu_2 = 1$ and $L_2 = 83.33$. Figures (3.35) and (3.36) illustrate the impact of the permittivity and permeability for the LHM layer in the averages of reflectance and transmittance, where they are matching with the TE and TM cases.

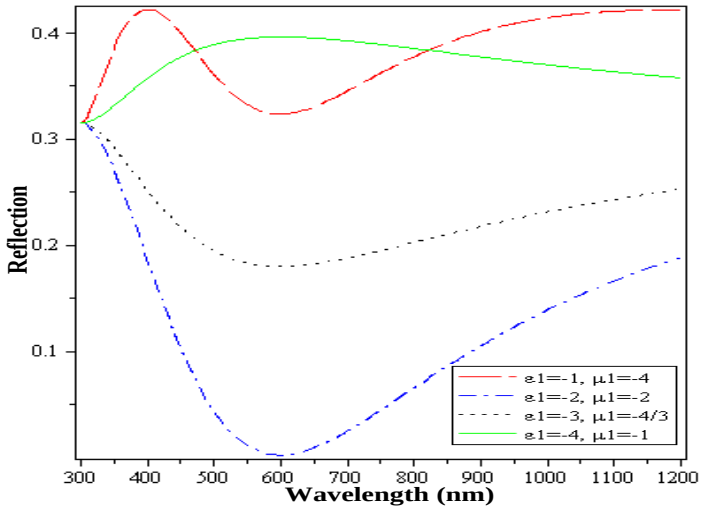

Figure (3.35): The average of reflectance versus the wavelength for different ε_1 and μ_1 under normal incidence, $L_1 = 75\,nm, L_2 = 83.33\,nm,\ \varepsilon_2 = 1.8^2$ and $\mu_2 = 1$.

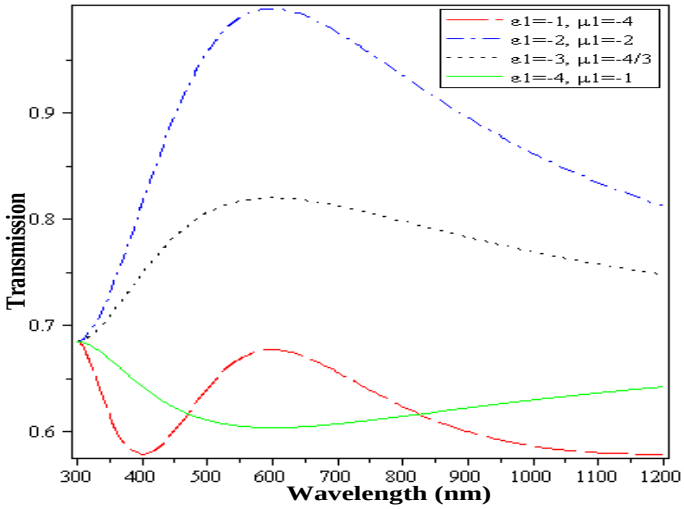

Figure (3.36): The average of Transmittance versus the wavelength for different ε_1 and $\mu_1$under normal incidence, $L_1 = 75\ nm, L_2 = 83.33\ nm,\ \varepsilon_2 = 1.8^2$ and $\mu_2 = 1$.

The preferable value of ε_1 and μ_1 are -2 and -2, where they give a minimum reflection and maximum transmission superior than the other values in the above figures, but the all of value in it can give the same results in deferent wavelength as in Figures (3.37) and (3.38).

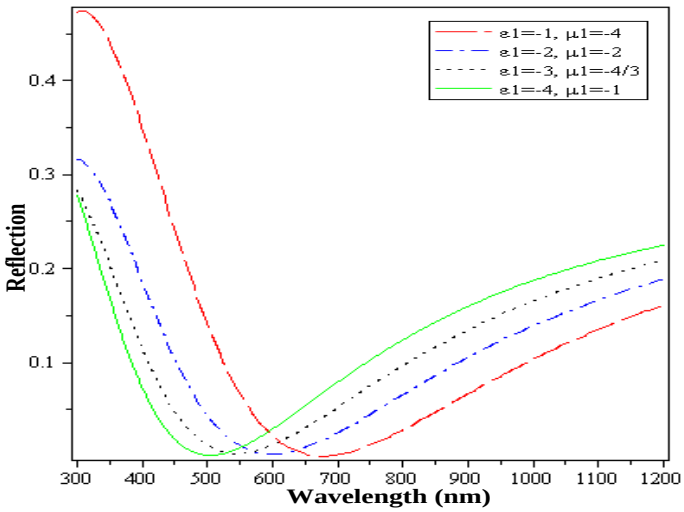

Figure (3.37): The average of reflectance versus the wavelength for different ε_1 and $\mu_1$under normal incidence, $\varepsilon_2 = 1.8^2$, $\mu_2 = 1$, $L_1 = 10$ nm and $L_2 = 83.33\ nm$.

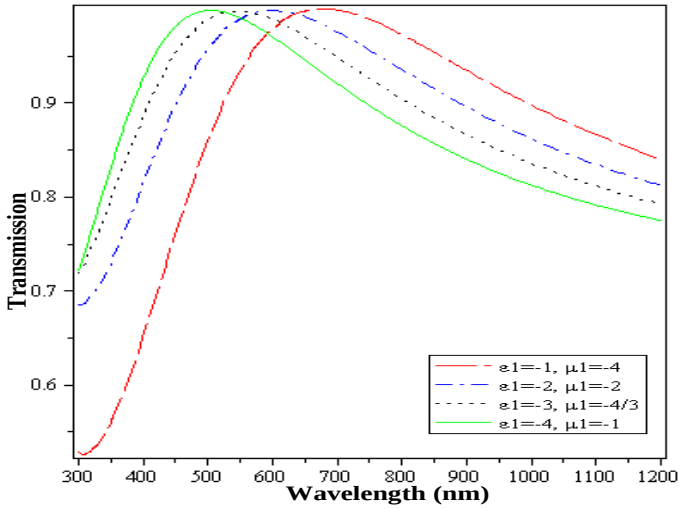

Figure (3.38): The average of transmittance versus the wavelength for different ε_1 and $\mu_1$under normal incidence, $\varepsilon_2 = 1.8^2$, $\mu_2 = 1$, $L_1 = 10$ nm and $L_2 = 83.33\ nm$.

In the last figures we change the thickness of the LHM layer from the relation $L_1 = 75$ nm to $L_1 = 10$ nm, we find several low reflections and high transmissions in different wavelength, but we use -2 and -2 as a value to ε_1 and μ_1 because it give the minimum reflectance in the center of the response light for solar cells.

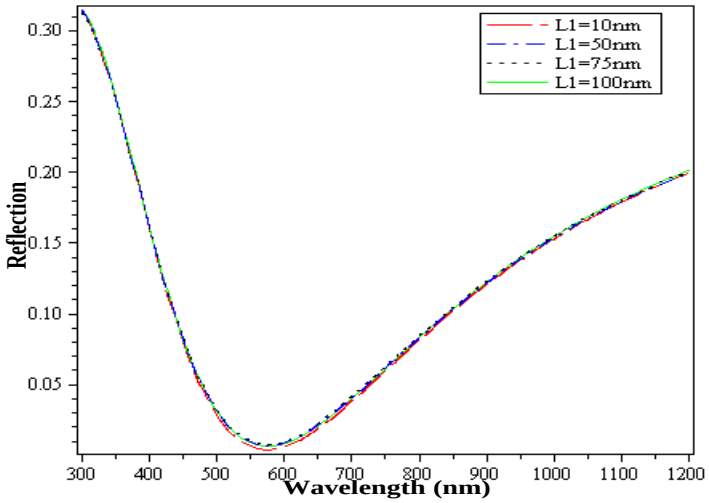

Figure (3.39): The average of reflectance versus the wavelength for different L_1, $\varepsilon_1 = \mu_1 = -2$, $\varepsilon_2 = 1.8^2$, $L_2 = 83.33\ nm\ and\ \theta_0 = 30^{\circ}$.

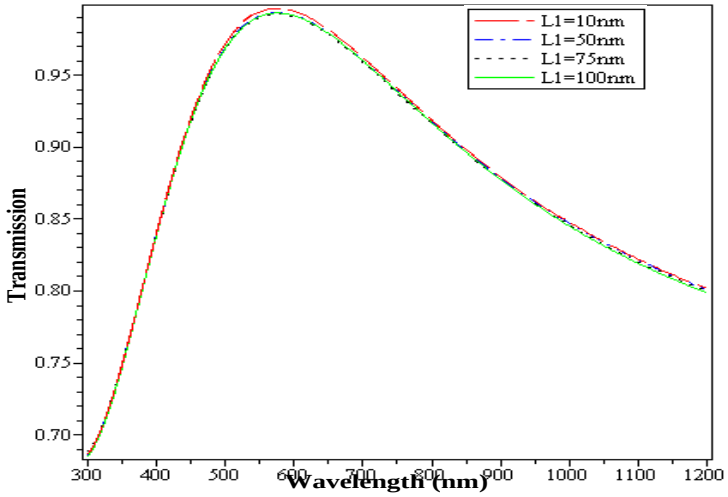

Figure (3.40): The average of transmittance versus the wavelength for different L_1, $\varepsilon_1 = \mu_1 = -2$, $\varepsilon_2 = 1.8^2$, $L_2 = 83.33\ nm\ and\ \theta_0 = 30^\circ$.

In Figures (3.39) and (3.40) the average of reflectance and transmittance are plotted versus the wavelength for different thickness of the LHM layer L_1. All of the thicknesses in the last figures can give the same results of reflectance and transmittance at $\theta_0 = 30^\circ$, but the chosen thickness for the LHM layer is $L_1 = 10$ nm, which gives a very small different. For more analysis of the effect of the thickness in the reflection and transmission Figures (3.41) and (3.42) illustrate this effect against the angle of incidence at 600 nm wavelength, where all of the thicknesses give approximately the same results until $\theta_0 = 35^\circ$, then there are some thicknesses characterized when the angle of incidence increase.

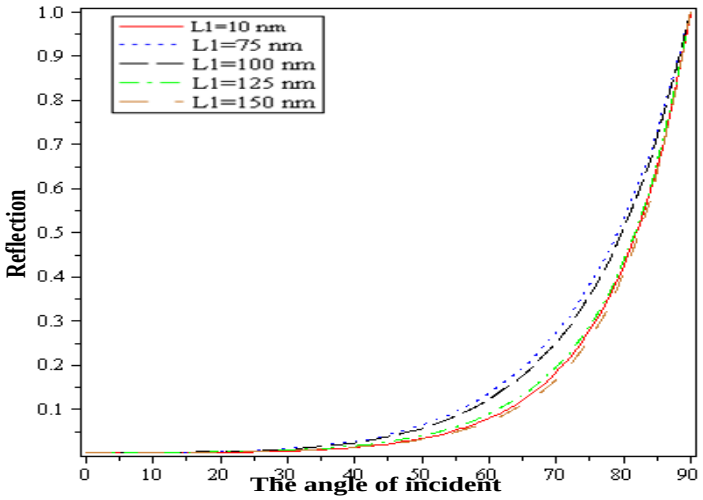

Figure (3.41): The average of reflectance versus the angle of incidence at 600 nm wavelength for different L_1, $\varepsilon_1 = \mu_1 = -2$, $\varepsilon_2 = 1.8^2$ and $L_2 = 83.33\ nm$.

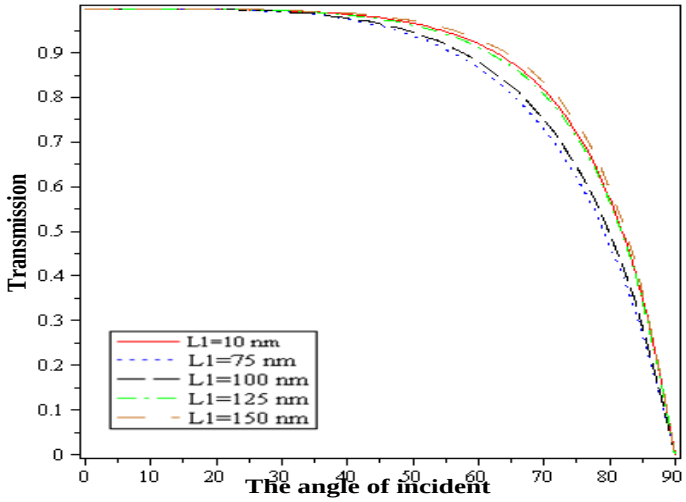

Figure (3.42): The average of transmittance versus the angle of incidence at 600 nm wavelength for different L_1, $\varepsilon_1 = \mu_1 = -2$, $\varepsilon_2 = 1.8^2$ and $L_2 = 83.33\ nm$.

Now to examine the dielectric layer (SiN_x), assume the LHM layer with $\varepsilon_1 = -2$, $\mu_1 = -2$ and $L_1 = 10$ nm, Figures (3.43) and (3.44) indicate the impact of ε_2 for SiN_x layer in the average of reflection and transmission against the wavelength, where ε_2 is chosen between 1.8^2 to 2.4^2.

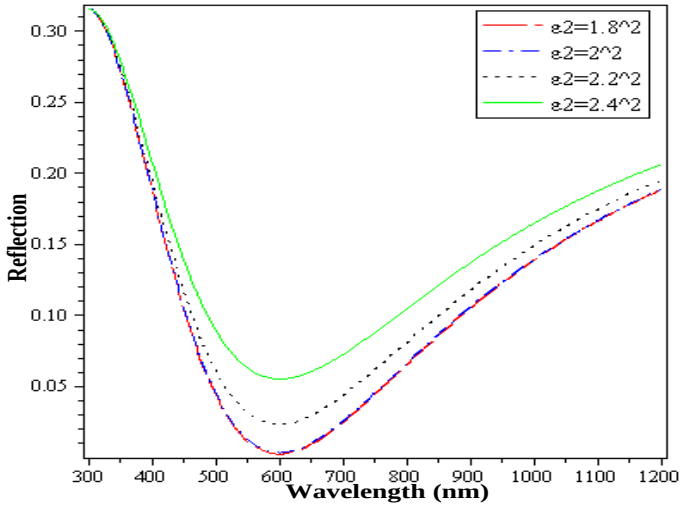

Figure (3.43): The average of reflectance versus the wavelength for different ε_2 under normal incidence, $\varepsilon_1 = \mu_1 = -2$, $L_1 = 10\text{nm}$, and $L_2 = 83.33\ nm$.

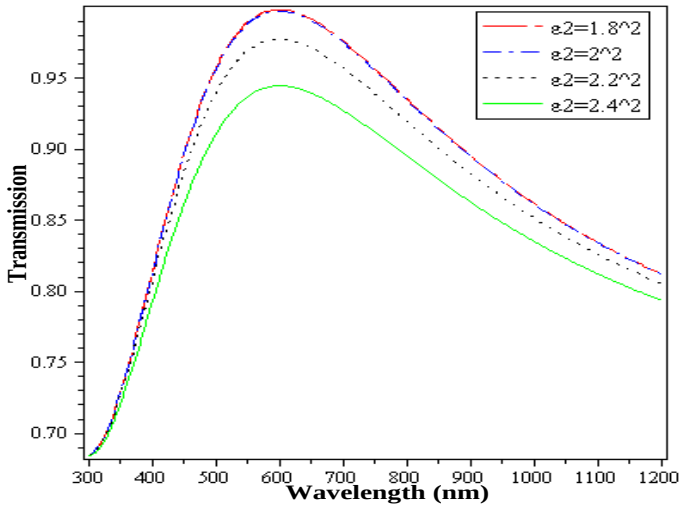

Figure (3.44): The average of transmittance versus the wavelength for different ε_2 under normal incidence, $\varepsilon_1 = \mu_1 = -2$, $L_1 = 10\text{nm}$ and $L_2 = 83.33\ nm$.

The above average figures give the same results to TE and TM polarization, where the optimal value of ε_2 for SiN_x can tack two values (1.8^2 and 2^2) to give a minimum reflection and maximum transmission at the case of normal incidence, but $\varepsilon_2 = 1.8^2$ is chosen, where it gives a better results than the others when the angle of incidence is changed.

Now to obtain the thickness of the SiN_x layer, assume $\varepsilon_2 = 1.8^2$ and the angle of incidence equal 30° and by changing the thickness of the SiN_x (L_2) between (50-

125) nm, there are several thicknesses can give the same results at different wavelength as in Figures (3.45) and (3.46).

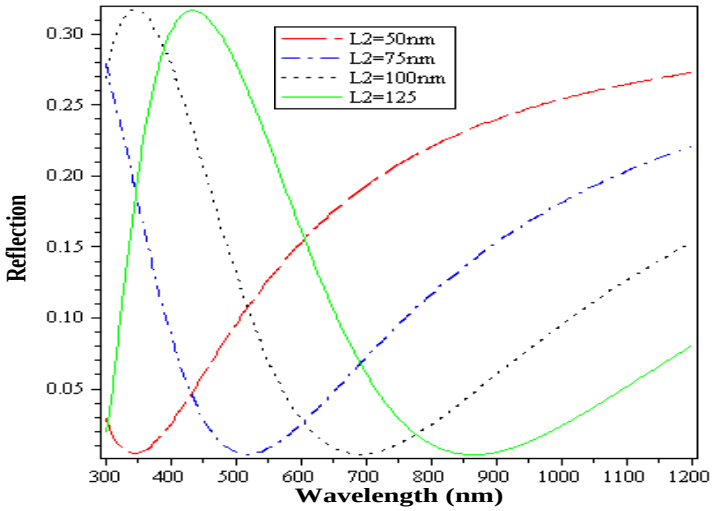

Figure (3.45): The average of reflectance versus the wavelength for different L_2. Here, $\varepsilon_1 = \mu_1 = -2$, $\varepsilon_2 = 1.8^2$, $\mu_2 = 1$, $L_1 = 10nm$ and $\theta_0 = 30^\circ$.

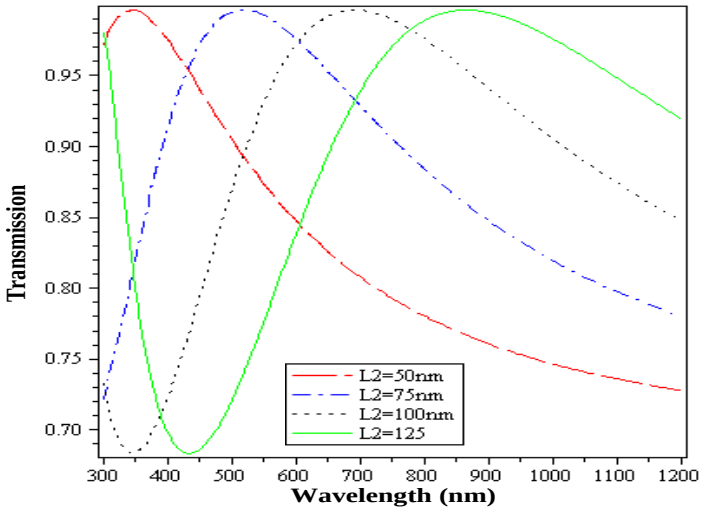

Figure (3.46): The average of transmittance versus the wavelength for different L_2. Here, $\varepsilon_1 = \mu_1 = -2$, $\varepsilon_2 = 1.8^2$, $\mu_2 = 1$, $L_1 = 10nm$ and $\theta_0 = 30^\circ$.

Reflectance minima and transmittance maxima are all the same for various values of L_2 but they are shifted to the right with higher values. The best behavior is seen for the two middle values (75 nm and 100 nm) since they occur in the desired range of the photon flux (400-800 nm wavelength) in good agreement with the best value of L_2=83.33nm which is calculated from the relation: $L_x = \lambda/4|\sqrt{\varepsilon_x \mu_x}|$ at 600 nm wavelength.

As we illustrate in TE and TM cases, the angle of incidence must be consider to get minimum reflection for the ARC at the required wavelength. To verify the effect of angle of incidence these values of parameters are put into consideration: $\varepsilon_2 = 1.8^2$ and $L_2 = 83.33$ nm are considered for the SiN_x layer and the LHM with $\varepsilon_1 = -2$, $\mu_1 = -2$ and $L_1 = 10$ nm. Figures (3.47) and (3.48) illustrate plottings of the average of reflectance and transmittance versus the wavelength for different angles of incidence, where the taken angles are $\theta_0 = (0^\circ, 15^\circ, 30^\circ, 45^\circ \; and \; 60^\circ)$.

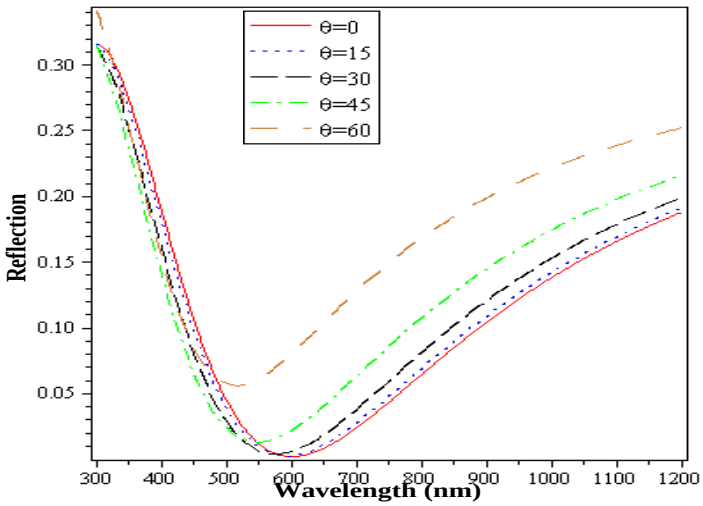

Figure (3.47): The average of reflectance versus the wavelength for different angles of incidence θ_0. Here, $\varepsilon_1 = \mu_1 = -2$, $L_1 = 10$ nm, $\varepsilon_2 = 1.8^2$ and $L_2 = 83.33$ nm.

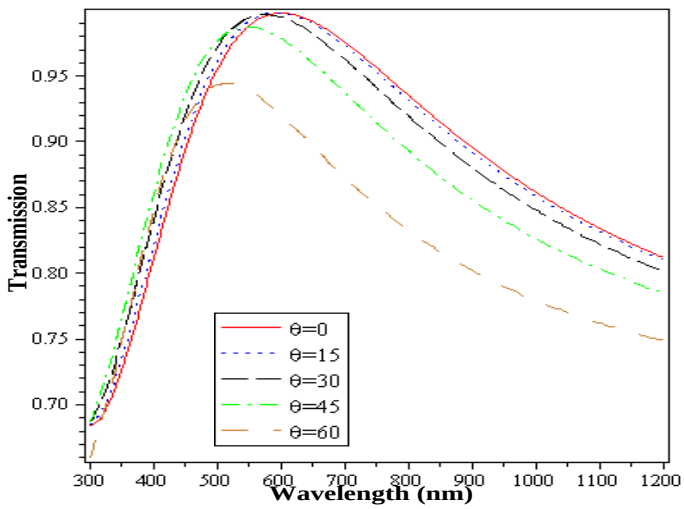

Figure (3.48): The average of transmittance versus the wavelength for different angles of incidence θ_0. Here, $\varepsilon_1 = \mu_1 = -2$, $L_1 = 10$ nm, $\varepsilon_2 = 1.8^2$ and $L_2 = 83.33$ nm.

As the TE and TM modes the effective angles that give the minimum reflection and maximum transmission at 600 nm wavelength is closed to the normal incidence even 45° and when the angle increases , the optimal values of reflectance and transmittance are shifted towards higher energy spectra but their extremes become no longer optimal. Figures (3.49) and (3.50) display in other way the effect of the angles of incidence on the average of reflectance and transmittance, It's clear from these two figures that the reflection is very close to zero and transmission is nearly unity when the angle of incidence is less than 45° at 600nm. When the angle of incidence increases, the reflection increases but there is another wavelength giving a low reflection when the angle of incidence from 45° to 65° at 500nm. When the angle of incidence is greater than 65° the reflection increases significantly for all the range of wavelength.

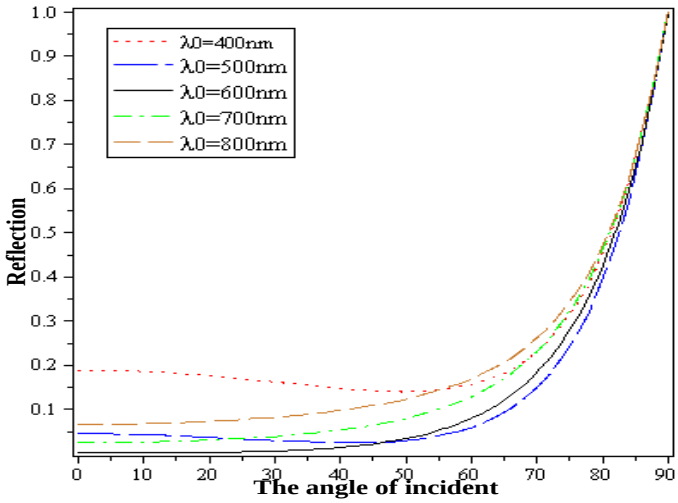

Figure (3.49): The average of reflectance versus the angle of incidence θ_0 for different wavelengths. Here, $\varepsilon_1 = \mu_1 = -2$, $L_1 = 10$ nm, $\varepsilon_2 = 1.8^2$ and $L_2 = 83.33$ nm.

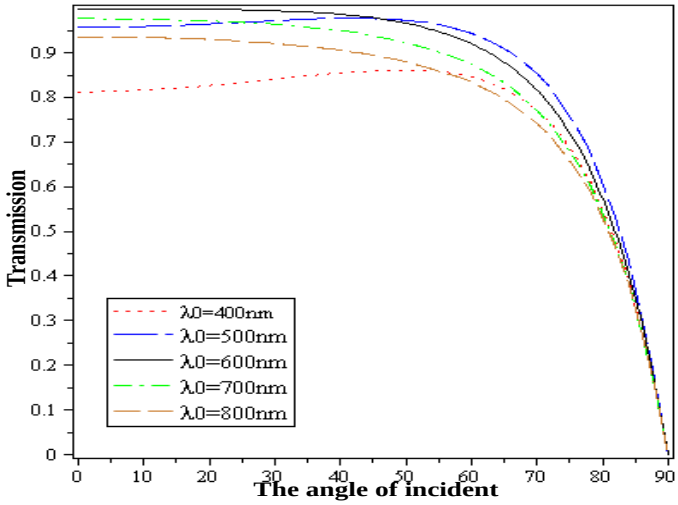

Figure (3.50): The average of transmittance versus the angles of incidence θ_0 for different wavelengths. Here, $\varepsilon_1 = \mu_1 = -2$, $L_1 = 10$ nm, $\varepsilon_2 = 1.8^2$ and $L_2 = 83.33$ nm.

Chapter 4
Optimize the Absorption for GaAs Solar Cells

Chapter 4

Optimize the Absorption for GaAs Solar Cells

4.1 Introduction

The idea of solar cells based on the concept of the photovoltaic effect, where the incidence photons with energy equal or higher than the band gap of the receiving material are absorbed as we explained in chapter 1. To increase the efficiency of solar cells and, the substrate is chosen from semiconductors with band gap between 1.0 to 1.8 ev, where the energy distribution of the solar spectrum is considered (Zeman, 2003). Gallium Arsenide (GaAs) is one of the optimum semiconductors for solar cells applications, where it has a band gap of 1.424 ev (Zdanowicz et al., 2005).

There are several investigations had been implemented to enhance the efficiency of GaAs solar cells, where ARCs and other ways are used as a method of light trapping and increase the transmission and absorption. Nakayama et al. (Nakayama, Tanabe, and Atwater, 2008) used plasmonic nanoparticles to improve light absorption in GaAs solar cells. Bahrami et al. studied the effects of ARCs on the performance of GaAs solar cells. Different materials are used in the ARCs and early the LHMs are deposited as a layer of it to enhance the absorption and decrease the reflection (Bahrami et al., 2013). Chen et al. presented to ARC using LHM for GaAs solar cells (Chen et al., 2010). Hamoche and Shabat give an investigation into ARC consist of glass/silicon nitride/LHM on a silicon substrate to enhance the absorption for silicon solar cells (Hamouche and Shabat, 2016).

In this chapter, we study the absorption of ARC that cause by the LHM in TE and TM polarization and compute the average of the both cases. Transfer matrix method and Maple 13 program are used to verify the results.

4.2 The Model Structure

In order to achieve high absorption for solar cells, we assume a multilayers ARC consist of four layers that similar to the structure mentioned in Figures (3.1) with replacement the sites of the LHM and dielectric layers as Figure (4.1) demonstrate. we consider the first layer is air with $\varepsilon_0 = 1$ and $\mu_0 = 1$, the second layer is $Si N_x$ as a dielectric material with electric permittivity (ε_1) take the values

between 1.8^2 to 2.4^2 (Lee et al., 2012), where we assume its magnetic permeability $\mu_1 = 1$, the third layer is LHM with different electric permittivity ε_2 and the magnetic permeability μ_2 is assumed to be -1 (Hamouche and Shabat, 2016) and the last layer is GaAs as a substrate with $\varepsilon_s = 12.7$ and $\mu_s = 1$.

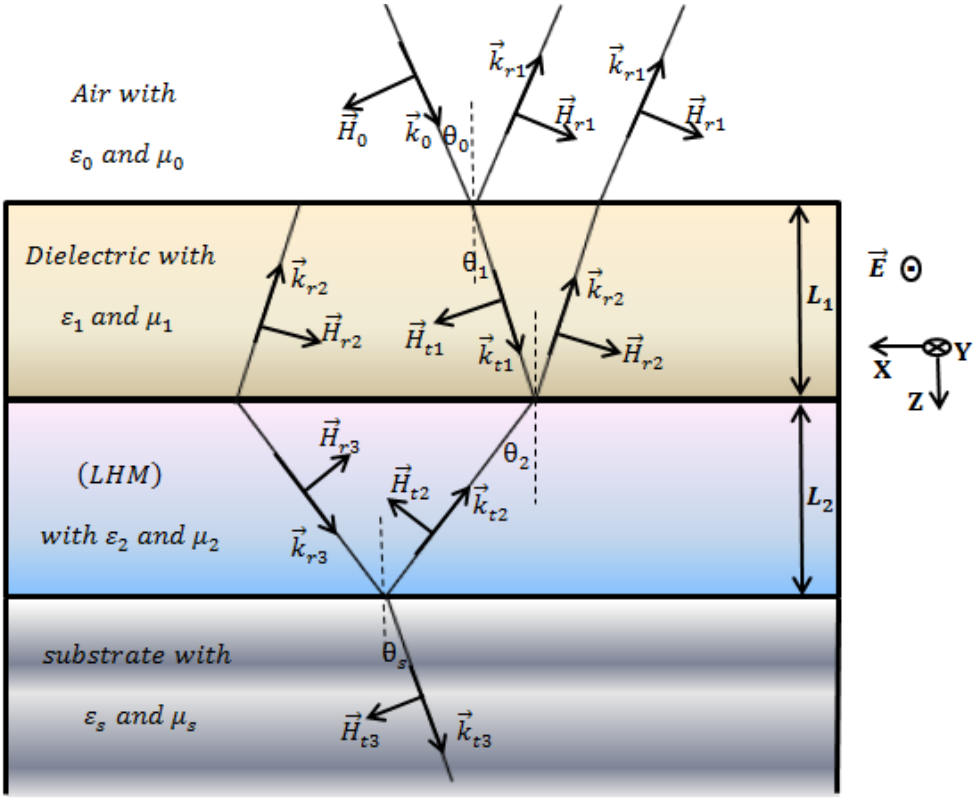

Figure (4.1): Four layers ARC under TE polarization of light.

The angles in the above figures $\theta_0, \theta_1, \theta_2$ *and* θ_s represent the angles of incidence in air, refraction in the dielectric, refraction in the LHM and refraction in the substrate respectively. The SiN_x layer takes the thickness $L_1 = 70\ nm$ and the thickness of the LHM is $L_2 = 3.97\ \mu m$ (Hamouche and Shabat, 2016).

4.3 Optimize the Absorption in TE Mode

To compute the absorption for the four layers ARC in the previous section we need to determine the reflectance and transmittance by using equations (3.13) and (3.16) for the TE polarization then the absorbances can be determined from the relation:

$$A(\lambda) = 1 - R(\lambda) - T(\lambda) \tag{4.1}$$

In the beginning of checking the ARC parameter, we start from the electric permittivity for the LHM (ε_2), which can be calculate from the relation $\varepsilon_2 = -(n_2)^2$, where different values of n_2 have been used at different wavelengths (Hamouche and Shabat, 2016) as Figures (4.2), (4.3) and (4.4) indicate.

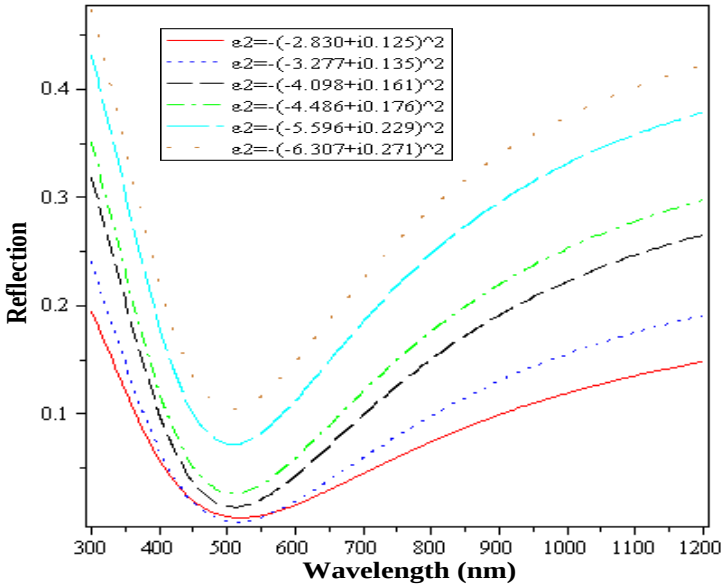

Figure (4.2): The reflectance versus the wavelength for different ε_2 for the LHM under normal incidence in TE case, $\varepsilon_1 = 1.8^2$, $L_1 = 70\ nm$ and $L_2 = 3.97\ \mu m$.

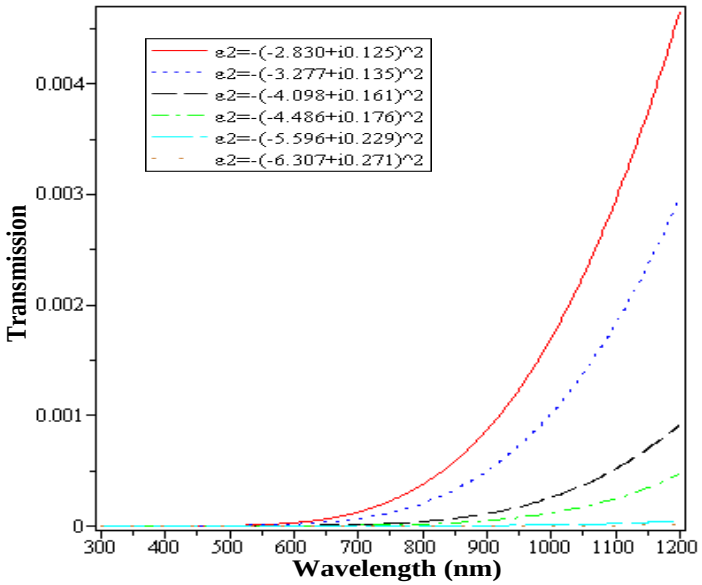

Figure (4.3): The transmittance versus the wavelength for different ε_2 for the LHM under normal incidence in TE case, $\varepsilon_1 = 1.8^2$, $L_1 = 70\ nm$ and $L_2 = 3.97\ \mu m$.

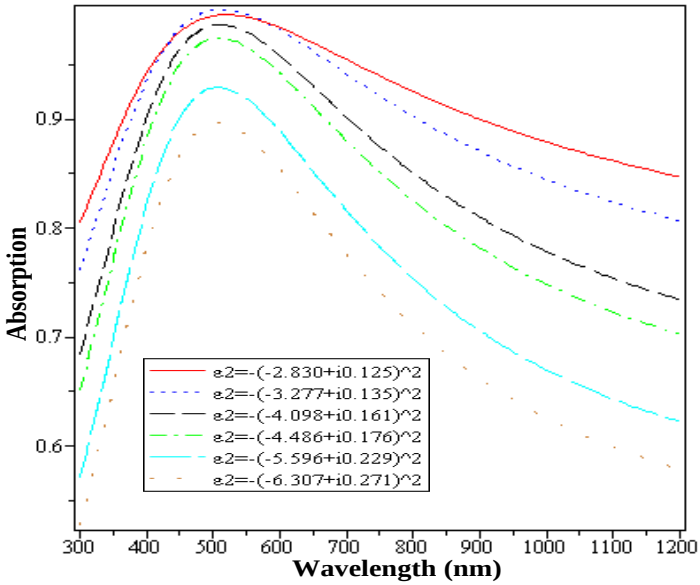

Figure (4.4): The absorbance versus the wavelength for different ε_2 for the LHM under normal incidence in TE case, $\varepsilon_1 = 1.8^2$, $L_1 = 70\ nm$ and $L_2 = 3.97\ \mu m$.

The above figures illustrate the reflection, transmission and absorption for different values of ε_2 in range of wavelength between (300-1200) nm, where the electric permittivity for the SiN_x layer is assumed to be 1.8^2 in the case of normal incidence. The minimum values of reflection and maximum values of absorbances appear when the permittivity of the LHM layer $\varepsilon_2 = -(-3.277 + i0.135)^2$ at (450-550) nm wavelength, but in the out of that range of wavelength $\varepsilon_2 = -(-2.830 + i0.125)^2$ can give results better than the previous value as in Figures (4.2) and (4.4). Figure (4.3) shows the transmittance, which goes to zero for all values of ε_2 until 600 nm wavelengths and after that wavelength it is starting rise, but their value is still close to zero where it can be neglected.

If the permittivity for SiN_x (ε_1) is changed between 1.8^2 to 2.4^2, all of values of ε_2 in the last figures can give a good results in different wavelength as Figures (4.5), (4.6), (4.7), (4.8), (4.9) and (4.10) indicate.

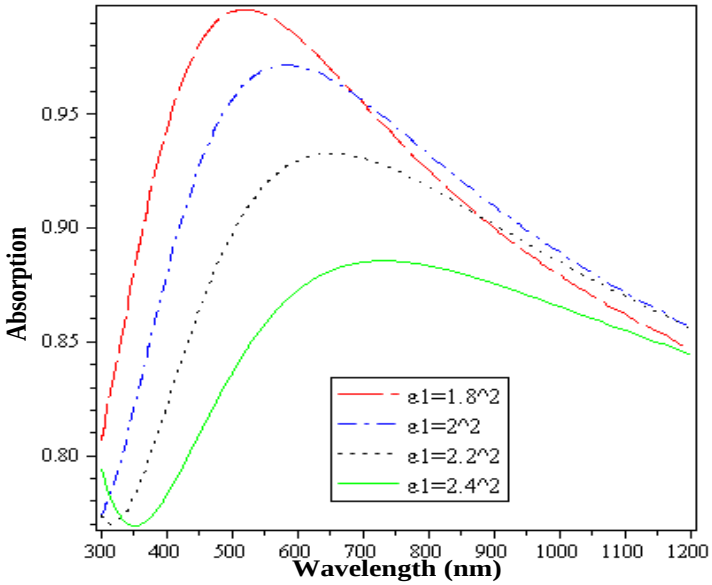

Figure (4.5): The absorbance versus the wavelength for different ε_1 for SiN_x under normal incidence in TE case, $\varepsilon_2 = -(-2.830 + i0.125)^2$, $L_1 = 70\ nm$ and $L_2 = 3.97\ \mu m$.

In the previous figure, the optimal value of ε_1 for SiN_x is 1.8^2 when $\varepsilon_2 = -(-2.830 + i0.125)^2$, which gives 99.56% absorption at 520 nm wavelength and at the boundary of effective wavelength for solar cells give 80.57% and 84.69% absorption at 300 nm and 1200 nm wavelength respectively, these results make it a perfect absorbent ARC.

Figure (4.6) illustrates the effect of ε_1 for SiN_x when $\varepsilon_2 = -(-3.277 + i0.135)^2$, which the optimal results are given by $\varepsilon_1 = 1.8^2$. The maximum value of absorption for this structure is better than the previous, which give 99.99% absorption at 515 nm wavelength, but in the boundary of the supposed range of wavelength the previous structure seem better, where the present structure takes 76% and 80.64% absorbances at 300 nm and 1200 nm wavelengths; respectively.

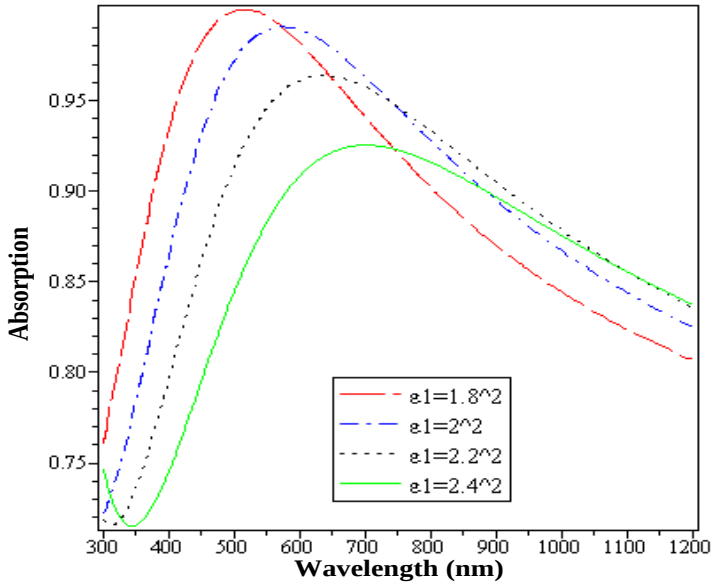

Figure (4.6): The absorbance versus the wavelength for different ε_1 for SiN_x under normal incidence in TE case, $\varepsilon_2 = -(-3.277 + i0.135)^2$, $L_1 = 70\ nm$ and $L_2 = 3.97\ \mu m$.

Figure (4.7) indicates the variation in the absorption against the wavelength for the different values of ε_1 for SiN_x when $\varepsilon_2 = -(-4.098 + i0.161)^2$ for the LHM layer, where the maximum absorption reach 99.98% and appears at 570 nm wavelength when $\varepsilon_1 = 2^2$. In contrast, the minimum value of absorption amount to 63.78% at 300 nm wavelength.

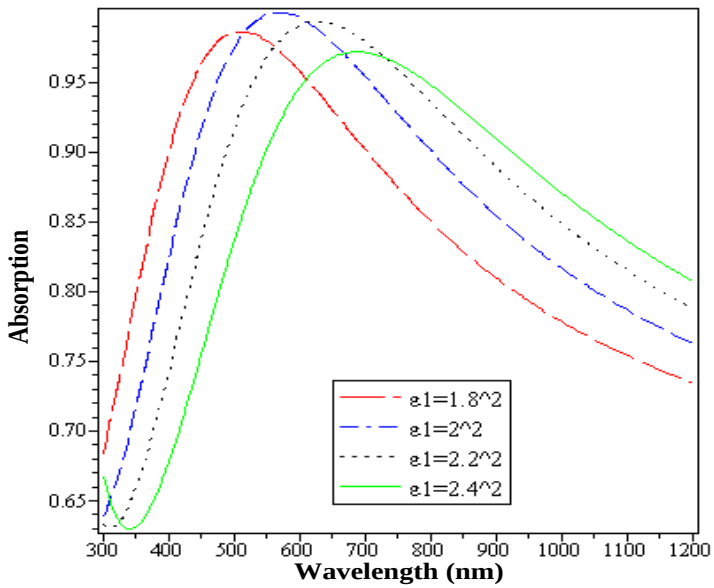

Figure (4.7): The absorbance versus the wavelength for different ε_1 for SiN_x under normal incidence in TE case, $\varepsilon_2 = -(-4.098 + i0.161)^2$, $L_1 = 70\ nm$ and $L_2 = 3.97\ \mu m$.

The below figures indicate the absorbance versus the wavelength for different ε_1 for SiN_x, where each figure deals with different ε_2 for LHM. In Figure (4.8), the LHM layer takes $\varepsilon_2 = -(-4.486 + i0.176)^2$, which gives 99.86% absorption with $\varepsilon_1 = 2.2^2$ at 625 nm wavelength, also it can give 99.65% absorption with $\varepsilon_1 = 2^2$ at 570 nm wavelength. In Figures (4.9), we consider $\varepsilon_2 = -(-5.596 + i0.229)^2$, which has 99.98% absorption at 680 nm wavelength with $\varepsilon_1 = 2.4^2$ and when $\varepsilon_1 = 2.2^2$ it has 99.45% absorption at 625 nm wavelength. For the value $\varepsilon_2 = -(-6.307 + i0.271)^2$ in Figure (4.10), we can get 99.78% absorption at 680 nm wavelength.

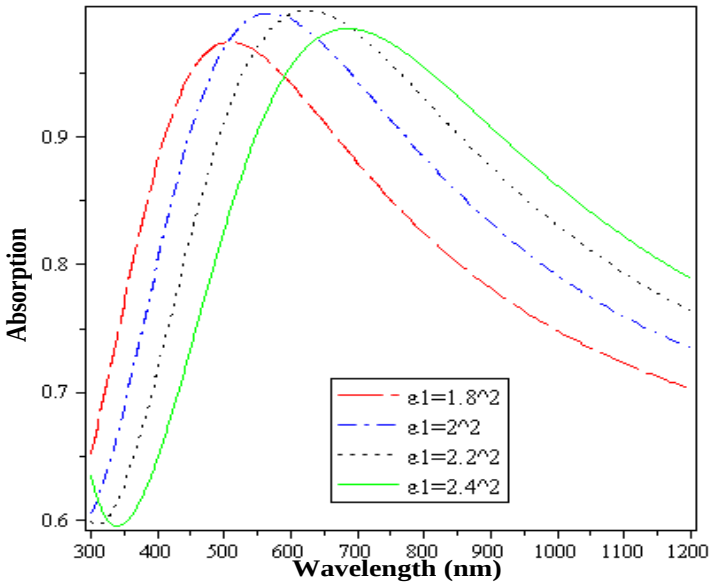

Figure (4.8): The absorbance versus the wavelength for different ε_1 for SiN_x under normal incidence in TE case, $\varepsilon_2 = -(-4.486 + i0.176)^2$, $L_1 = 70\ nm$ and $L_2 = 3.97\ \mu m$.

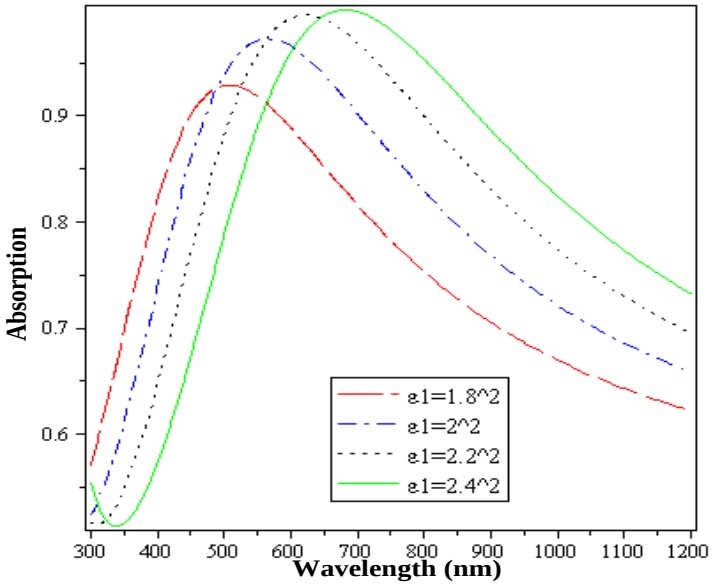

Figure (4.9): The absorbance versus the wavelength by changing ε_1 for SiN_x under normal incidence in TE case, $\varepsilon_2 = -(-5.596 + i0.229)^2$, $L_1 = 70\ nm$ and $L_2 = 3.97\ \mu m$.

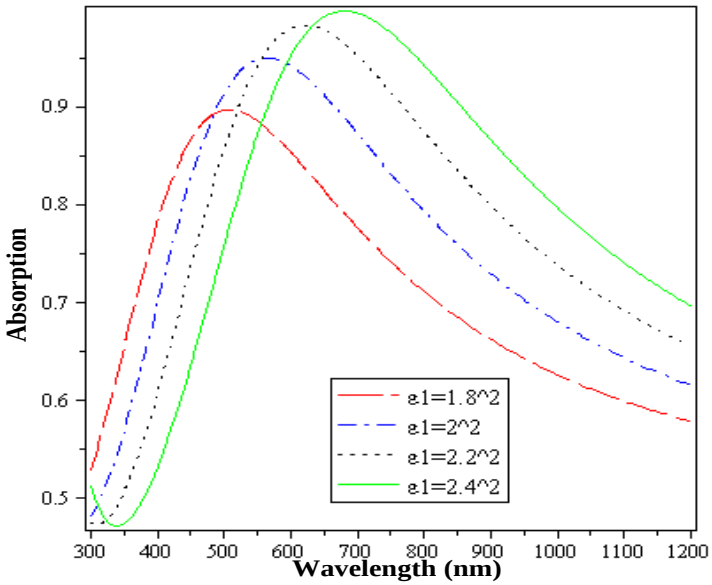

Figure (4.10): The absorbance versus the wavelength for different ε_1 for SiN_x under normal incidence in TE case, $\varepsilon_2 = -(-6.307 + i0.271)^2$, $L_1 = 70\ nm$ and $L_2 = 3.97\ \mu m$.

Although of the high maximum value of absorption in the last four figures, it still have low minimum value at the boundary of the effective wavelength for solar cells with respect to Figures (4.4) and (4.5), so the values $\varepsilon_2 = -(-2.830 + i0.125)^2$ and $\varepsilon_2 = -(-3.277 + i0.135)^2$ for the LHM with $\varepsilon_1 = 1.8^2$ for the SiN_x layer are adopted.

To search on the effect of angle of incidence on the absorbance, the next figures illustrate the variation in absorption against wavelength for different angles of incidence, where Figure (4.11) use $\varepsilon_2 = -(-2.830 + i0.125)^2$ for LHM and Figures (4.12) use $\varepsilon_2 = -(-3.277 + \mathrm{i}0.135)^2$ for LHM and $\varepsilon_1 = 1.8^2$ for SiN_x to the both figures. We can get good results for this structure, when the angle of incidence is below 45°.

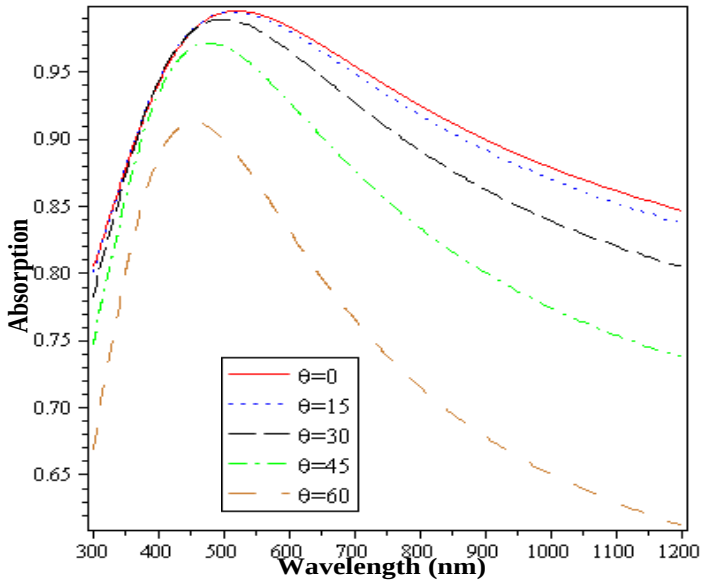

Figure (4.11): The absorbance versus the wavelength for different angles of incidence with $\varepsilon_1 = 1.8^2$, $L_1 = 70\ nm$, $L_2 = 3.97\ \mu m$ and $\varepsilon_2 = -(-2.830 + \mathrm{i}0.125)^2$ in TE case.

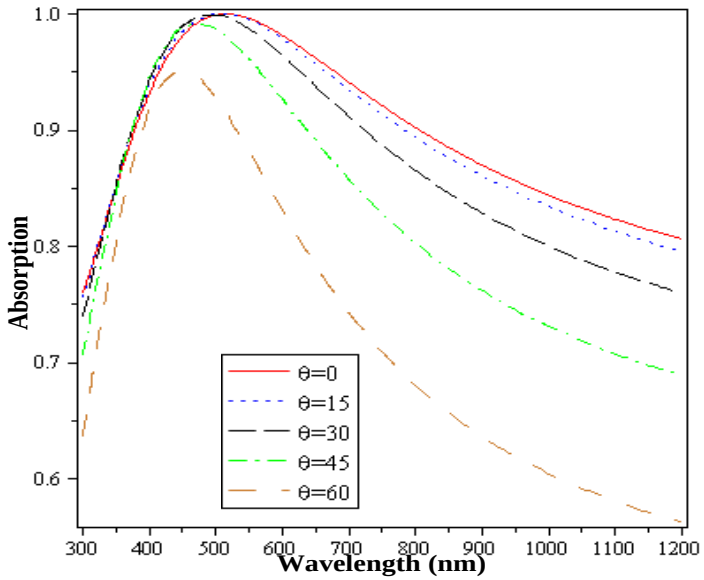

Figure (4.12): The absorbance versus the wavelength for different angles of incidence with $\varepsilon_1 = 1.8^2$, $L_1 = 70\ nm$, $L_2 = 3.97\ \mu m$ and $\varepsilon_2 = -(-3.277 + \mathrm{i}0.135)^2$ in TE case.

As the angle of incidence increases, the optimal values of reflectance and transmittance are shifted towards higher energy spectra but their extremes become no longer optimal.

Figures (4.13) and (4.14) illustrate in other way the effect of the angle of incidence on the absorbance for different wavelengths and prove the previous results, where the angle of incidence has high absorption until 45° and then the absorption is decreasing clearly and rapidly.

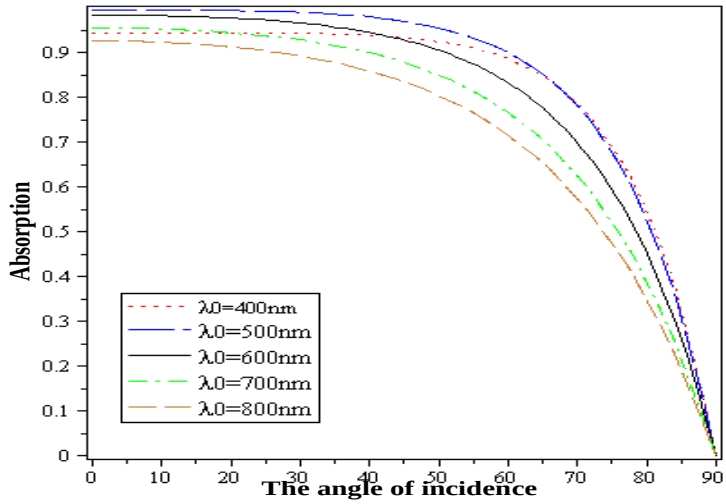

Figure (4.13): The absorbance versus the angles of incidence for different wavelengths with $\varepsilon_1 = 1.8^2, L_1 = 70\ nm, L_2 = 3.97\ \mu m$ and $\varepsilon_2 = -(-2.830 + i0.125)^2$ in TE case.

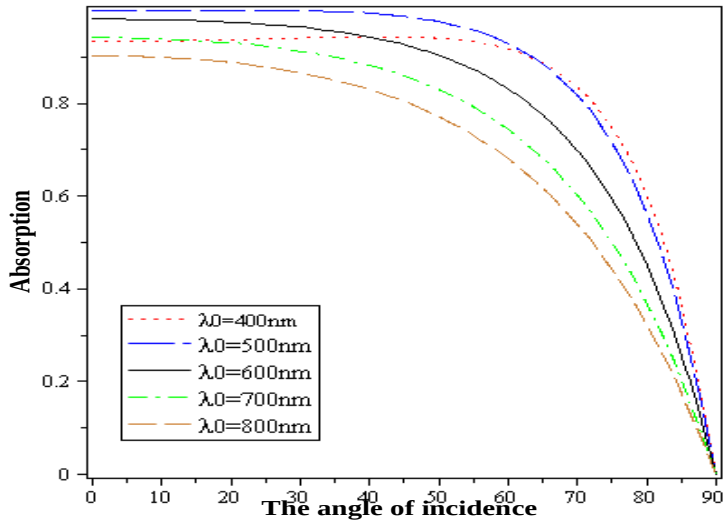

Figure (4.14): The absorbance versus the angles of incidence for different wavelengths with $\varepsilon_1 = 1.8^2, L_1 = 70\ nm, L_2 = 3.97\ \mu m$ and $\varepsilon_2 = -(-3.277 + i0.135)^2$ in TE case.

4.4 Optimize the Absorption in TM Mode

Consider the proposed structure and the values of each layer in section 4.2, in this section the effect of LHM in absorbance for TM polarization is determined, where equations (3.28), (3.30) and (4.1) are used.

If we chose $\varepsilon_1 = 1.8^2$ for SiN_x to determine the effective value of ε_2 for LHM, Figures (4.15), (4.16) and (4.17) illustrate the reflection, transmission and absorbances; respectively, where the reflectance goes to zero when ε_2 take the value $-(-3.277 + i0.135)^2$ and all of incidence light between (450-550) nm wavelengths are absorbed approximately. Due to the low values of the transmittance for all values of ε_2, the transmission can be omitted.

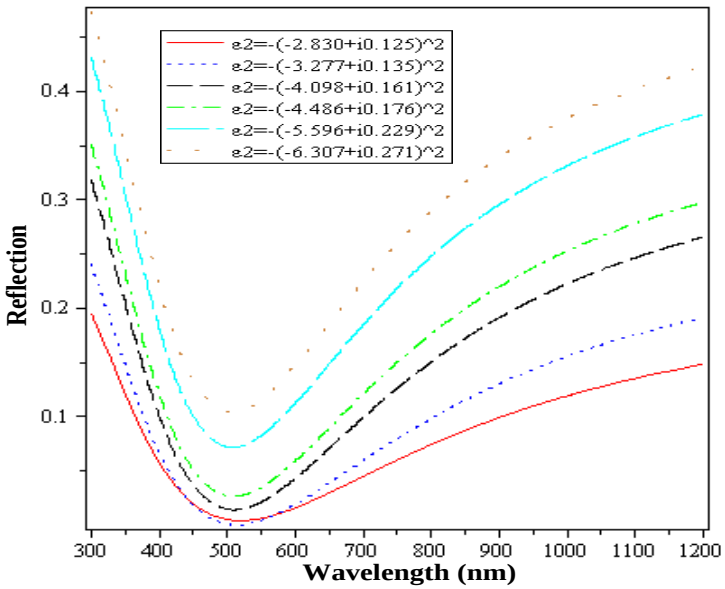

Figure (4.15): The reflectance versus the wavelength for different ε_2 for the LHM under normal incidence in TM case, $\varepsilon_1 = 1.8^2$, $L_1 = 70\ nm$ and $L_2 = 3.97\ \mu m$.

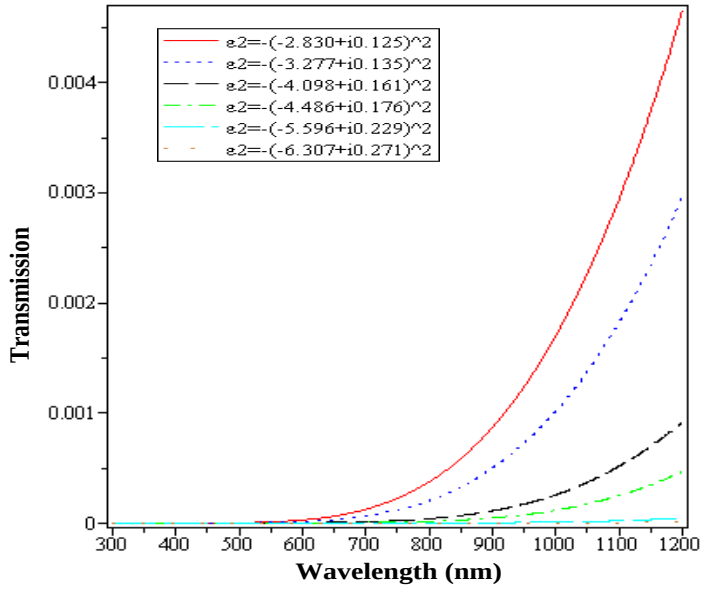

Figure (4.16): The transmittance versus the wavelength for different ε_2 for the LHM under normal incidence in TM case, $\varepsilon_1 = 1.8^2$, $L_1 = 70\ nm$ and $L_2 = 3.97\ \mu m$.

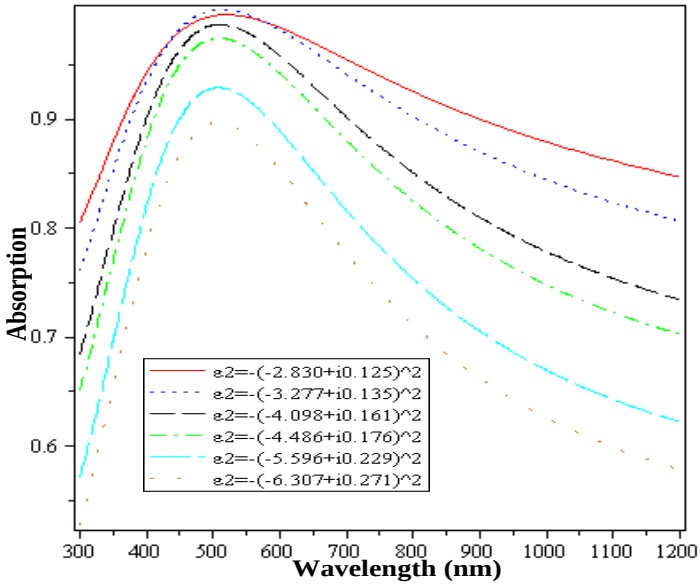

Figure (4.17): The absorbance versus the wavelength for different ε_2 for the LHM under normal incidence in TM case, $\varepsilon_1 = 1.8^2$, $L_1 = 70\ nm$ and $L_2 = 3.97\ \mu m$.

Although of the optimum maximum value of absorption for $\varepsilon_2 = -(-3.277 + i0.135)^2$, $\varepsilon_2 = -(-2.830 + i0.125)^2$ can get better results near the boundary of the required wavelength as the above figures show.

To study the effect of the permittivity for SiN_x (ε_1), where it can take the values between 1.8^2 to 2.4^2, the below figures from (4.18) to (4.23) illustrate the

absorbance versus the wavelength by changing ε_1, where each figure deals with different value of ε_2 for LHM layer. In Figure (4.18) the value of ε_2 is equal $-(-2.830 + i0.125)^2$, which give 99.56% absorption at 520 nm wavelength when ε_1 for SiN_x equals 1.8^2. The value $\varepsilon_2 = -(-3.277 + i0.135)^2$ can give preferable maximum absorption with the same value of ε_1, where it achieve 99.99% absorption at 515 nm wavelength as in Figure (4.19), but it has minimum values of absorption at the boundary of the supposed wavelength lower than the previous.

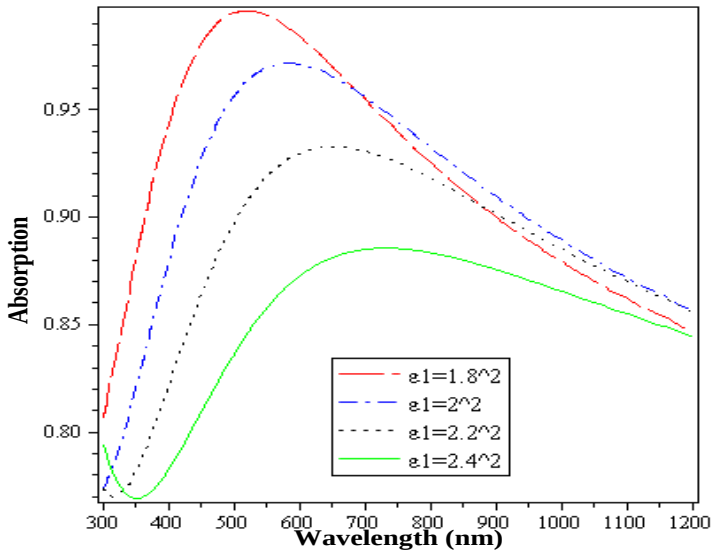

Figure (4.18): The absorbance versus the wavelength for different ε_1 for SiN_x under normal incidence in TM case, $\varepsilon_2 = -(-2.830 + i0.125)^2$, $L_1 = 70\ nm$ and $L_2 = 3.97\ \mu m$.

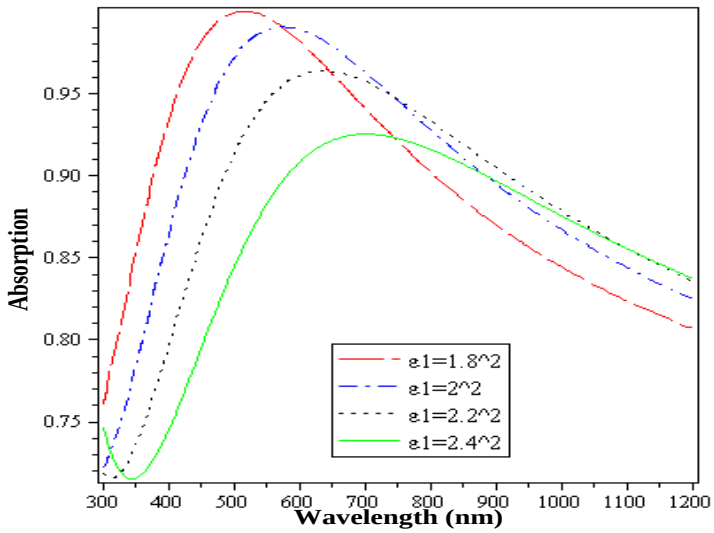

Figure (4.19): The absorbance versus the wavelength for different ε_1 for SiN_x under normal incidence in TM case, $\varepsilon_2 = -(-3.277 + i0.135)^2$, $L_1 = 70\ nm$ and $L_2 = 3.97\ \mu m$.

In Figure (4.20) ε_2 has a value of $-(-4.098 + i0.161)^2$, which gives the maximum absorption with $\varepsilon_1 = 2^2$ for SiN_x and reach to 99.32% absorption at 630 nm wavelength. The value $\varepsilon_2 = -(-4.486 + i0.176)^2$ for LHM has two maximum values, where it has 99.65% absorption at 570 nm wavelength with $\varepsilon_1 = 2^2$ and 99.86% absorption at 625 nm wavelength with $\varepsilon_1 = 2.2^2$ as in Figure (4.21).

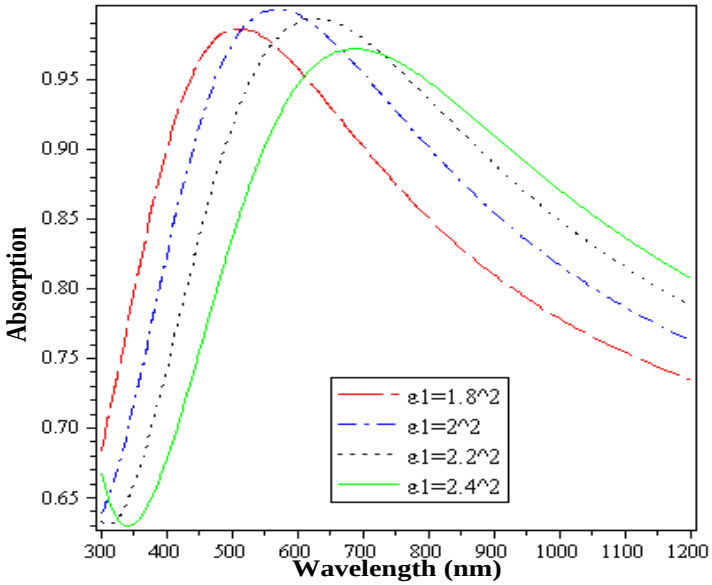

Figure (4.20): The absorbance versus the wavelength for different ε_1 for SiN_x under normal incidence in TM case, $\varepsilon_2 = -(-4.098 + i0.161)^2$, $L_1 = 70\ nm$ and $L_2 = 3.97\ \mu m$.

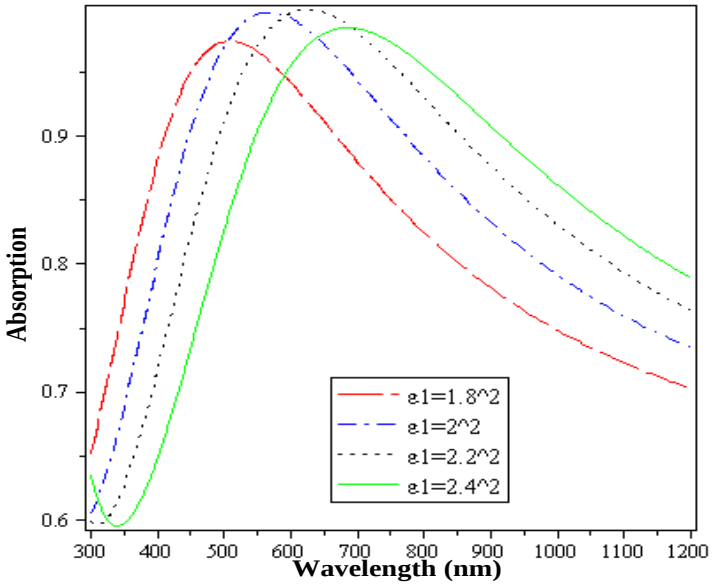

Figure (4.21): The absorbance versus the wavelength for different ε_1 for SiN_x under normal incidence in TM case, $\varepsilon_2 = -(-4.486 + i0.176)^2$, $L_1 = 70\ nm$ and $L_2 = 3.97\ \mu m$.

Figure (4.22) illustrates that the value $\varepsilon_2 = -(-5.596 + i0.229)^2$ also can take two perfect maximum absorption as the previous, where it gives 99.45% absorption at 625 nm wavelength with $\varepsilon_1 = 2.2^2$ and 99.98% absorption at 680 nm wavelength with $\varepsilon_1 = 2.4^2$. In Figure (4.23) the maximum absorption reaches 99.78% at 680 nm wavelength for the value $\varepsilon_2 = -(-6.307 + i0.271)^2$ with $\varepsilon_1 = 2.4^2$.

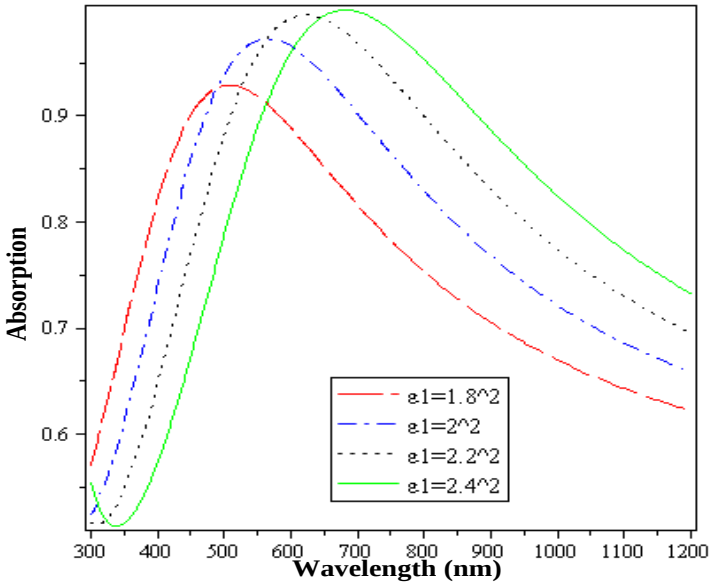

Figure (4.22): The absorbance versus the wavelength for different ε_1 for SiN_x under normal incidence in TM case, $\varepsilon_2 = -(-5.596 + i0.229)^2$, $L_1 = 70\ nm$ and $L_2 = 3.97\ \mu m$.

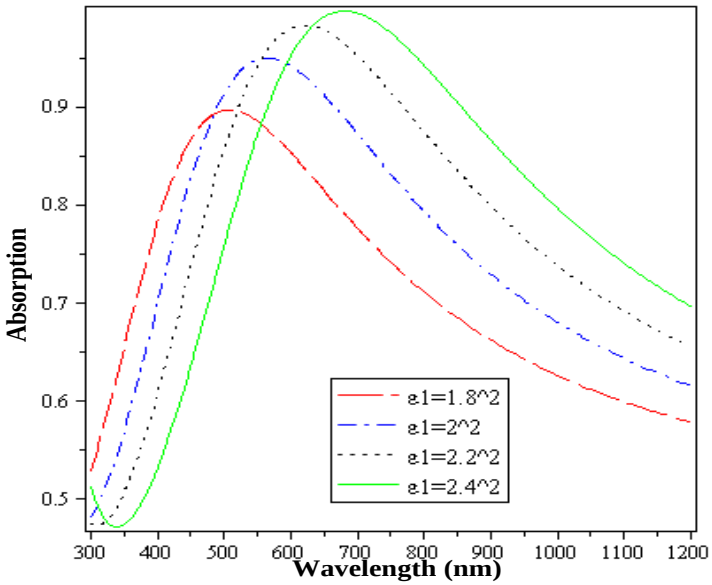

Figure (4.23): The absorbance versus the wavelength for different ε_1 for SiN_x under normal incidence in TM case, $\varepsilon_2 = -(-6.307 + i0.271)^2$, $L_1 = 70\ nm$ and $L_2 = 3.97\ \mu m$.

It is noted that all of the above results of normal incidence are matching with the TE polarization.

Figures (4.24) and (4.24) indicate the effect of the angle of incidence on the absorbance versus the wavelength for $\varepsilon_2 = -(-2.830 + i0.125)^2$ and $\varepsilon_2 = -(-3.277 + i0.135)^2$; respectively, with $\varepsilon_1 = 1.8^2$ to the both, where they illustrate the angles until 60° can give a good absorption and that results in TM polarization is considered better than from the results for TE case in the previous section, where the better absorption was considered until 45°.

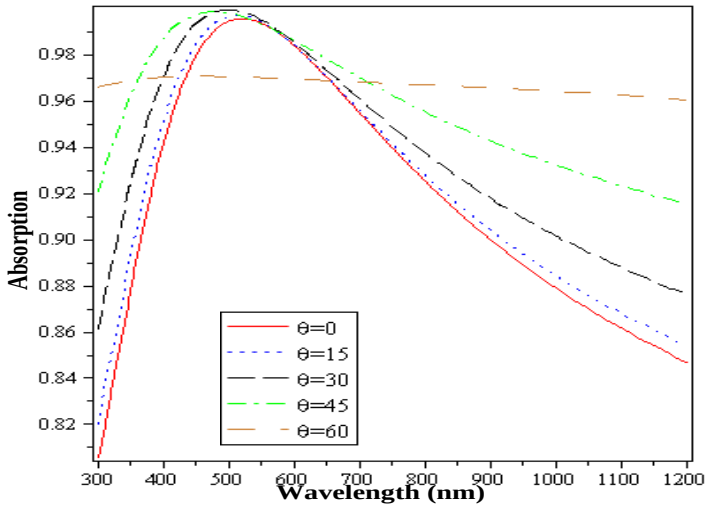

Figure (4.24): The absorbance versus the wavelength for different angles of incidence with $\varepsilon_1 = 1.8^2$, $L_1 = 70\ nm$, $L_2 = 3.97\ \mu m$ and $\varepsilon_2 = -(-2.830 + i0.125)^2$ in TM case.

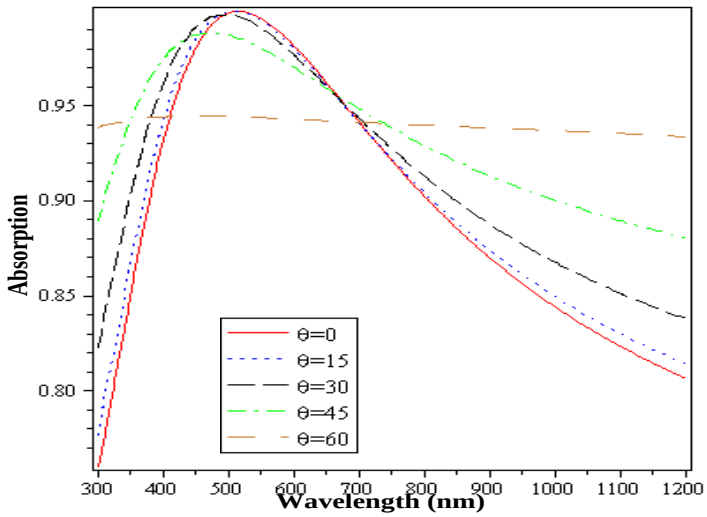

Figure (4.25): The absorbance versus the wavelength for different angles of incidence with $\varepsilon_1 = 1.8^2$, $L_1 = 70\ nm$, $L_2 = 3.97\ \mu m$ and $\varepsilon_2 = -(-3.277 + i0.135)^2$ in TM case.

Figures (4.26) and (4.27) indicate the previous results, where they show the effect of the angle of incidence on the absorbance for different wavelengths in the range of the desired photon flux and it's clear that when the angle of incidence increase from 60° the absorption start decay significantly.

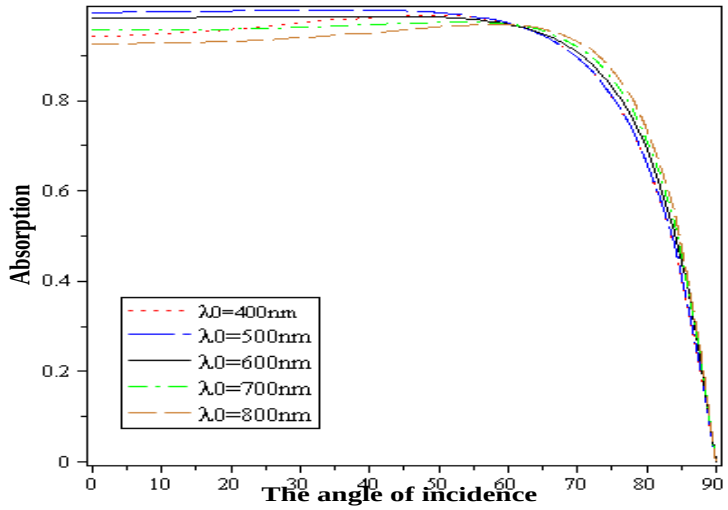

Figure (4.26): The absorbance versus the angles of incidence for different wavelengths with $\varepsilon_1 = 1.8^2$, $L_1 = 70\ nm$, $L_2 = 3.97\ \mu m$ and $\varepsilon_2 = -(-2.830 + i0.125)^2$ in TM case.

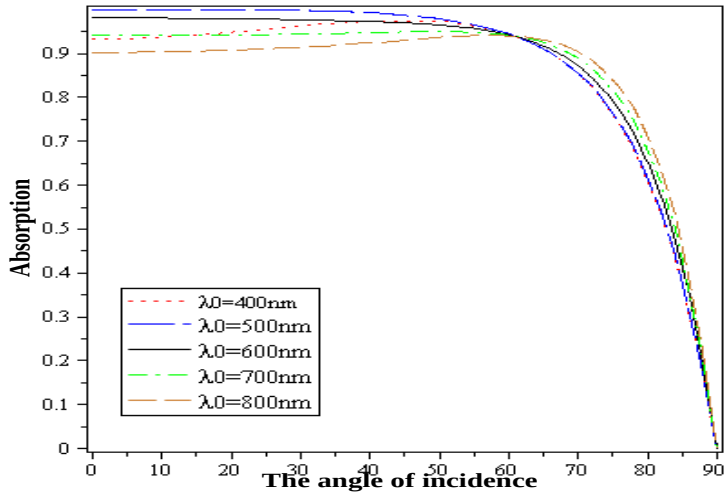

Figure (4.27): The absorbance versus the angles of incidence for different wavelengths with $\varepsilon_1 = 1.8^2$, $L_1 = 70\ nm$, $L_2 = 3.97\ \mu m$ and $\varepsilon_2 = -(-3.277 + i0.135)^2$ in TM case.

4.5 The Average of Absorption for TE and TM Polarization

Depending on the values of each layer of the structure in section 4.2 and the results for TE and TM polarizations in sections 4.2 and 4.3; respectively, to calculate the average of absorption, which is given by:

$$A_{ave} = \frac{A_s + A_p}{2} \tag{4.2}$$

To determine the optimal value of ε_2 for the LHM layer, ε_1 for SiN_x layer is assumed to be 1.8^2. The below figures indicate the reflection, transmission and absorbances against wavelength for different ε_2, where the results are completely agree with the TE and TM results, where $\varepsilon_2 = -(-2.830 + i0.125)^2$ and $\varepsilon_2 = -(-3.277 + i0.135)^2$ are chosen.

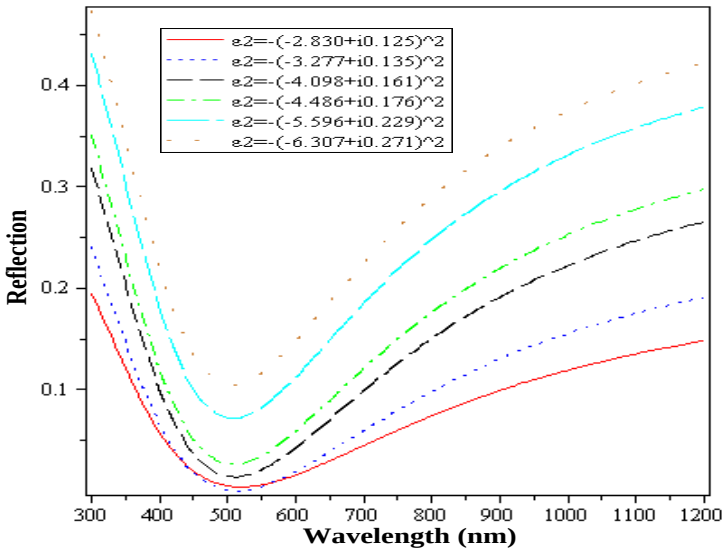

Figure (4.28): The average of reflectance versus the wavelength for different ε_2 for the LHM with $\varepsilon_1 = 1.8^2$, $L_1 = 70\ nm$ and $L_2 = 3.97\ \mu m$ under normal incidence.

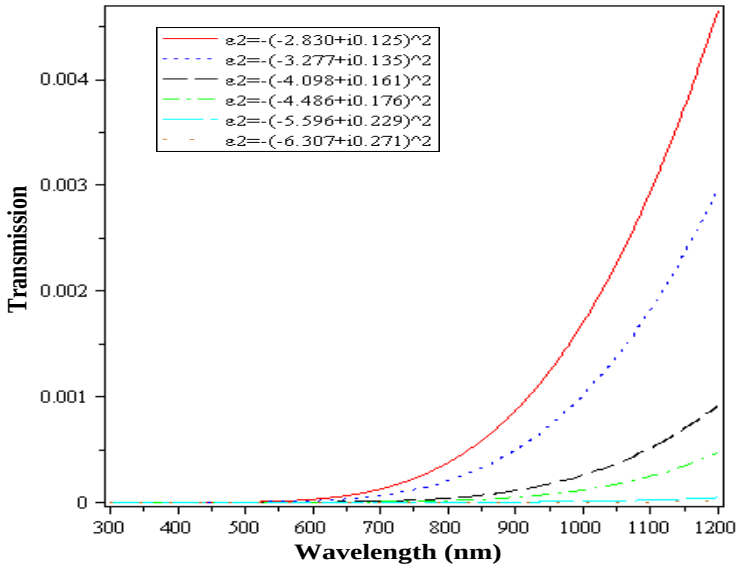

Figure (4.29): The average of transmittance versus the wavelength for different ε_2 for the LHM with $\varepsilon_1 = 1.8^2$, $L_1 = 70\ nm$ and $L_2 = 3.97\ \mu m$ under normal incidence.

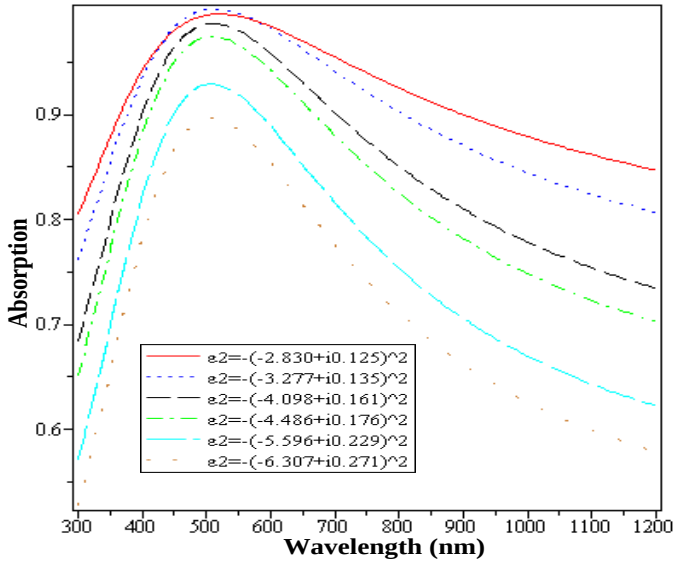

Figure (4.30): The average of absorbance versus the wavelength for different ε_2 for the LHM with $\varepsilon_1 = 1.8^2$, $L_1 = 70\ nm$ and $L_2 = 3.97\ \mu m$ under normal incidence.

It is worth mentioning that under normal incidence all of the average results of the two polarizations are matching with TE and TM polarizations, so all of the values of ε_2 in the previous figures can give a good results with different ε_1 for the SiN_x layer as in sections 4.3 and 4.4, but it is still neglected due to the low absorption with respect to $\varepsilon_2 = -(-2.830 + i0.125)^2$ and $\varepsilon_2 = -(-3.277 + i0.135)^2$ results in the boundary of the desired rang of wavelength, also the value of ε_1 that gives the perfect results with the last two values of ε_2 is 1.8^2 in the normal incidence case as the previous.

Now, to examine the effect of the angle of incidence on the average of absorbance, Figures (4.31) and (4.32) illustrate the change in the average of absorption versus the wavelength for different angles, where the first figure uses $\varepsilon_2 = -(-2.830 + i0.125)^2$ for the LHM which gives acceptable results with angles of incidence less than 60°, the second figure dials with $\varepsilon_2 = -(-3.277 + i0.135)^2$ for the LHM which can take the same behavior as the first with some small different in the upper and lower values of absorption.

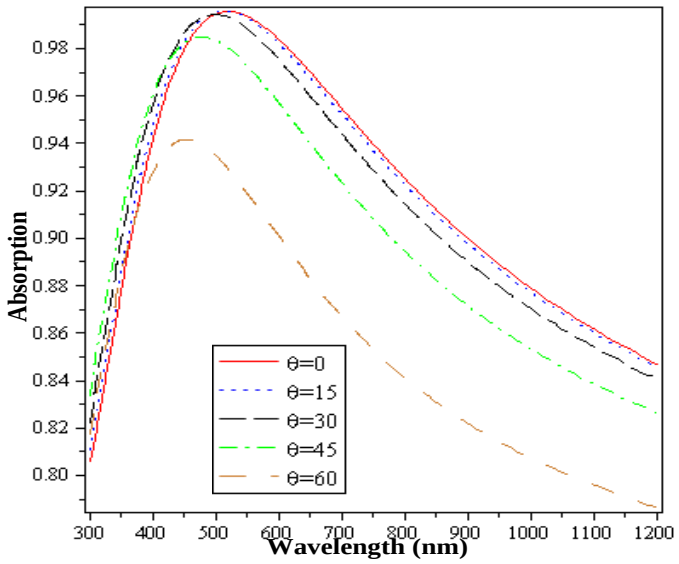

Figure (4.31): The average of absorbance versus the wavelength for different angles of incidence with $\varepsilon_1 = 1.8^2$, $L_1 = 70\ nm$, $L_2 = 3.97\ \mu m$ and $\varepsilon_2 = -(-2.830 + i0.125)^2$.

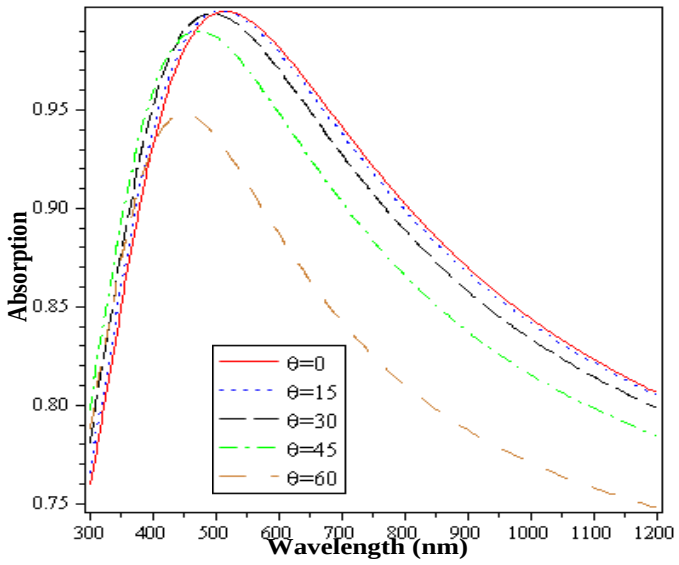

Figure (4.32): The average of absorbance versus the wavelength for different angles of incidence with $\varepsilon_1 = 1.8^2$, $L_1 = 70\ nm$, $L_2 = 3.97\ \mu m$ and $\varepsilon_2 = -(-3.277 + i0.135)^2$.

The below two figures explain the change in the average of absorption versus the angle of incidence for different wavelengths with the two values of ε_2. They confirm the previous results, where the average of absorption falling dawn significantly when the angle of incidence getting more than 60°.

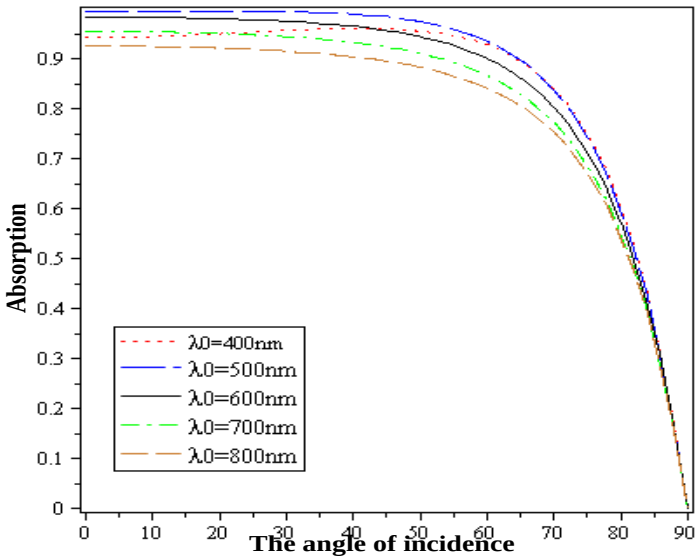

Figure (4.33): The average of absorbance versus the angles of incidence for different wavelengths with $\varepsilon_1 = 1.8^2$, $L_1 = 70\ nm$, $L_2 = 3.97\ \mu m$ and $\varepsilon_2 = -(-2.830 + i0.125)^2$.

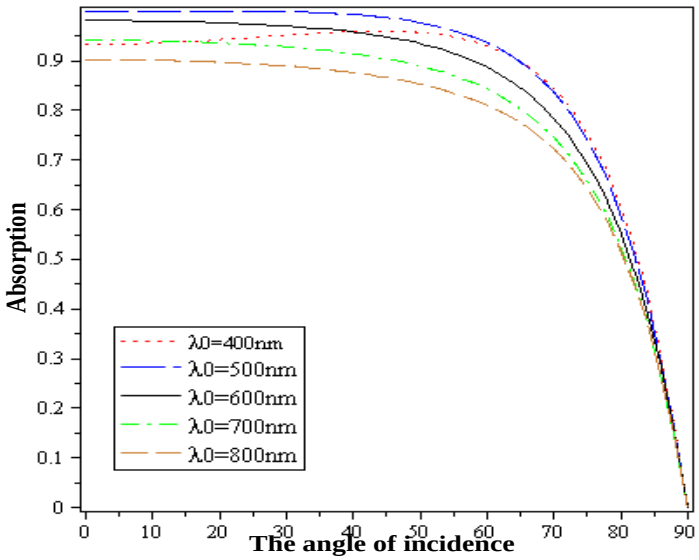

Figure (4.34): The average of absorbance versus the angles of incidence for different wavelengths with $\varepsilon_1 = 1.8^2$, $L_1 = 70\ nm$, $L_2 = 3.97\ \mu m$ and $\varepsilon_2 = -(-3.277 + i0.135)^2$.

Chapter 5

Conclusion

Chapter 5

Conclusion

The basic purpose of this thesis is to design a new multilayer ARC structure containing LHM for solar cells applications. A theoretical analysis for the proposed structure was carried out for the TE and TM polarizations. Both reflection and transmission of the structures were studied in detail. Moreover, an investigation of the absorption for another structure had been implemented.

For the first ARC structure, the following remarks have been observed:

- The transmission and reflection for the TE and TM polarizations and their average as well are completely matching for the normal incidence case.
- Both reflection and transmission are slightly affected by changing the thickness of the LHM for TE and TM modes.
- The thickness of the LHM that gives maximum transmission and minimum reflection as the angle of incidence variation are different between the two polarization.
- All of the thicknesses around the minimum value that give a destructive interference at 600 nm wavelength, can give almost the same behaviors of reflection and transmission for the average of the two polarization.
- The minimum value of ε_2 for SiN_x layer gives the best results and when it is increasesd, the transmittance become no longer optimal for the normal incidence case.
- When the thickness of SiN_x layer increases over than the minimum thickness that gives a destructive interference, the maximum transmittance is shifted towards smaller energy spectra for the both polarizations with a small deviation between the two polarization about 50 nm wavelength in the horizontal line .
- As the angle of incidence increases in TE polarization, the optimal values of reflectance and transmittance are shifted towards higher energy spectra, but in TM polarization they are shifted towards smaller energy spectra, but their extremes become no longer optimal for the both polarizations.

- The average of the TE and TM polarizations obeys almost the TE polarization for the transmittance and reflectance because its deviation is stronger than TM polarization.

With respect to the second ARC structure, where the LHM layer and the SiN_x layer for the first structure are interchanged, the basic conclusion remarks can be summarized as:

- There are several values of ε_2 for the LHM layer that give good maximum absorptions with different permittivity values of SiN_x.
- As the angle of incidence increases, the maximum absorption decreases and shifts slightly towards higher energy spectra, and the angles until 60° can give an acceptable absorption for solar cells.

The LHM can be a good candidate to make structures of the ARCs to enhance the transmission or the absorption and then the efficiency of solar cells applications as a future work.

References

References

Al-Turk, S. (2011). *Analytic Optimization Modeling of Anti-Reflection Coatings for Solar Cell*. (Unpublished Master Thesis). McMaster University, Hamilton, Ontario, Canada.

Bahrami, A., Mohammadnejad, S., Abkenar, N. J., & Soleimaninezhad, S. (2013). Optimized single and double layer antireflection coatings for GaAs solar cells. *International Journal of Renewable Energy Research (IJRER), 3*(1), 79-83.

Beye, M., Faye, M. E., Ndiaye, A., Ndiaye, F., & Maiga, A. S. (2013). Optimization of SiNx Single and Double Layer ARC for Silicon Thin Film Solar Cells on Glass. *Research Journal of Applied Sciences, Engineering and Technology*, *6*(3), 412-416.

Bouhafs, D., Moussi, A., Chikouche, A., & Ruiz, J. M. (1998). Design and simulation of antireflection coating systems for optoelectronic devices: Application to silicon solar cells. *Solar Energy Materials and Solar Cells*, *52*(1), 79-93.

Chen, H. T., Zhou, J., O'Hara, J. F., Chen, F., Azad, A. K., & Taylor, A. J. (2010). Antireflection coating using metamaterials and identification of its mechanism. *Physical review letters*, *105*(7), 073901.

Chew, W. C. (2005). Some reflections on double negative materials. *Progress In Electromagnetics Research*, *51*, 1-26.

Cory, H., & Zach, C. (2004). Wave propagation in metamaterial multi-layered structures. *Microwave and Optical Technology Letters*, *40*(6), 460-465.

Crabtree, G. W., & Lewis, N. S. (2007). Solar energy conversion. *Physics today*, *60*(3), 37-42.

El-Amassi, D. M., El-Khozondar, H. J., Shabat M. M. (2015). Efficiency Enhancement of Solar Cell Using Metamaterials. *International Journal of Nano Studies & Technology (IJNSST), 4*(2), 84-87.

Engheta, N. (2003). Metamaterials with negative permittivity and permeability: background, salient features, and new trends. *Departmental Papers (ESE)*, 9.

Goodman, J. W. (2005). *Introduction to Fourier optics*. (3rd ed.). Roberts and Company Publishers.

Hamouche, H., & Shabat, M. M. (2016). Enhanced absorption in silicon metamaterials waveguide structure. *Applied Physics A*, *122*(7), 1-7.

Hashmi, M. H. I., & Shahida Rafique, G. (2013). Towards high efficiency solar cells: Composite metamaterials. *Global Journal of Research In Engineering*, *13*(10).

Heavens, O. S. (1991). *Optical properties of thin solid films*. Courier Corporation.

Jackson, J. D. (1999). *Classical electrodynamics*. (3rd ed.). John Wiley and Sons, New York.

Kim, K. Y., Cho, Y. K., Tae, H. S., & Lee, J. (2006). Guided mode propagations of grounded double-positive and double-negative metamaterial slabs with arbitrary material indexes. *JOURNAL-KOREAN PHYSICAL SOCIETY*, *49*(2), 577.

Kong, J. A. (2002). Electromagnetic wave interaction with stratified negative isotropic media. *Progress In Electromagnetics Research*, *35*, 1-52.

Lee, Y., Gong, D., Balaji, N., Lee, Y. J., & Yi, J. (2012). Stability of SiN X/SiN X double stack antireflection coating for single crystalline silicon solar cells. *Nanoscale research letters*, *7*(1), 1.

Macleod, H. A. (2001). *Thin-film optical filters*. (3ed ed.). CRC press.

Markoš, P., & Soukoulis, C. M. (2008). *Waves Propagation From Electrons to Photonic Crystals and Left-Handed Materials*. (1st ed.). New Jersey: Princeton University Press.

Nakayama, K., Tanabe, K., & Atwater, H. A. (2008). Plasmonic nanoparticle enhanced light absorption in GaAs solar cells. *Applied Physics Letters*, *93*(12), 121904.

Nelson, J. (2003). The physics of Solar Cells, vol. 57.

Oraizi, H., & Abdolali, A. (2009). Mathematical formulation for zero reflection from multilayer metamaterial structures and their notable applications. *IET microwaves, antennas & propagation*, *3*(6), 987-996.

Pedrotti, F. L., & Pedrotti, L. S. (1993). *Introduction to optics*. (2nd ed.). New Jersey: Prentice Hall.

Pendry, J. B., Holden, A. J., Robbins, D. J., & Stewart, W. J. (1998). Low frequency plasmons in thin-wire structures. *Journal of Physics: Condensed Matter*, *10*(22), 4785.

Pendry, J. B., Holden, A. J., Stewart, W. J., & Youngs, I. (1996). Extremely low frequency plasmons in metallic mesostructures. *Physical review letters*, *76*(25), 4773.

Reza, A. (2008). *The optical properties of metamaterial waveguide structures*. (Unpublished Master Thesis). Queen's University, Kingston, Ontario, Canada.

Sabah, C., & Uckun, S. (2007). Electromagnetic wave propagation through frequency-dispersive and lossy double-negative slab. *Opto-Electronics Review*, *15*(3), 133-143.

Sabah, C., Ogucu, G., & Uckun, S. (2006). Reflected and transmitted powers of electromagnetic wave through a double-negative slab. *Journal of Optoelectronics and Advanced Materials*, *8*(5).

Schubert, M. F., Mont, F. W., Chhajed, S., Poxson, D. J., Kim, J. K., & Schubert, E. F. (2008). Design of multilayer antireflection coatings made from co-sputtered and low-refractive-index materials by genetic algorithm. *Optics express*, *16*(8), 5290-5298.

Shabat, M. M., & Ubeid, M. F. (2014). Antireflection coating at metamaterial waveguide structures for solar energy applications. *Energy Procedia*, *50*, 314-321.

Shelby, R. A., Smith, D. R., & Schultz, S. (2001). Experimental verification of a negative index of refraction. *science*, *292*(5514), 77-79.

Smith, D. R., & Kroll, N. (2000). Negative refractive index in left-handed materials. *Physical Review Letters*, *85*(14), 2933.

Smith, D. R., Padilla, W. J., Vier, D. C., Nemat-Nasser, S. C., & Schultz, S. (2000). Composite medium with simultaneously negative permeability and permittivity. *Physical review letters*, *84*(18), 4184.

Ubeid, M. F., Shabat, M. M., & Sid-Ahmed, M. O. (2011). Effect of negative permittivity and permeability on the transmission of electromagnetic waves through a structure containing left-handed material. *Natural science*, *3*(04), 328.

Ubeid, M. F., Shabat, M. M., & Sid-Ahmed, M. O. (2012, a). Maximum and minimum transmittance of a structure containing N identical pairs of left-and right-handed materials. In *Electromagnetics in Advanced Applications (ICEAA), 2012 International Conference on* (pp. 75-78). IEEE.

Ubeid, M. F., Shabat, M. M., & Sid-Ahmed, M. O. (2012, b). Numerical study of a structure containing left-handed material waveguide. *Indian Journal of Physics*, *86*(2), 125-128.

Ubeid, M. F., Shabat, M. M., & Sid-Ahmed, M. O. (2013, a)(PHD). Reflection and transmission powers of electromagnetic waves through a structure containing left-handed material, Sudan University of Science and Technology, Sudan.

Ubeid, M. F., Shabat, M. M., & Sid-Ahmed, M. O. (2013, b). Effect of dissipation factor on reflected and transmitted powers of a structure containing left-handed material waveguide. *International Letters of Chemistry, Physics and Astronomy*, *3*, 1-11.

Veselago, V. G. (1968). The electrodynamics of substances with simultaneously negative values of ϵ and μ .*Soviet physics uspekhi*, *10*(4), 509.

Xiong, X. Y., & Sha, W. E. I. (2013). The FDTD method: Essences, evolutions, and applications to nano-optics and quantum physics. *Computational Nanotechnology Using Finite Difference Time Domain*, 37-82.

Yeh, C., & Shimabukuro, F. I. (2008). *The essence of dielectric waveguides* (p. 68). New York: Springer.

Yu, K., & Chen, J. (2008). Enhancing solar cell efficiencies through 1-D nanostructures. *Nanoscale Research Letters*, *4*(1), 1.

Zdanowicz, T., Rodziewicz, T., & Zabkowska-Waclawek, M. (2005). Theoretical analysis of the optimum energy band gap of semiconductors for fabrication of solar cells for applications in higher latitudes locations. *Solar Energy Materials and Solar Cells*, *87*(1), 757-769.

Zeman, M. (2003). Introduction to photovoltaic solar energy [Electronic Version]. *Delft University of Technology*, *2*(6), 1- 139.